Institut für Entwicklungsgenetik
GSF-Forschungszentrum für Umwelt und Gesundheit

The molecular and functional analyses of neurochondrin mouse mutant

Ruzanna Istvanffy

Vollständiger Abdruck der von der Fakultät Wissenschaftszentrum Weihenstephan für Ernährung, Landnutzung und Umwelt der Technischen Universität München zur Erlangung des akademischen Grades eines

Doktors der Naturwissenschaften

genehmigten Dissertation.

Vorsitzender:	Univ.-Prof. Dr. Erwin Grill
Prüfer der Dissertation:	1. Univ.-Prof. Dr. Wolfgang Wurst
	2. Univ. Prof. Dr. Kay H. Schneitz

Die Dissertation wurde am 06.09.2006 bei der Technischen Universität München eingereicht und durch die Fakultät Wissenschaftszentrum Weihenstephan für Ernährung, Landnutzung und Umwelt am 30.11.2006 angenommen.

„Der Mensch hat dreierlei Wege klug zu handeln: erstens durch nachdenken, das ist der edelste, zweitens durch nachahmen, das ist der leichteste, und drittens durch Erfahrung, das ist der bitterste.“

Konfuzius

The aim of this study was the phenotypic and functional analyses of neurochondrin (*Ncdn*) gene–trap mouse mutant. This mouse line was generated from the embryonic stem (ES) cell clone W044B06 (http://genetrap.de) trapped with the pT1*βgeo* gene trap vector, which integrated in the 3'UTR of exon 7. The *Ncdn* gene-trap mice express a truncated form of *Ncdn*, lacking only the C-terminal part of the protein and therefore represent a hypomorphic allele of this gene. The mutant mice develop normally till the adulthood. The homozygous females are subfertile due to ovulation failure, suggesting a possible involvement of *Ncdn* in the regulation of female reproduction. This is supported by strong expression of *Ncdn* in the neuroendocrine system, particularly in the arcuate nucleus of the hypothalamus and in the anterior and intermediate lobes of the pituitary. The analyses of factors involved in the regulation of the female fertility revealed dramatically elevated level of prolactin (PRL) expression in the pituitary of female mutants. The pituitaries itself were enlarged and contained an increased number of proliferating lactotrophs, as a consequence of decreased Erk1/2 activity in the anterior lobe. In fact, PRL expression and lactotroph proliferation are under negative control of neurotransmitter dopamine (DA) via activation of the dopamine receptor 2 (D2R), anchored in the lactotroph cell membrane. Interestingly, the *Ncdn*-binding-domain was identified in the cytoplasmic tail of D2R during homology PSI BLAST analyses of protein sequences. Moreover, the expression patterns of D2R and *Ncdn* overlapped in the pituitary and some brain regions, suggesting acting in the same pathway. Furthermore the pituitary phenotype of *Ncdn* homozygous females strongly resembles the one of D2R knock-outs (Saiardi et al., 1997). However, *Ncdn* homozygous females displayed decreased PRL in the blood contrary to the increased PRL in the blood of D2R null females. This discrepancy can be addressed to a selective binding of *Ncdn* to one of two D2R isoforms, which are known to play diverse roles in the regulation of PRL production and release (Usiello et al. 2000). On the other side, *Ncdn* was shown to bind with phospatidic acid (Ksistakis et al. 2003) which is involved in the exocytotic machinery in neuroendocrine cells (Vitale et al., 2001) suggesting a possible role for *Ncdn* in PRL release from the lactotroph cells aside of D2R signalling.

Das Ziel dieser Studie war die phenotypische und funktionale Analyse von neurochondrin *(Ncdn)* Mausmutanten. Die verwendete Mauslinie wurde aus dem Stammzellenklon W044B06 (http://genetrap.de) gezogen, die mit dem pT1*βgeo* Gen-trap Vector manipuliert wurde, der sich in den 3'UTR von exon 7 integriert. Die *Ncdn* gen-trap Mäuse exprimiren eine verkürzte Form von *Ncdn,* dem lediglich der C-Terminus des Proteins fehlt und das dadurch ein hypomorphisches Allele dieses Gens darstellt.

Die Mäuse entwickeln sich normal bis ins Erwachsenenalter. Die homozygoten Weibchen sind aufgrund von Ovulationsversagen unterdurchschnittlich fruchtbar, was einen möglichen Einfluss von *Ncdn* auf den Ablauf der weiblichen Fortpflanzung nahe legt. Diese Annahme wird durch starke Exprimierung von *Ncdn* im neuroendokrinen System, besonders im Arcuate Nucleus des Hypothalamus und im vorderen und mittleren Lappen der Hypophyse unterstützt. Die Analyse der Faktoren mit Einfluss auf die weibliche Fruchtbarkeit zeigte einen stark erhöhten Prolactinspiegel (PRL) in der Hypophyse der weiblichen Mutanten. Die Hypophysen selbst waren stark vergrößert und enthielten eine erhöhte Anzahl von wuchernden Laktotrophen aufgrund von reduzierter Erk1/2 Aktivität im vorderen Lappen. Offensichtlich stehen PRL Exprimierung und die Laktotrophenwucherung unter negativer Kotrolle des Neurotransmitters Dopamin aufgrund der Aktivierung des Dopaminrezeptors 2 (D2R), der in der Zellmembrane der Laktotrophen verankert ist. Während der PSI BLAST Analyse der Protein Sequenzen wurde die „*Ncdn*-binding-domain" im zytoplasmatischen Bereich des D2R identifiziert. Des Weiteren wurde festgestellt, dass die Exprimierungsmuster von D2R und *Ncdn* in der Hypophyse und in einigen Hirnregionen überlappen, was auf die Mitwirkung in einem Signalweg hinweist. Außerdem weist der Hypophysen Phenotype von *Ncdn* homozygoten Weibchen starke Ähnlichkeit mit dem von D2R knock-outs (Saiardi et al., 1997) auf. *Ncdn* homozygote Weibchen weisen jedoch reduziertes PRL auf, im Gegensatz zu erhöhtem PRL im Blut von D2R null Weibchen. Diese Diskrepanz kann mit spezifischer Binding von *Ncdn* an eine der beiden D2R Isoformen, die bekanntermaßen eine Rolle in der Produktion und Ausschüttung von PRL spielen (Usiello et al. 2000), erklärt werden. Andererseits wurde auch gezeigt, dass *Ncdn* sich an die Phosphatsäure bindet (Ksistakis et al. 2003), welche eine Rolle in der Exocytose aus den neuroendocrinen Zellen spielt (Vitale et al., 2001). Dies legt den Schluss nahe, dass möglicherweise *Ncdn* eine Rolle in der PRL Ausschüttung von Lactotrophen unabhängig von dem D2R Signalweg spielen könnte.

INDEX OF CONTENT

1 INTRODUCTION

1.1 Neurochondrin gene-trap female mutants are subfertile

Initially, neurochondrin (*Ncdn)* was identified in the large screen for genes inducing long-term potentiation (Shinozaki et al. 1997). *Ncdn* gene is located on the mouse chromosome 4 and consists of seven exons. *Ncdn* is a cytoplasmic protein and exist in two isoforms *Ncdn 1* and *Ncdn 2*, arising due to alternative ATG in exon 1. *Ncdn* orthologous are widely represented within eucaryots. There were identified in higher plants (*Arabidopsis thaliana, Oryza sativa*), invertebrates (*Drosophila melanogaster*) and vertebrates (*Xenopus laevis, Gallus gallus, Mus musculus, Rattus norvegicus and Homo sapience*). Interestingly, the Arabidopsis orthologue of *Ncdn* (*Accession number*: NP_194933) contains SPX domain, which was originally identified in the SYG1 yeast protein. SYG1 inhibits the transduction of the mating pheromone signal via direct binding to a G-protein beta subunit, suggesting an involvement in G-protein associated signal transduction.

The previously published *Ncdn* null mouse mutants are embryonically lethal (between 3.5 and 6.5 days *post coitum* (dpc)) suggesting an important role of *Ncdn* during early embryogenesis (Moshizuki et al., 2003). The study of *Ncdn* gene functions in the adulthood is only possible by generating conditional or hypomophic alleles of the *Ncdn* gene. Recently, conditional *Ncdn* knockout mutants (NC $^{lox/lox}$Cre) were generated using Cre/loxP-recombinant system (Dateki et al., 2005). In those mutants *Ncdn* was targeted specifically in the neural tissue by breeding of the mouse line with mutated allele of *Ncdn* gene (exon1 flanked by loxP sites) with mice expressing Cre recombinase in neuronal and glia cell precursors under the control of the rat nestin promoter and enhancer (Tronche et al., 1999). In the hippocampus of the NC $^{lox/lox}$Cre mice phosphorylation and activity of Ca(2+)/calmodulin-dependent protein kinase II (CaMK II) were increased. This suggested a possible role for *Ncdn* as a negative regulator of CaMK II activity (Dateki et al., 2005). Additionally, some of the mutants displayed epileptic seizures (~24% of NC $^{lox/lox}$Cre) when they aged over 6 months.

Another *Ncdn* mouse mutant, presented in this study, was generated from the German Gene Trap Consortium (GGTC) clone W044B06, trapped with the pT1*βgeo* gene-trap vector. These mice express a truncated form of *Ncdn*, lacking only the C-terminal part of

the protein and therefore represent a hypomorphic allele of this gene. The mutant mice develop normally till the adulthood, while homozygous females are subfertile due to ovulation failure and hormonal imbalance, suggesting a possible involvement of *Ncdn* in the regulation of female reproduction.

1.2 Reproduction and it's genetic

Biological reproduction is a complex biological process by which new individual organisms are produced. The main types of reproduction: sexual and asexual. Asexual reproduction is the biological process by which an organism creates a genetically-similar or identical copy of itself without a contribution of genetic material from another individual. Bacteria divide asexually via binary fission; viruses take control of host cells to produce more viruses; Hydras and yeasts are able to reproduce by budding; most of plants are capable of vegetative reproduction (without seeds and spores). Sexual reproduction is the biological process by which organisms create descendants that have a combination of genetic material contributed from usually two different members of the species. It is characterised by generation of haploid germ cells (meiosis) of either sex, fertilisation, which leads to fusion of two gametes and the restoration of the original number of chromosomes. During meiosis, the chromosomes of each pair usually cross over to achieve genetic recombination. Almost all plants and animals reproduce primarily sexually. The physiological regulation of reproductive processes is well understood, while few is known about it's genetics. The study of mammalian reproduction is hindered by two major obstacles. First, mammalian germ cells in culture fail to survive, due to absent autocrine/paracrine or direct cell-to-cell support from supporting cells of somatic origin (Staub et al., 2001; Matzuk et al., 2002). The second is an inability to develop *in vitro* proper conditions for development of gametes with retained ability to fertilize and produce healthy offspring from undifferentiated germ cells. Although, meiosis-competent germ cells generated from undifferentiated embryonic stem cells, were shown to fertilize oocytes and produce blastocytes (Hubner *et al.* 2003, Toyooka et al. 2003, and Geijen et al. 2004), there is no data available suggesting that these progress to produce live offspring. Therefore, study of molecular mechanisms of mammalian reproduction is largely dependent on the generation of loss-of-function mouse mutants. Till now approximately 300 mouse knock outs that manifest defects in

reproduction were generated (Matzuk and Lamb, 2002). These mutations target genes, which are involved in the development and differentiation of reproductive system and proper functioning of it during reproductive age.

In this thesis major focus was on genes which define fertility, an ability of sexually reproducing organisms to generate haploid germ cells of either sex in order to produce healthy offspring in abundance. Therefore, development and differentiation of female gametes with associated surrounding somatic cells (folliculogenesis and ovulation) as well as genetic regulation of those processes are presented further in details.

The population of oocytes is already defined in the female at birth in contrast to the continuous proliferation of male germ cells. In the mouse, two days after birth, naked oocytes become surrounded by three to five somatic cells termed “pre-granulosa” cells to form the primordial follicle (Fig.1).

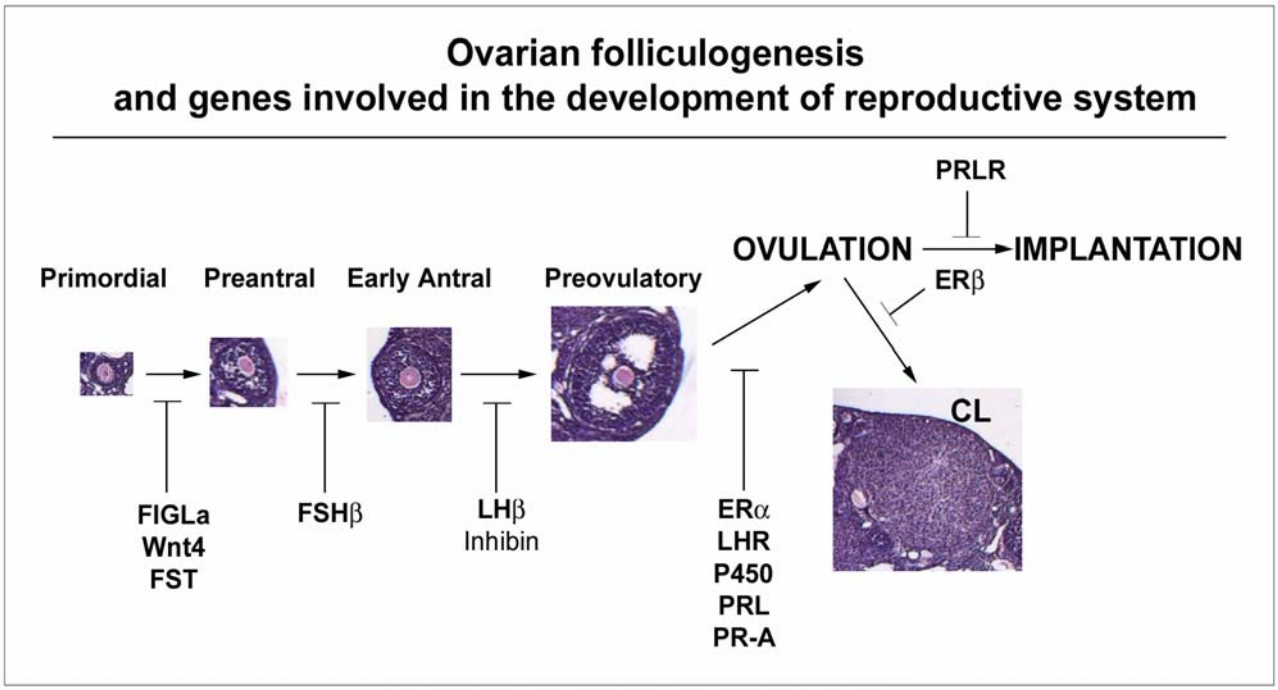

Fig.1 Genes involved in the regulation of the ovarian folliculogenesis

Primordial follicles in response to the intragonadal factors (FIGLa, Wnt4, FST) start to growth rapidly and develop to preantral follicles, surrounded with several layers of granulosa and thecal cells. Up to this stage follicles start to respond to extragonadal factors (FSH, LH and inhibin). The preovulatory follicle is characterised by oocyte protruded from the follicular wall on a well-developed stalk into a large antral cavity. Ovulation (oocyte release from the follicle) appears in response to preovulatory surge of LH and PRL. Granulosa cells remaining in the postovulatory follicle undergo luteinization and form CL.

Null mutations of presented genes result in an arrest in the development of the reproductive system.

Abbreviations: *CL* Corpora lutea

Some of primordial follicles and associated somatic cells start to differentiate and grow in response to intragonadal factors, such as basic helix-loop-helix transcription factor Factor in the Germ Line a (FIGLa), present specifically in the female germ cells. The ovaries of *Figla* $^{-/-}$ mouse mutants are completely devoid of primordial follicles by postnatal day (pd) 2 (Soyal et al. 2000). Other factors derived from somatic cells appeared to be necessary for the folliculogenesis, and as Wnt4 and follistatin (FST). Ovaries of *Wnt4* $^{-/-}$ mouse mutants at pd1 have a dramatic reduction in the number of meiotic-stage oocytes and most oocytes degenerate shortly thereafter (Vainio et al. 1999). A similar phenotype was observed in the ovaries of FST-deficient mice (Yao et al. 2004). Most of the preantral follicles, developed from primordial follicles, suffer atresia characterised by apoptotic death of granulosa cells. Few of preantral follicles start to respond to extragonadal factors, namely follicle stimulating hormone (FSH) and luteinising hormone (LH) and develop further. FSH and LH are produced by gonadotroph cells of anterior pituitary and belong to the family of glycoprotein hormones as well placental human chorionic hormone (hCG), produced by the placenta and thyroid stimulating hormone (TSH) produced by thyrotroph cells of the anterior pituitary. All four proteins are composed of a common α-subunit (Cα) and a hormone specific β-subunit, coupled by non-covalent interaction (Gharib et al., 1990). FSH and LH transmit their signal via activation of FSH and LH receptors (FSHR and LHR) located in the granulosa and theca interna cell membrane. Both receptors belong to the rhodopsin/β2-adrenergic receptor-like family A of seven transmembrane G protein coupled receptors (GPCRs) (Simoni et al, 1997; Heckert and Griswold 2002; Menon et al, 2003).

FSH and LH, by binding to their receptors activate several transduction pathways: cAMP-PKA (Walker et al., 1995; Ascoli et al. 2002); MAP kinase pathway (Crepieux et al, 2001; Salvador et al. 2002; Srisuparp et al. 2003). FSHR was reported to activate calcium pathway in sertoli cells (Gorczynska et al. 1994; Lalevee et al. 1997); phosphatidylinositol 3-kinase (PI3-K) pathway in granulosa and sertoli cells (Gomzalez-Robayna et al. 2000, Meroni et al. 2002) and phospholipase A_2 (PLA_2) pathway (Jannini et al. 1994). LHR, activated by its ligands LH and hCG, was shown to stimulate phospholipase C (PLC) signalling (Davis et al. 1984, Gudermann et al. 1992) and to mediate the activation of Janus kinase-signaling pathways (JAK) (Carvalho et al. 2003).

Interestingly, analyses of knock out mouse mutants for FSH β (*Fshb*) and LHβ (*Lhb*) subunits, as well as for the FSHR (*Fshr*) and LHR (*Lhr*) revealed non-redundant roles in both sexes. In males, a loss of FSH signalling resulted in smaller testis size, reduced spermatogenesis, and impaired sperm motility although the males were fertile (Kumar et al. 1997; Dierich et al. 1998). Females deficient for FSH signalling are sterile with thin uteri and hypoplastic ovaries, due to a block in folliculogenesis prior to the formation of antral follicles (Kumar et al., 1997). In contrast, the absence of LH signalling either by loss of LH or LHR, led to infertility and hypogonadism in both sexes (Lei et al., 2001; Zhang et al. 2001; Ma et al 2004). Moreover, in the females with deficiency in LH signalling folliculogenesis is arrested at early antral stage. Similarly, in males lacking of LH signalling a block of spermatogenesis at the round spermatid stage was reported. In summary, FSH is essential for the progression from secondary to early antral follicle stage (Rao et al, 1978), while LH is required for further development of follicles in females and maturation of the haploid gametic cells in males. Additionally to the regulation of folliculogenesis, FSH and LH stimulate steroidogenesis in somatic cells associated with the oocyte. Thereby, LH stimulates mainly androgen (testosterone) production from thecal cells, while FSH induces proliferation of granulosa cells and trigger signal transduction pathways to activate expression of cytochrome P450 aromatase (CYP19) for aromatization of testosterone to estrogen (Richards, 1994). Steroid hormones (testosterone, estrogen and progesterone) have been long believed to play essential roles in the development, differentiation and proper function of female and male reproductive systems. Testosterone signalling appears via activation of nuclear androgen receptor (AR). The Sertoli cell specific knockout mutants of AR revealed an essential role of testosterone signalling for spermatogenesis but not for gonadal functions (Chang et al., 2004; De Gendt et al., 2004). In females, absence of AR resulted in the reduced fertility with increased defective folliculogenesis, reduced corpora lutea (CL) formation and longer estrous cycle, suggesting an essential role of testosterone in the proper functioning of the female reproductive system (Hu et al., 2004). Estrogen directly influences proliferation and differentiation of follicles (Hisaw , 1947; Drummond et al., 1999; Richards 2001) and acts via two types of nuclear receptors ERα and ERβ. Deletion of ERβ leads to subfertility (Krege et al. 1998) due to defects in granulosa cell development (Dupont et al. 2000), while disruption of ERα results in female infertility due to complete lack of ovulation with ovaries displaying

hemorrhagic cysts (Lubahn et al. 1993; Dupon et al. 2000). ERα knock out males are infertile as well and display degenerated seminiferous tubules and disrupted spermatogenesis (Eddy et al. 1996; Hess et al. 1997). Furthermore, the female knock out mutants for P450 aromatase, which are not able to produce endogenous estrogen, are infertile, due to folliculogenesis arrested at the antral stage. In the ovaries, CL does not get formed and levels of gonadotropins and testosterone are increased in the blood (Fisher et al., 1998). Summarizing, estrogen is obligatory for gametogenesis in both sexes; in females it regulates follicular development beyond the antral stage and maintenance of the female phenotype of ovarian somatic cells. Additionally to local ovarian functions, estrogen in the feedback loop induces preovulatory surge of LH and inhibits FSH release from the pituitary (Greco et al. 1993; Disfalusy et al. 1998, Simpson, 2003).

In response to the LH surge, oocyte are being released (ovulate) from the preovulatory follicle, which is characterised by oocyte protruded from the follicular wall on a well-developed stalk into a large antral cavity. The preovulatory surge of LH is accompanied by a surge of prolactin (PRL), secreted from the lactotroph cells of the anterior pituitary (Arbogast et al., 1988). Interestingly, ovulation can be blocked by pentobarbital infusions that inhibit the preovulatory surge of both LH and PRL in rats, indicating an important role of both hormones in female reproduction (Ishikawa, 1992). PRL along with growth hormone (GH) and placental lactogens (PLs) form a family of group I of the helix bundle protein hormones (Bole-Feysot et al. 1998; Boulay et al. 1992; Horzeman et al., 1994). PRL signalling is mediated by membrane anchored PRL receptor, which belongs to the class 1 cytokine receptor superfamily. This superfamily includes receptors for several interleukins, oncostatin M, erythropoietin and obesity factor leptin (Finidori et al., 1995; Wells et al., 1996). Mice lacking PRL and PRL receptor (PRLR) are infertile and display decreased levels of steroid hormones in the blood. In PRL knock out mice infertility is caused by ovulation failure (Horseman et al., 1997), while PRLR knock out females are infertile due to implantation defects caused by progesterone deficiency, while ovulation rates and estrous cycle are not affected (Grosdemouge et al., 2003). PRL signalling was shown to be necessary for the expression of LHR and therefore potentiates steroidogenic effects of LH in the granulosa-luteal cells (Gafvels et al., 1992; Bjurulf et al., 1994). Moreover, PRL as a factor regulating formation and destruction of CL seems to play a major role in modulating the physiological status of estrous, pregnancy and

lactation (Bowen et al.1996; Boy-Feysot et al., 1998; Risk et al., 2001). CL gets formed by induced luteinization of granulosa cells remaining in the postovulatory follicle (Freeman et al., 2000). The luteinization involves exit of the cells from the cell cycle, cellular hypertrophy, acquisition of the steroidogenic morphology, and expression of the cytochrome P450 cholesterol side chain cleavage. CL, which is a highly vascularized, transient endocrine organ, produces progesterone essential for uterine preparation and maintenance of pregnancy. Absence of progesterone signalling which is mediated via two isoforms of progesterone receptor, namely PR-A and PR-B result in the female infertility due to defects in ovulation with associated uterine inflammation and disruption of the mammary gland morphogenesis (Lydon et al. 1995). Knock out mutants for each isoform revealed essential role of PR-A in ovulation and uterine physiology, while PR-B was shown to be important for mammary gland development (Mulac-Jericevic et al. 2000, 2003).

Another ovarian hormone, a glycoprotein inhibin has been shown to be involved in the regulation of fertility. Expression of α and β subunits of inhibin is stimulated by FSH, while inhibin in the feedback loop negatively regulates FSH release (Coerver et al., 1996; Li et al., 1998). Inhibin is a member of TGFβ superfamily of growth factors, which includes bone morphogenic proteins and Müllerian inhibitory substance. Inhibin is a heterodimer and consists of a α subunit and either a β_A or β_B subunits (Risbridger et al., 2001). Both sexes of inhibin-deficient mutant mice generated by targeted mutation of inhibin α subunit gene developed gonadal sex-cord stromal tumors with very high penetrance, suggesting an important role of the protein in gonadal cell-cycle regulation (Matzuk et al., 1992, 1994, 1996; Coerver et al., 1996; Li et al., 1998). Additionally, Inhα deficient mice displayed increased level of FSH in blood (Matzuk et al., 1992), indicating regulatory role of inhibin in FSH release.

Primarily, the production and release of gonadotropins (FSH and LH) from the anterior pituitary are regulated by gonadotropin releasing hormone (GnRH), secreted from the specific neuronal populations of the hypothalamus (Wierman 1996; Neill 2002; Gore, 2002). The *hpg* (hypogonadal) mice of both sexes with a naturally occurring deletion in the GnRH gene are infertile with a reduction in the size of the gonads and accessory sex organs as well as a block in gametogenesis (Mason et al. 1986). GnRH is produced by a loose network of neurons (about 800 in rodents) located in the basal hypothalamus (Tobet et al., 2001). In rodents, GnRH cell bodies are distributed from the medial

septum and diagonal band of Broca to the ventral anterior hypothalamus (Smith et al., 2001). Major axonal projections of GnRH releasing neurons extend to the median eminence (ME) through periventricular and subventricular pathways and are relevant to the control of anterior pituitary functions. GnRH is secreted in pulsatile manner and is delivered by portal blood to the anterior pituitary; there it binds selectively to GnRH receptor (GnRHR) located on the surface of gonadotroph cells (Norwitz et al., 1999). GnRHR belongs to the family of GPCRs (Kakkar et al., 1992) and activates diverse signalling pathways in the anterior pituitary (Ruf et al., 2003). Coupling of GnRHR to Gq/11 proteins activates phospholipase C which transmits its signal to diacylglycerol (DAG) and inositol 1,4,5-trisphosphate (IP3) (Kraus et al. 2001, McArdle et al. 2002, Krsmanovic et al. 2003, Ruf et al. 2003). DAG activates the intracellular protein kinase C (PKC) pathway and IP3 stimulates the release of intracellular calcium. PKC activation in response to GnRH also leads to increases in the mitogen-activated protein kinase (MAPK) pathways including ERK1,2, ERK5, p38MAPK and JNK in pituitary cells (Kraus et al. 2001, McArdle et al. 2002, Ruf et al. 2003). The active MAPKs move to the nucleus where they activate a variety of transcription factors to modulate gene expression. These pathways then differentially regulate the synthesis and secretion of the LHβ and FSHβ subunits in the anterior pituitary, selectively modulating gonadotropin synthesis and/or release from pituitary cells.

Interestingly, GnRH secretion from the hypothalamic nerve terminals appears in pulsatile manner observed *in vivo* from rodents (Martinez de la Escalera et al., 1992; Wetsel et al., 1992; Weiner and Martinez de la Escalera,1993). An oscillatory GnRH release is modulated by exogenous signals such as adrenergic (Herbison et al., 1989; Herbison, 1997), glutamatergic (Brann and Mahesh, 1994), and GABAergic (Herbison and Dyer, 1991). Moreover, there is considerable evidence that the circadian biological clock is an important modulator of the GnRH secretion (Chapell et al, 2003).

GnRH pulsatile secretion induces cyclic changes in FSH and LH release from the pituitary (Lloyd et al., 1994). Thereby, alterations in FSH and LH secretion regulate secretory patterns of the steroid hormones estrogen and progesterone that induces recurring physiologic changes, named estrous cycle. Estrous cycles start after puberty in sexually mature females and are interrupted by anestrous phases. Lengths of estrous cycles are different among species and are determined primarily by duration of the luteal phase. Luteal phases of larger mammals are long compared to species of lesser body

stature. Small animals are subject to predation, and therefore have short non pregnant cycles. Moreover, they have short gestation and their offspring attain puberty quickly. In the table 1 an average length of estrous and estrous cycles of different species is presented in days.

SPECIES	ESTROUS	ESTROUS CYCLE
Mouse, Rat	0.5	4
Hamster	1	4
Guinea pig	0.5	16
Sheep	2	17
Horse	5	21
Elefant	4	22
Human	1	28

Table 1. Average length of an estrous and estrous cycle in different species

As it is shown in the table 1 an average length of estrous cycle in rodents takes four days and consists of four stages (Gordon, 1977): proestrous, estrous; metestrous and diestrous. During proestrous the CL regresses (progesterone declines) and a preovulatory follicle undergoes its final growth phase (estradiol increases). Ovulation usually occurs during estrous. Proestrous and estrous comprise the follicular phase. CL develops during metestrus and function at optimum during diestroues. Metestrous and diestrous make up the luteal phase. Thereby, fluctuations in the steroid hormone release induce changes in the vaginal cytology. Therefore, stages of an estrous cycle can be evaluated by monitoring of vaginal cytology (Fig.2). In the proestrus, largely small round, nucleated cells are present singly or in sheets and no leucocytes are present. In estrus hundreds of large cornified cells (squames) with degenerated nucleus can be observed. Towards the end of the estrous the smear becomes “cheesy” and masses of adherent cornified cells are present. In metestrous many leucocytes and few cornified cells can be observed. In the diestrous vaginal smear is strongly mucous with entangled many leucocytes and a few nucleated cells.

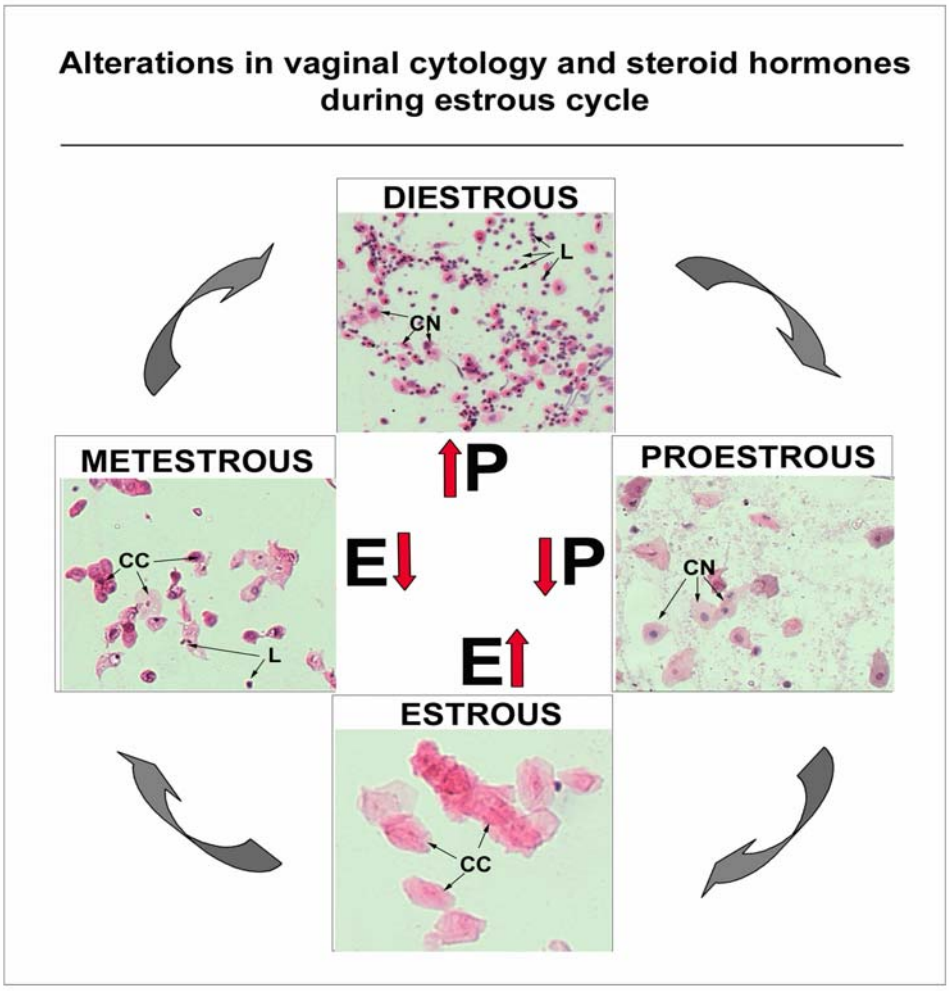

Fig. 2 Vaginal cytology at different stages of estrous cycle and fluctuation in steroid hormones
In proestrous largely small round, nucleated cells are present singly or in sheets. There are no leucocytes. The progesterone level starts to decline. In estrus– hundreds of large cornified cells (squames) with degenerated nucleus are present and estrogen level start to increase. In metestrous, many leucocytes and few cornified cells are present, estrogen level declines. In the diestrous - vaginal smear is strongly mucous with entangled many leucocytes and a few nucleated cells. The progesterone level increases.
Abbreviations: *CC* cornified cells; *CN* nucleated cells; *E* estrogen; *L* leucocytes; *P* progesterone

The reproductive organs also undergo changes during the estrous cycle influenced by cyclic hormonal changes. The oviducts and uterus are motile under the influence of estradiol; progesterone has the opposite effect. The endometrium undergoes proliferation during the follicular phase in response to rising circulatory titer of estradiol. Progesterone causes endometrial glands to become branched and secretory. Estradiol primes the endometrial response to progesterone (expressed during the luteal phase) by stimulating synthesis of receptors for progesterone (which inhibits synthesis of

receptors for estradiol). The cervix becomes dilated in the follicular phase and constricted in the luteal phase; correspondingly, cervical mucus is of either a watery or denser consistency. Each of the noted changes in the reproductive tract of the female has relevance to gamete transport and pregnancy.

2 RESULTS

The aim of this work was the phenotypic and functional analyses of neurochondrin (*Ncdn*) gene–trap mouse mutant. *Ncdn* gene-trap mutants were generated from the embryonic stem (ES) cell clone W044B06 (http://genetrap.de) trapped with the pT1*βgeo* gene trap vector. This clone was identified in the large-scale gene-trap screen at the Institute of Developmental Genetics, GSF. The endogenous expression of *Ncdn* was reflected by whole mount X-gal staining of the embryos and showed strong expression in the developing CNS (Fig.3).

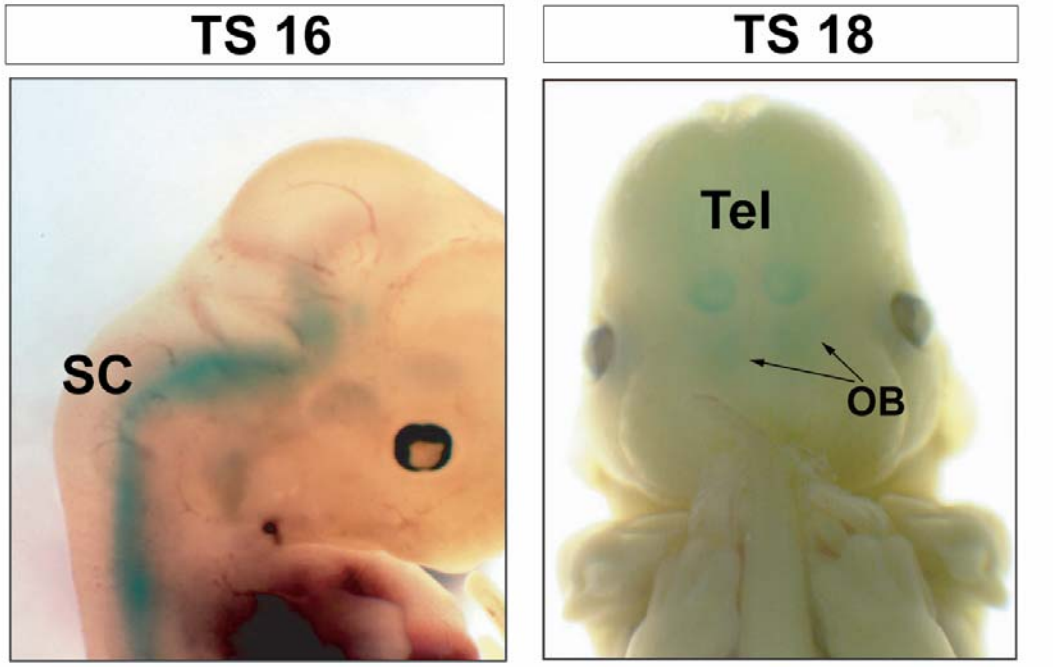

Fig.3 The expression of the *Ncdn/β-geo* fusion protein visualized by X-gal staining on the embryos TS 16 and TS 18

The primary expression analysis of the trapped *Ncdn* gene was performed by X-gal staining of the mutant embryos at TS 16 and TS18 (courtesy of Dr. T. Floss). The strong blue staining in the spinal cord, olfactory bulbs and telencephalon reflect the expression of the *Ncdn* gene in the CNS during embryonic development.

Abbreviations: *OB* olfactory bulb, *SC* spinal cord, *Tel* telencephalon

2.1 Establishment of the *Ncdn* gene-trap mouse line

2.1.1 The pT1*βgeo* gene-trap vector

Gene-trapping is a high throughput method in order to introduce insertional mutations across the mouse genome. Gene-trap vectors simultaneously mutate and report endogenous gene expression and provide DNA tags for the rapid identification of the trapped gene.

The pT1*βgeo* gene-trap vector, which was used for trapping of the *Ncdn* gene, contains a promotorless *β-galactosidase* (*β-gal*) gene from *E.coli* fused in frame with the *neomycin phosphotransferase* (*neo*) gene from *E.coli*. After integration into the genome the expression of the *neo* gene allows selection for expressed genes, while the *β-gal*-reporter is used for the primary expression analysis of the trapped gene. The *β-geo* reporter-selector cassette is flanked by an upstream 3' splice consensus sequence (splice acceptor from the mouse *Engrailed 2* gene) and a downstream polyadenylation site (polyA) from the simian virus (SV 40) (Wiles et al., 2000). Splice acceptor and polyA enable trapping even in case of intron integration. After determination of the vector integration site into the genome by 5'RACE analysis, the ES cell clone with the trapped gene of interest is used for the generation of the mouse mutant line.

2.1.2 The generation of the *Ncdn* mouse mutants

The trapped clone was injected into the blastocyte of C57BL/6N female mice followed by transfer into the *uteri* of pseudopregnant CD-1 foster mice. Due to the pluripotency of ES cells, the trapped allele of *Ncdn* gene can be transmitted into the germ line. Five chimaeras with more then 90% agouti coat colour were bred to C57 BL/6N mice. Agouti offspring was genotyped by southern blot analysis with internal *neo* probe on genomic DNA, digested with *HindIII* or *EcoRI* enzymes. The digestion with *HindIII* enzyme was used to determine a number of independent vector integrations, because *HindIII* restriction sites are lost after integration of the pT1*βgeo* vector. Using *EcoRI* cutting tandem integrations of the vector can be determined,

since the *EcoRI* restriction site is present in the *βgeo* cassette (Wiles et al., 2000). As a hybridisation control the *En1* probe was used. The *neo* probe was excised by *PstI* from the pKJ-1 vector (Adra et al., 1987) and the *En1* probe was created by digestion of the "ESEN1" vector (kindly provided by Dr. J. Guimera) with *EcoRI* and *SalI* enzymes. In the southern blot on the mutant DNA, digested with *HindIII* only one band (8 kb) corresponding to the mutant allele of the *Ncdn* gene was detected. The control band (6 kb) corresponding to the *En1* gene was present in all samples (Fig.2b). Similarly, the southern blot on the DNA, digested with *EcoRI* only one signal was determined (data not shown). These data indicated a single-copy integration of the pT1*βgeo* in the *Ncdn* gene. The heterozygous animals wined from the two of five chimeras were twice backcrossed to C57BL/6N mice and further bred to the homozygosity.

2.1.3. The pT1βgeo vector integrated in the 3'UTR region of the exon 7 of the *Ncdn* gene

According to the primary 5´RACE analysis the pT1*β-geo* gene-trap vector had integrated into the 3'UTR of *Ncdn* exon 7. In order to determine the genomic integration site a PCR analysis was performed on genomic DNA of the animals using primers inside of the 3'UTR of the exon7 sequence (F7 - forward primer) and the *β-gal* sequence (Lac2 - reverse primer) (Fig.4a). The sequencing of amplified PCR products revealed the integration of the gene-trap vector at 13.412 bp of *Ncdn* gene (NCBI: Mus musculus chromosome 4; Accession number: NT_109317), nucleotides inside of exon 7 between the stop and polyA signal.

To be able to distinguish between heterozygote and homozygote animals a genotyping triplex PCR established by N. Uez with own modifications was utilized (Fig.4a and c).

2.1.4 *Ncdn* homozygous mutants are viable and are born at mendelian ratio

Genomic DNA for the genotyping assay was isolated from mouse tails (4.3.1). The PCR products were amplified using primers F7 (forward primer in exon 7 prior to vector integration site), Lac2 (reverse primer inside of *β-gal*) and R7U (reverse primer in exon 7 after the vector integration site) and included 400 bp (wild type allele) and 620 bp fragments (mutant allele of the *Ncdn* gene) (Fig. 4c).

Genotyping of F2 offspring revealed the viability of *Ncdn* homozygous mutants. The progeny obtained from the *Ncdn* heterozygous mice followed the expected mendelian ratio, suggesting that the embryonic development of the *Ncdn* gene-trap mice is normal. The distribution of the pups of each genotype in 3 litters wined from heterozygous crosses was the following: 6 wild types (26 %); 12 heterozygous animals (52,2 %) and 5 homozygous animals (21,7 %).

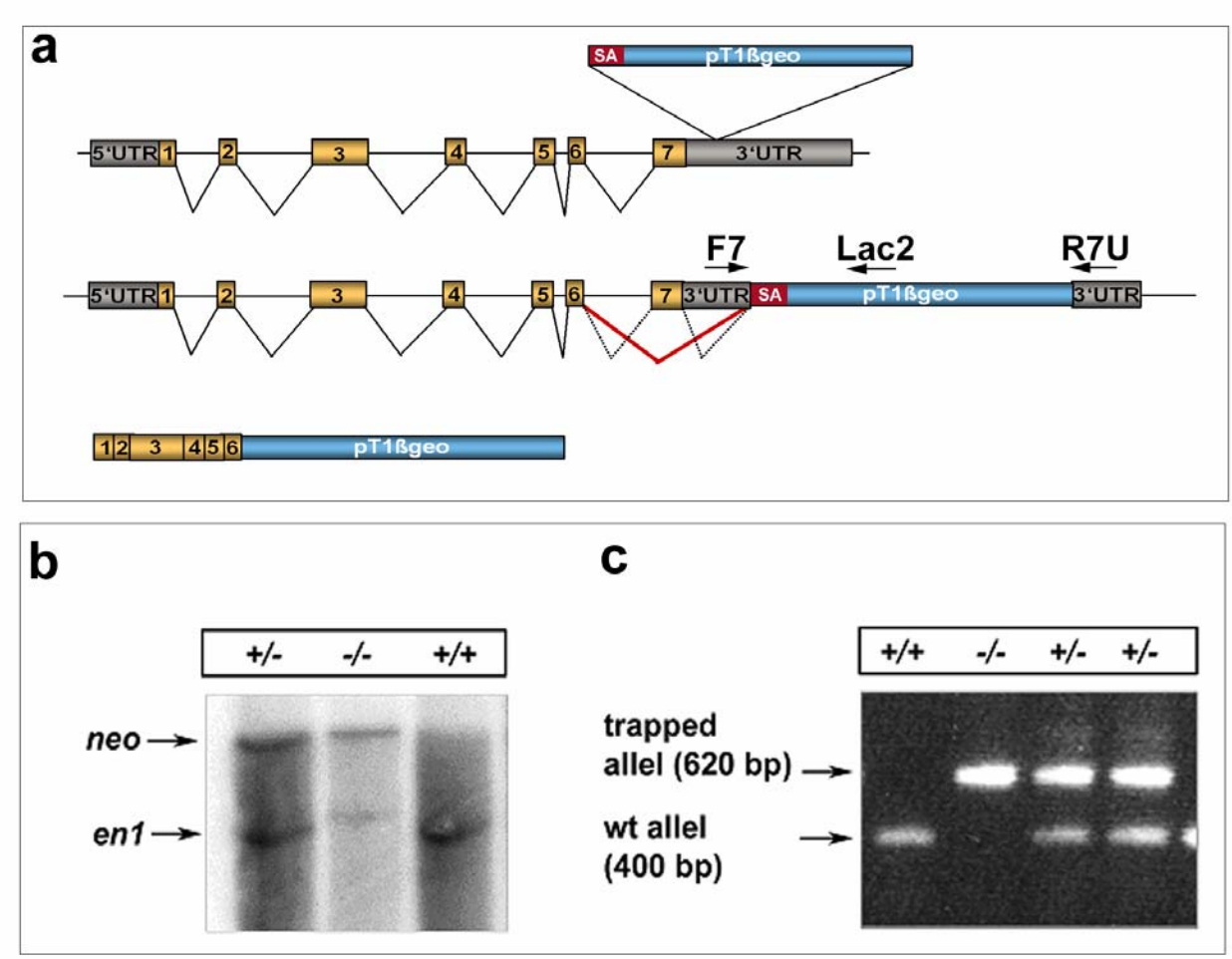

Fig.4 The pT1*β-geo* vector integrated in the 3'UTR of exon 7 of the *Ncdn* gene

Southern blot analysis was used for the genotypic of mutant mice. Genomic DNA was digested with *HindIII* and hybridised with *neo* (800 bp) and *En1* (760 bp) probes at the same time. In wild type DNA only one band was detected corresponding to *En1*. Two bands were observed corresponding to *neo* and *en1* in heterozygous and homozygous mutants (b). Triplex PCR analysis with primers designed homologous to 3'UTR sequence prior and behind the vector integration site (F7-forward, R7U-reverse primer) and homologous to the *β-gal* sequence of the vector (Lac2 reverse primer) (a). The amplified products with a size of 400 bp and 620 bp, corresponded to wild type and trapped alleles of *Ncdn* gene respectively (c).

2.2 Analysis of the *Ncdn* gene-trap mouse line

Ideally, gene-trap vectors with splice acceptors mutate an endogenous gene by splicing of the reporter/selector cassette to the exon adjacent to the vector integration site. Fusion transcripts from the mutated alleles are finally translated into fusion proteins.

In order to analyse if the vector insertion in the *Ncdn* gene resulted in truncation of the endogenous sequence and a fusion transcript which eventually get translated into a fusion protein, the RT-PCR and western blot analysis were performed.

2.2.1 Integration of the pT1*βgeo* resulted in the absence of exon 7 in the fusion transcript and accordant truncation of the C-terminal part in the fusion protein

RNA was prepared from adult brains of mice heterozygous and homozygous for the vector insertion by RT-PCR in order to analyse the mutant transcripts. Primers for RT-PCR were designed homologous to sequences of exon 6 (F6 - forward), exon 7 (R7 – reverse) and *β-gal* (LacZ –reverse) (Fig.5a). As expected, in the wild type only one RT-PCR product (460 bp) was amplified corresponding to the sequence between primers F6+R7 (wild type allele of the *Ncdn* gene). Similarly, in homozygous mutant only one RT-PCR product (1200 bp) corresponding to the trapped allele of the *Ncdn* gene was amplified, while in the heterozygous mice both RT-PCR products were present (Fig.5b). The amplified products were sequenced and confirmed the proper use of the splice acceptor of the vector. Additionally, there were no wild type transcripts detected in the mutant mice, indicating that no splicing around the vector occurred in the trapped allele of the *Ncdn* gene. Interestingly during transcription, the vector got spliced directly to exon 6, instead of expected splicing to the adjacent to the vector integration site exon 7. This resulted in the absence of the entire exon 7 sequence in the fusion transcript. Therefore it was concluded that exon skipping occurred due to the stronger splice acceptor of pT1*βgeo*, as related to *Ncdn* exon 7.

On the protein level the absence of the C-terminal part of the *Ncdn* protein (coded by exon 7) was verified by western blot analysis using a specific C-terminal *Ncdn* antiserum (kindly gift of Prof. K. Maruyama, Japan). This antiserum recognizes the last 5 amino acids (aa) of the C-terminal part of Ncdn protein. Total protein was isolated from adult brains and from the whole embryo (TS21) (5.7.1). As expected, a 79 kDa band corresponding to the wild type protein was observed only in samples isolated from wild type and heterozygous animals. No wild type protein was detected

in the homozygous mutants. These results confirmed the absence of exon 7 in the fusion transcript which results in the truncation of the C-terminal part in the Ncdn protein (Fig.5c). Thus, the mutant fusion protein lacks the C-terminal 145 aminoacids (Fig.5d).

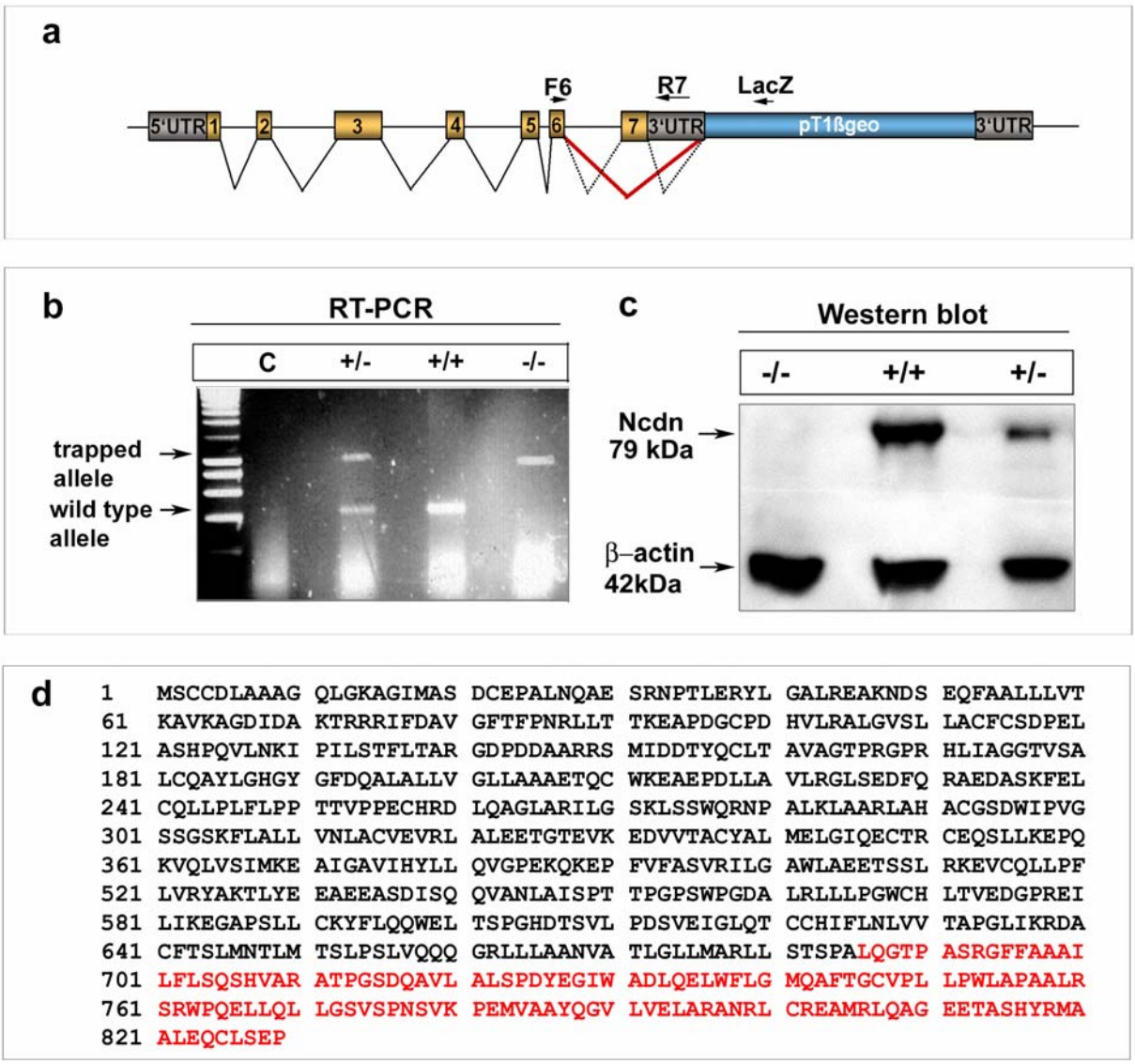

Fig.5 Absence of exon 7 in fusion transcript and fusion protein

The RT-PCR was done with primers designed homologous to exon 6 (F6 - forward primer); 3'UTR prior to vector integration site (R7-reverse primer) of *ncdn* gene and *β-geo* sequence (LacZ - reverse primer) of the vector (a). The amplified products corresponded to 1200 bp (trapped allele of *Ncdn* gene) and 480 bp (wild type allele). In the wild type and homozygous mutant only one band corresponded to 480 bp and 1200 bp respectively were observed. In the heterozygous mutant both products were present (b). The first lane is a negative control for the RT-PCR. The absence of the

terminal exon 7was demonstrated by western blot analysis with specific *Ncdn* C-terminal antiserum directed against last five amino acids of the protein. The wild type *Ncdn* (79 kDa) was detected only in protein extracts from wild type and heterozygous animals and not in the homozygous mutants. As a loading control staining with β-actin was used (c). The fusion protein lacks last 145 aa of the C-terminal part indicated in red (d).

In order to determine whether a fusion protein of *Ncdn* (exons 1 to 6) and the β-geo is formed western blot analysis with an N-terminal *Ncdn* antiserum (kindly provided by Prof. K. Maruyama, Japan) and a β–galactosidase (β–gal) antibody was performed. The N-terminal *Ncdn* antiserum recognizes first 5 aa of the N-terminal part of *Ncdn* protein. The β–gal antibody recognizes the β–gal protein encoded by *β-gal* reporter gene of the vector. Expectedly, using the β–gal antibody a fusion protein was detected only in heterozygous and homozygous mutants (Fig.6a). As a positive control for the β–gal antibody protein samples isolated from adult brains of the non-related gene-trap mouse mutant “BRUCE” were used (Hitz et al., 2005). As a loading control staining with the β-actin antibody was used.

Using an *Ncdn* N-terminal antibody the wild type and fusion proteins were detected. In total protein isolated from wild type animals only wild type protein and in homozygous mutants only the fusion protein with an expected molecular weight of 243 kDa corresponding to the predicted sum of the truncated *Ncdn* (exon 1 to 6, expected size 63 kDa) and the β-geo (corresponding size 180 kDa) were detected (Fig.6b).

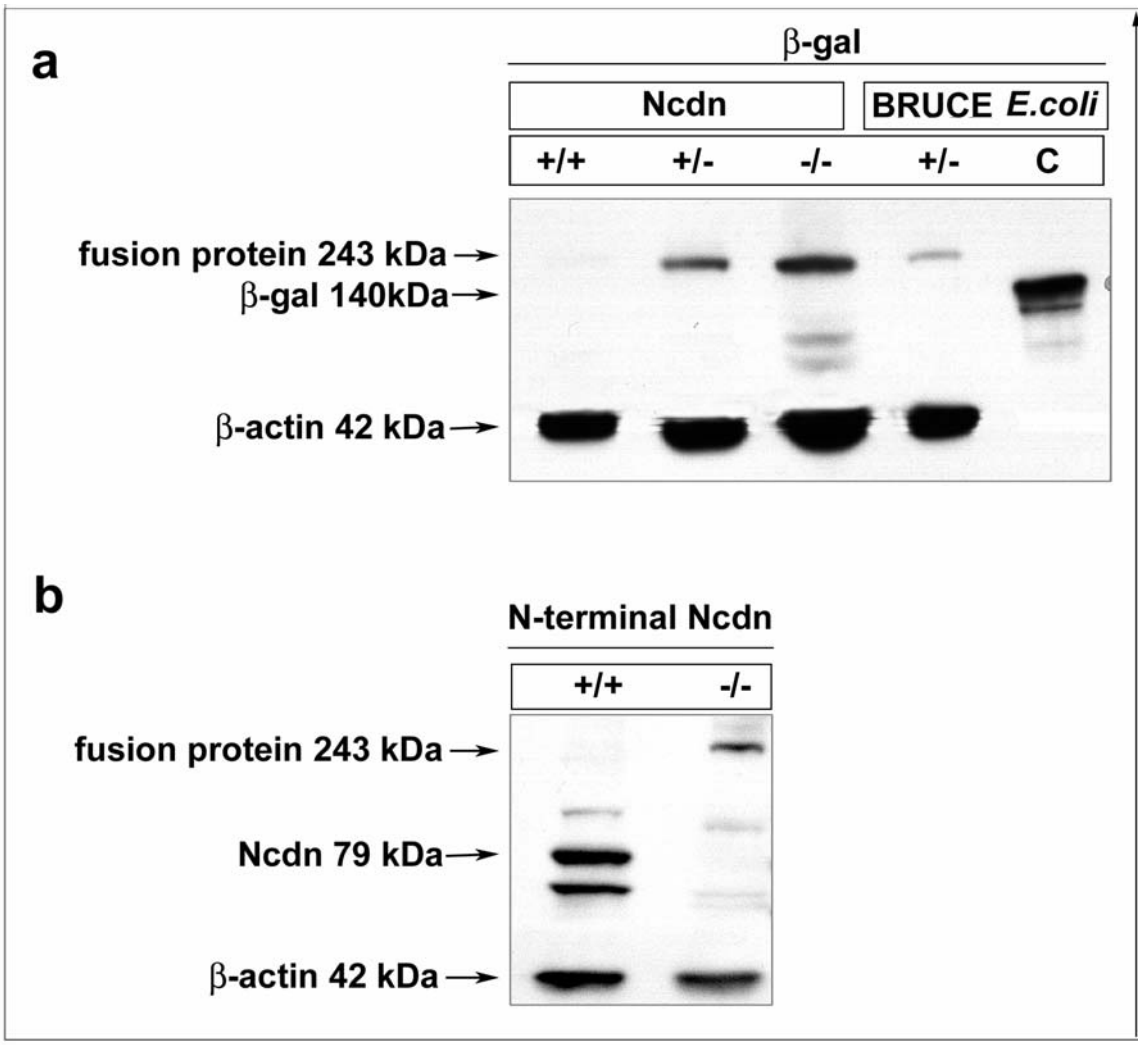

Fig.6 Fusion protein consist of truncated Ncdn and β-geo sequences

On the western blot loaded with total protein from the brain and incubated with the β-gal antibody only the *Ncdn/β-geo* fusion protein was detected in the *Ncdn* heterozygous and homozygous mice. As a positive control for β-gal staining, a protein extract from the homozygous "BRUCE" mutant mice and from the E.coli strain expressing *β-gal* were used (a). Using an *Ncdn* N-terminal antiserum in wild type a band corresponded to 79 kDa (wild type protein) and in the homozygous mice a band corresponding to 243 kDa (*Ncdn/β-geo* fusion protein) was detected. As a loading control the β-actin (42 kDa) was used.

In summary, the integration of the pT1*βgeo* gene-trap vector in the *Ncdn* gene resulted in the truncation of the exon 7 in the fusion transcript and the C-terminal part of the protein in the *Ncdn/β-geo* fusion protein respectively. The *Ncdn* gene-trap homozygous mutants are viable in contrast to embryonically lethal knock out mutants

supporting that truncation of the exon 7 resulted in the hypomorphic allele of *Ncdn* gene.

2.2.2 *Ncdn* is widely expresses in the CNS during embryogenesis and in the adult brain

The expression of the *Ncdn* gene during embryonic development was studied by *in-situ* hybridisation (ISH) of 8 µm thick paraffin sections (starting from Theiler stage (TS) 16 (corresponding to 10 dpc) to TS 26 (18dpc)) with *Ncdn* specific radioactively labelled riboprobe.

Ncdn starts to be expressed in the developing brain up to TS16. At TS18 *Ncdn* is strongly expressed in the ventral horn of the spinal cord, ventral mid/hindbrain and in the dorsal root ganglia (Fig.7 C, C', D, D'). At TS21, *Ncdn* expression was observed in more rostral brain regions such as the diencephalon (Fig. 7 A, A'). From this stage on, *Ncdn* is expressed in the developing cortical plate, the optic chiasm and in the olfactory bulb. In the developing eye *Ncdn* is strongly expressed in the elongated cell layer of the developing lens (Fig.7 A, A', B, B'). At this stage the expression in the ventral horn of the spinal cord and in dorsal root ganglia was still very strong (Fig.7 C, C', D, D'). Furthermore, the expression in cranial nerve ganglia was observed (data not shown). At TS26, *Ncdn* is expressed throughout the entire brain as decreasing gradient from caudal to rostral brain structures (Fig. 7 G, G'). At this stage strong expression in the developing cortex, piriform cortex, olfactory tubercle, striatum and even stronger in the lateral septum as well as in the developing hippocampus (Fig. 7 G, G', E, E') was detected. Also in the nuclei of the cranial nerves V (data not shown), VII and XII *Ncdn* was strongly expressed (Fig. 7 F, F').

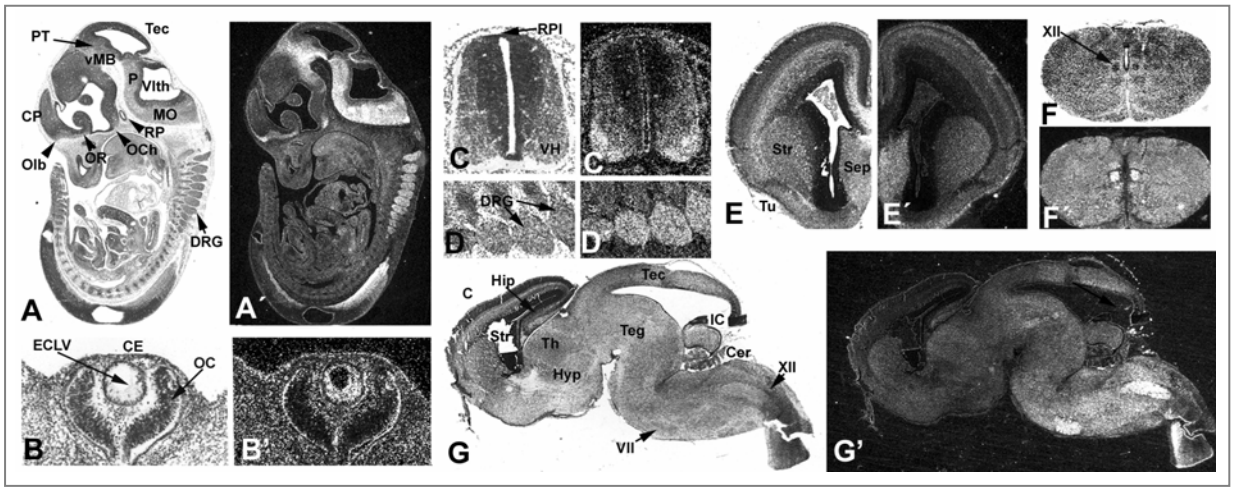

Fig.7 *Ncdn* expression at TS 21(A, B, C, D) and TS 26 (E, F, H, G)

The expression of the *Ncdn* gene was studied on 8 µm thick paraffin section of TS 21 whole embryo and on the brain of a TS 26 embryo with ISH using a *Ncdn* riboprobe. At TS 21 *Ncdn* was strongly expressed in ventral midbrain, pons, medulla oblongata, tectum, olfactory pit, Rathke's pouch (A,A'), dorsal root ganglia and ventral horn of the spinal cord (A, A'; C, C', D, D'). Strong expression was detected in the elongated cell layer of the developing lens (B, B'). At later stage TS 26 *Ncdn* is still strongly expressed in the brain with decreasing gradient from caudally to rostrally (G, G'). Strong expression was detected in the septum (E, E'), hypothalamus, tegmentum, tectum and in the nuclei of the cranial nerves VII and XII (G, G', F, F').

Abbreviations: *IVth* fourth ventricle, *VII* facial nucleus; *XII* hypoglossal nucleus, *C* cerebral cortex, *CE* corneal ectoderm, *Cer* cerebellum, *CP* cortical plate, *DRG* dorsal root ganglia, *ECLV* elongated cells of posterior wall of lens vesicle, *Hip* hippocampus, *Hyp* hypothalamus, *MO* medulla oblongata, *OC* optic cup, *OCh* optic chiasm, *Olb* olfactory lobe of the brain, *OR* optic recess, *P* pons, *PT* pretectal area, *RP* residual lumen of Rathke's pouch, *RPl* roof plate of the spinal cord, *Sep* septum, *Str* striatum, *Tec* tectum, *Teg* tegmentum, *Th* thalamus, *Tu* olfactory tubercle, *vMB* ventral midbrain, *VH* ventral horn of the spinal cord.

In the adult brain *Ncdn* is equally strong expressed in for-, mid- and hindbrain (Fig.8 A, A', B, B', C, C'). In the forebrain *Ncdn* expression was observed in the mitral and granule cell layers of the olfactory bulb (Fig. 8 G, G'), which project to the olfactory cortex and are mainly involved in olfaction. In the cortex *Ncdn* is expressed in all areas with the strongest signal in layers II and VI (Fig.8 J, J'). *Ncdn* is strongly expressed in the striatum, the core and shell of the nucleus accumbens, the islands of Calleja and in the piriform cortex (Fig.8 A, A', B, B', C, C'). Furthermore, *Ncdn* is expressed in all structures of the limbic system: hippocampus, amygdala and hypothalamus. In the hippocampus *Ncdn* expression is mostly restricted to the

granule cell layer of dentate gyrus, CA1–CA3 fields and hilus (Fig.8 H, H'). In the amygdala strongest *Ncdn* expression was observed in the central amygdaloid nucleus (Fig.8 B, B', C, C'). In the hypothalamus the strongest signal were observed in the paraventricular, ventromedial and arcuate nuclei (data not shown). In the thalamus *Ncdn* expression is restricted to the medial geniculate nucleus (Fig.8 C, C'). In the mid/hindbrain region *Ncdn* is strongly expressed in the intermediate layer of the superior colliculus, pons and dorsal cortex of the inferior colliculus (Fig.8 D, D'). In the cerebellum expression was restricted to the cerebellar nuclei and Purkinje cell layer in the cerebellar cortex (Fig.8 E, E', K, K'). In the caudal hindbrain *Ncdn* is expressed in sensory nuclei of the trigeminal nerve, motor and sensory nuclei of the facial nerve, hypoglossal nerve nuclei and cuneate nuclei (Fig.8 E, E', F, F' and data not shown). On the cellular level *Ncdn* was expressed specifically by large neurons.

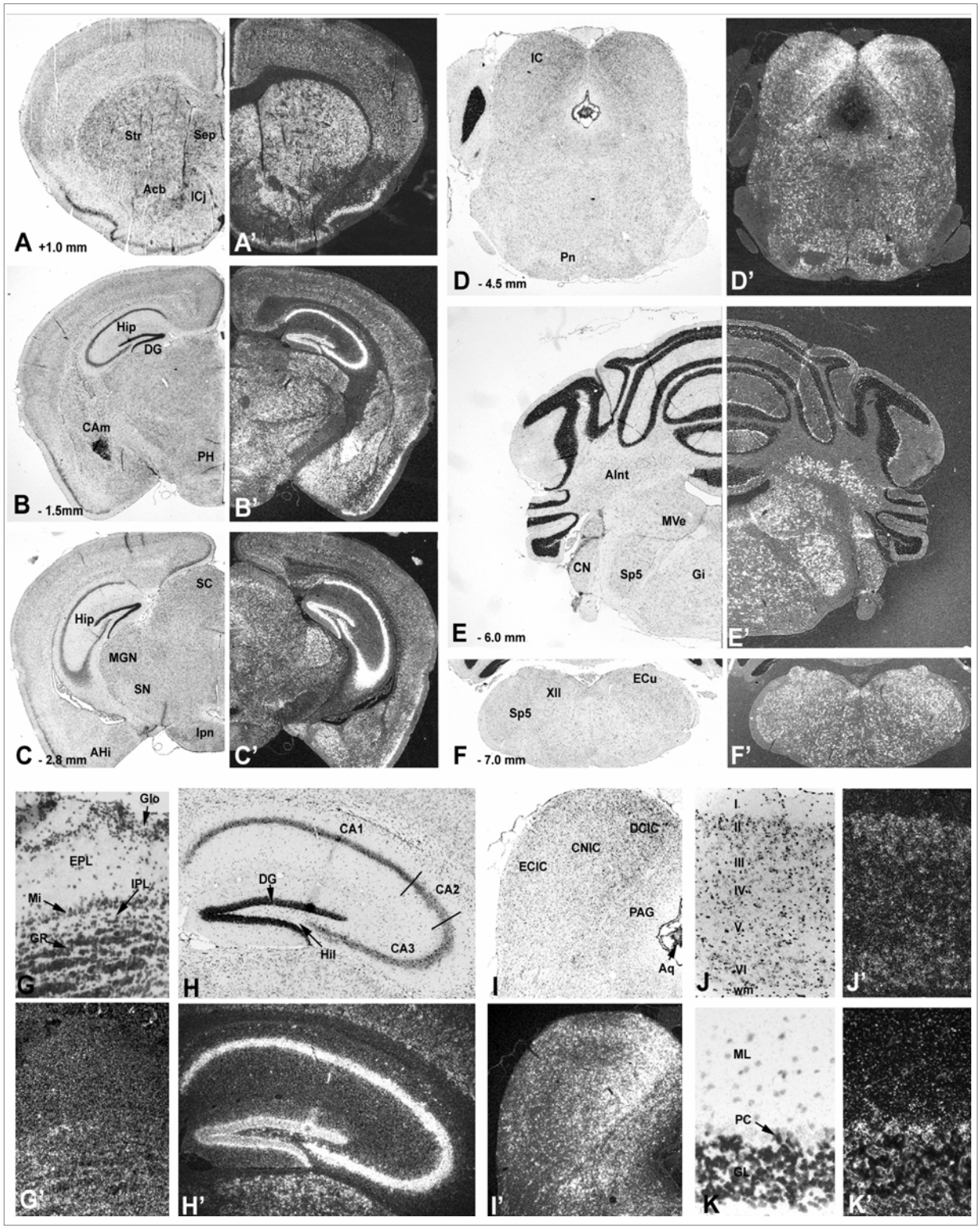

Fig.8 *Ncdn* expression in the adult brain

Ncdn expression in adulthood was studied by ISH on 8 µm thick coronal sections of the adult brains with an *Ncdn* riboprobe. *Ncdn* is strongly expressed in the mitral and the granular cell layers of olfactory bulb (G, G´). It is expressed in all areas of cortex with strongest signal in layer II and VI (J, J'). Strong signals were observed in the striatum, cortex medial septum, nucleus accumbens, islands of Calleja (A, A', B, B', C, C'). Also the amygdaloid complex shows strong *Ncdn* expression with a

prominent expression domain in the central nucleus of the amygdala (B,B').In the hippocampus, the signal is mostly restricted to the pyramidal cells of the hippocampal proper and granule cells of the dentate gyrus and hilus (H,H'). The thalamus shows restricted expression in specific nuclei with the strongest expression observed in the medial geniculate nucleus (C, C'). In the mid-/hindbrain region strongest expression was observed in the intermediate layer of superior colliculus, pons and dorsal cortex of the inferior colliculus (D, D', E, E'). In the cerebellum, expression was restricted to cerebellar nuclei and the Purkinje cell layer (E, E', K, K'). In caudal hindbrain strong signals were observed in sensory nuclei of the trigeminal nerve, motor and sensory nuclei of the facial nerve, nucleus of the hypoglossal nerve and cuneate nucleus (E,E',F,F').

Abbreviations: *I*, *II*, *III*, *IV*, *V*, *VI* Cortical layers; *XII* hypoglossal nucleus, *Acb* accumbens nucleus, *AHi* amygdalohippocampal area, *AInt* anterior interposed nucleus, *Aq* aqueduct, *CA1–3* subfields of hippocampus proper, *CAm* central amygdoloid nucleus, *CN* cochlear nucleus, *CNIC* central nucleus of inferior colliculus, *DCIC* dorsal cortex of inferior colliculus, *DG* dentate gyrus, *ECIC* external cortex of inferior colliculus, *ECu* external cuneate nucleus, *EPL* external plexiform layer of olfactory bulb, *Gi* gigantocellular reticular nucleus, *GL* granular layer, *Glo* glomerular cell layer of olfactory bulb, *GR* granular cell layer of olfactory bulb, *Hil* hilus, *Hip* hippocampus, *IC* inferior colliculus, *ICj* islands of Calleja, *IPL* internal plexiform layer of olfactory bulb, *Ipn* interpeduncular nucleus, *MGN* medial geniculate nucleus, *Mi* mitral cell layer of olfactory bulb, *ML* molecular cell layer, *Mve* medial vestibular nucleus, *PAG* periaqueductal gray, *PC* Purkinje cell layer, *PH* posterior hypothalamic area, *Pn* pontine nucleus, *SC* superior colliculus, *Sep* septum, *SN* substantia nigra, *Sp5* spinal trigeminal nucleus, *Str* striatum, *wm* white matter.

2.2.3 The X-gal staining of the reporter gene reflects expression of the *Ncdn* gene

To study the expression of the reporter gene (*β-gal*) the X-gal stain (4.9.3) was performed on 40 µm thick coronal cryosections of adult brains and TS 21 embryos. The expression of the integrated *β–gal* reported gene is dependent on the activity of endogenous promoter and can be detected by the X-gal staining. Therefore, the expression domains of the reporter gene turned blue due to enzymatic activity of *β-galactosidase* reflected the expression pattern of the *Ncdn* gene detected by ISH (Fig.9).

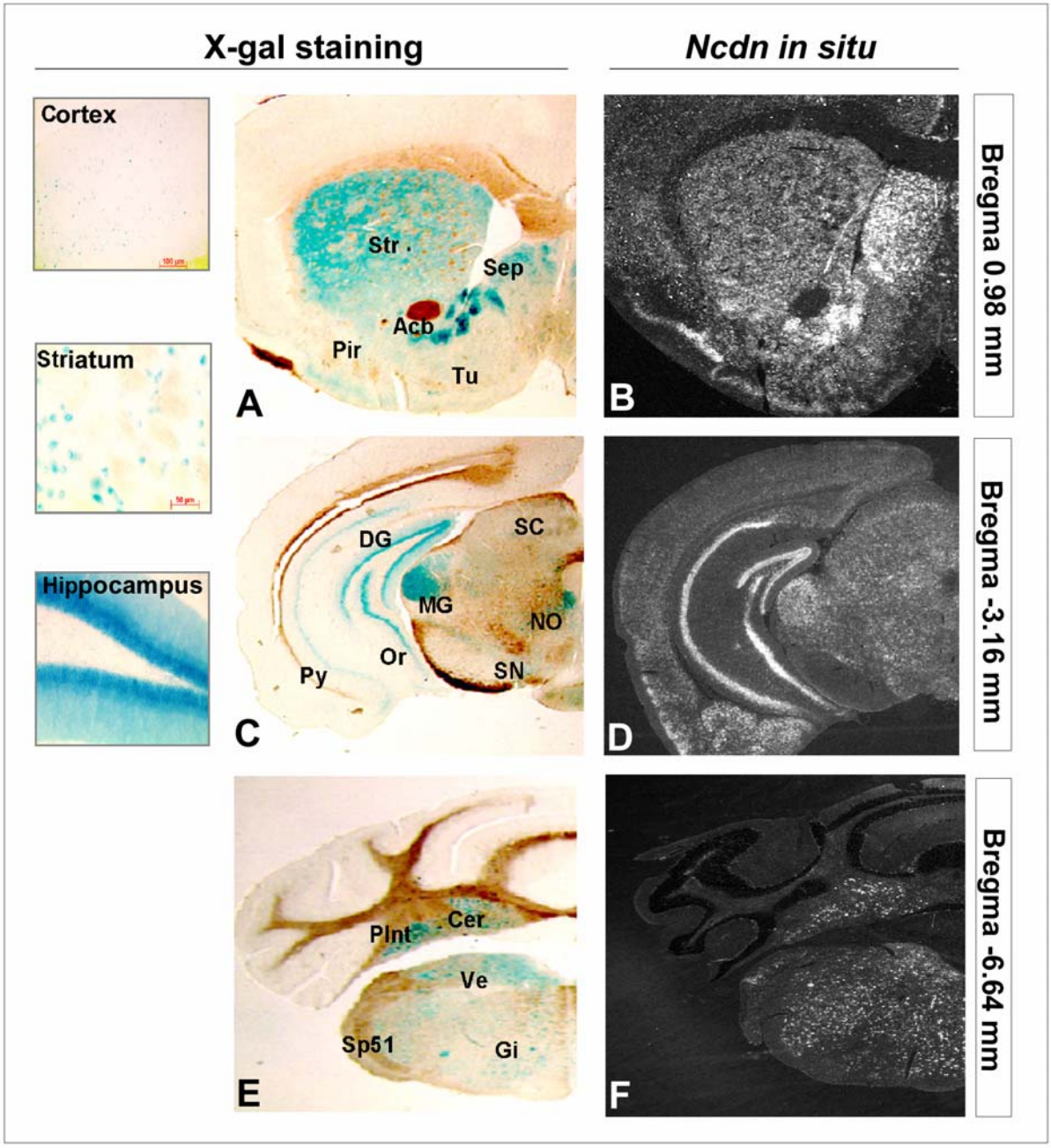

Fig. 9 X-gal staining reflects the *Ncdn* expression studied by ISH

The X-gal stain performed on 40µm thick cryosections of adult brains corresponded to the *Ncdn* expression detected by ISH. Strong X-gal activity was observed in the same domains were *Ncdn* is expressed, such as the striatum, septum, nucleus accumbens, olfactory tubercle, hippocampus, medial geniculate nuclei, superior colliculus, pyriform cortex, sustantia nigra, nucleus oculomotorius, cerebellar nuclei, vestibular nuclei, gigantocellural niclei. On the magnified pictures of the cortex, striatum and dentate gyrus strong blue staining was detected in the cell cytoplasm.

Abbreviations: *Acb* accumbens nucleus, *Cer* Cerebral nucleus; *DG* dentate gyrus, *Gi* gigantocellular reticular nucleus*; Hip* hippocampus, *MG* medial geniculate nucleus, *NO* nucleus oculomotorius; *Or*

Orient layer of hippocampus; *PC* Purkinje cell layer, *PInt* posterior interposed nucleus; *PH* posterior hypothalamic area, *Pn* pontine nucleus, *Py* pyriform cortex; *SC* superior colliculus, *Sep* septum, *SC* superior colliculus; *SN* substantia nigra, *Sp5* spinal trigeminal nucleus, *Str* striatum, *Tu* Olfactory tubercle; *Ve* vestibular nucleus

2.2.4 The major structures of the brain appeared morphologically not changed in the *Ncdn* mutant mice

The widespread expression of *Ncdn* in the developing and adult mouse brain suggested a possible involvement of it in the maintenance of neuronal populations. The integrity of the major brain structures and cell populations was analysed with a range of histochemical and immunohistochemical stains such as Nissl, Calbindine, Parvalbumin and AChE.

The Nissl stain is used to visualize brain morphology. The Nissl stain colours RNA in the Nissl bodies that are formed by clumps of ribosomes attached to portions of the endoplasmatic reticulum (raw endoplasmatic reticulum).

Staining with acetylcholine esterase (AChE) is used to visualize the cholinergic system. The AChE is a key enzyme of the cholinergic system, beside of choline acetyl transferase (ChAT), it is active in synaptic clefts of the cholinergic synapses. AChE cleaves neurotransmitter acetylcholine into constituents, acetate and choline, thus limiting the size and duration of the postsynaptic potential. The brain domains expressing AChE stain dark brown.

Immunostaining with a calbindin antibody is used to visualize the Purkinje neurons and their dendritic architecture. The parvalbumin antibody also detects a specific population of GABAergic interneurons which are thought to play a role in maintaining of the balance between excitation and inhibition in the cortex as well as the hippocampus.

No obvious morphological changes were detected in the brain structures, the cholinergic and GABAergic neuronal network was intact and the number and distribution of the Purkinje neurons were not changed in the homozygous mutants compared with their wild type littermates (Fig.10).

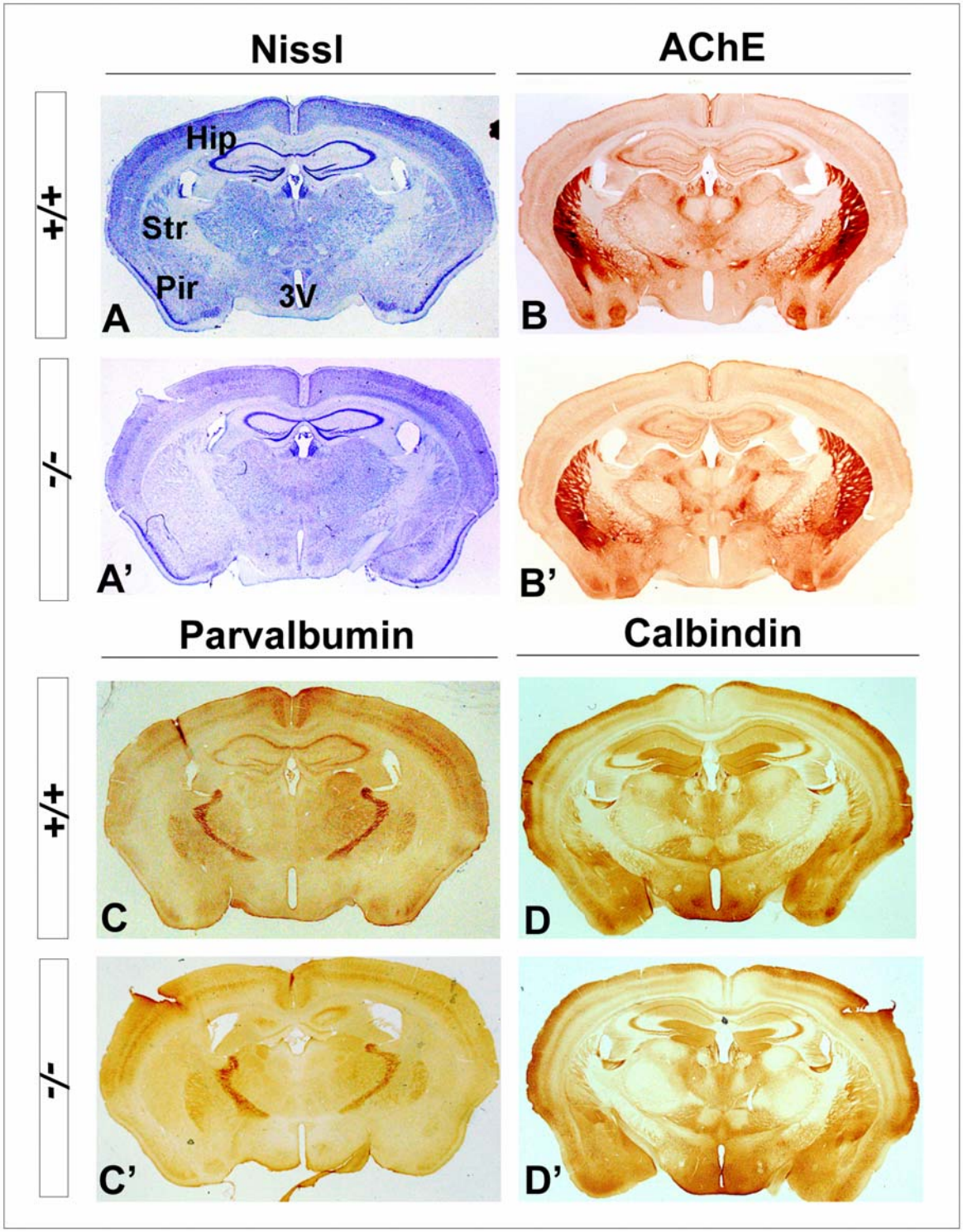

Fig.10 Nissle, AChE, Parvalbumin and Calbindin staining revealed no morphological changes in the brain archirecture of homozygous mutants

Nissle (A, A'), AChE (B, B'), Parvalbumin (C, C') and Calbindin (D, D') stains were performed on coronal 8 µm paraffin sections of the adult brains. No obvious differences in the main brain structures between homozygous mutants (A', B', C', D') and wild type mice (A, B, C, D) were observed.

Abbreviations: *3V* 3rd ventricle*; C* cortex; *Hip* hippocampus, *Str* striatum, *Pir* piriform cortex

2.2.5 Subfertility of *Ncdn* homozygous females

The fertility of heterozygous and homozygous *Ncdn* mutant mice was analysed by breeding of heterozygous and homozygous animals (n=5) during 8 month with a fertile partner. Heterozygous animals of both sexes and homozygous males were fertile (number of pups 6 to 8 from each mating). Homozygous females did not produce any offspring after 8 month of mating, indicating a fertility problem, while the disturbance in sexual behaviour was excluded due to observed seminal plugs. In order to understand reasons underlying the fertility problems of homozygous female mice, further the structural and functional integrity of reproductive organs, ovulation, estrous cycle and hormonal status were analysed.

The ovarian morphology analysed by hematoxilin-eosin (HE) staining of 8 µm thick paraffin sections (n=5). Follicles at all maturation stages and CL were present in the ovaries of homozygous mice. The oocytes in the follicles were surrounded by layers of the granulosa and theca interna cells (Fig.11).

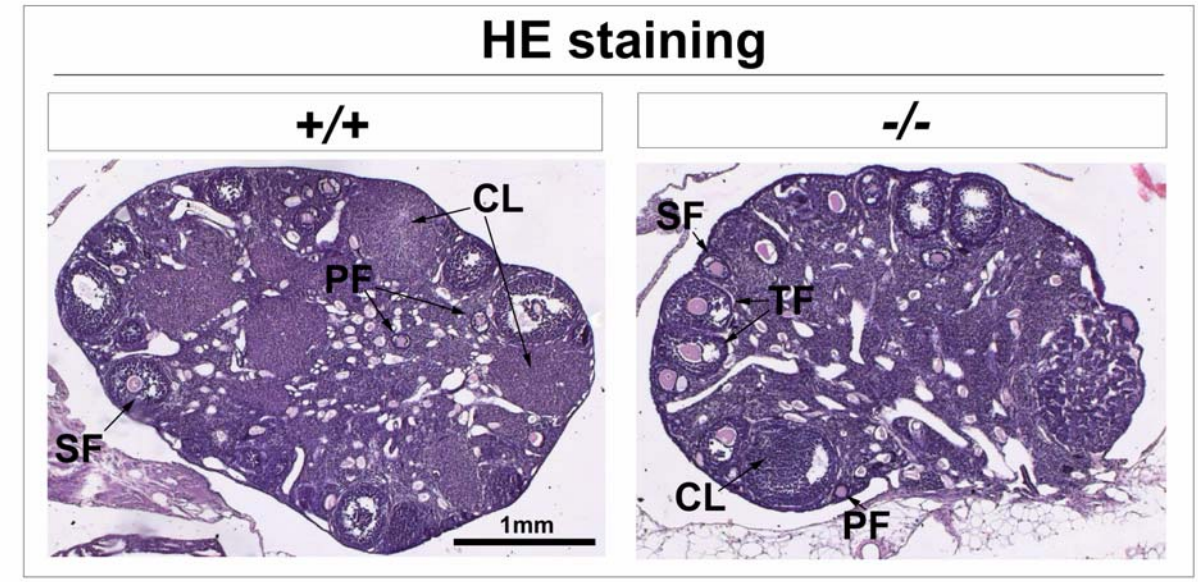

Fig.11 Hematoxilin-eosin staining of the ovaries

In the ovaries of wild type (A) and homozygous mutant mice (B), HE staining revelaed no obvious morphological differences between wild type (A) and homozygous (B) mutants were observed. The follicles at all stages of maturation (primary, secondary and tertial follicles) and also the corpora lutea were present in the ovaries of homozygous mutant females.

Abbreviations: *CL* corpora lutea; *PF* primary follicle; *SF* secondary follicle; *T*-tertial follicle

Since the ovaries of homozygous females appeared to be morphologically intact, in the next step the ovulation from the ovaries of naturally mated *Ncdn* homozygous females was analysed. Homozygous females and their wild type littermates (9 to 10 month old) were mated with fertile males. Only females with seminal plugs were sacrificed, the oocytes and zygotes were flushed out of oviducts, treated with hyaloronidase (Sigma; 100 µl type IV-S; 10 mg/ml) at 37^0 C for 5 min for dissociation from cumulus cells and counted. No oocyte and zygote ovulated from the ovaries of homozygous female mutants were detected in contrast to their wild type littermates (Fig. 12). Data were analysed by one-way analyses of variance (one-way ANOVA or two-way ANOVA). Post-hoc analysis was conducted using Student-T test. Data presented in the figure is mean ±S.E.

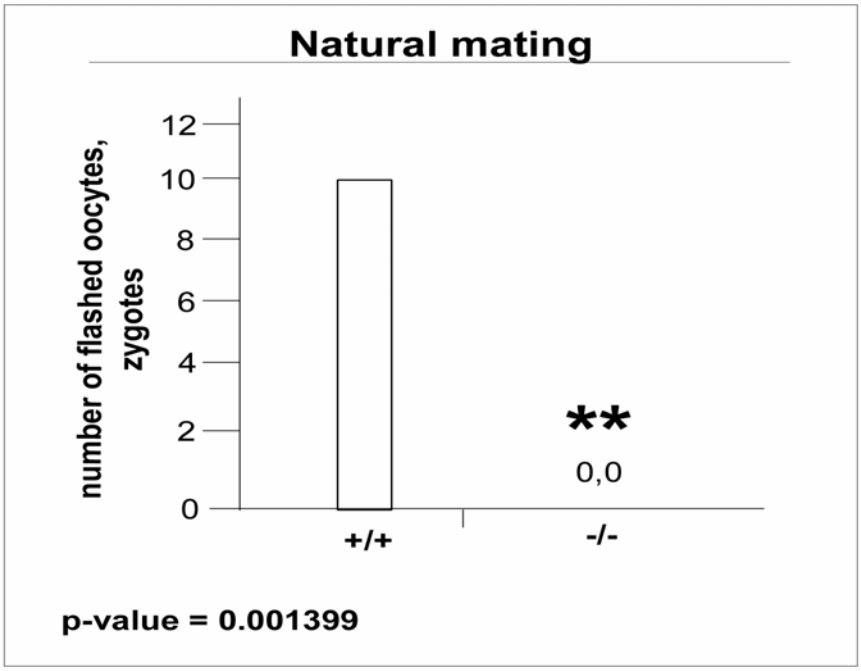

Fig. 12 Subfertility of the homozygous females is caused by ovulation failure

The mean number of the zygotes flushed from the oviducts is indicated on the Y-axis. There were no zygotes present in the naturally mated homozygous females (n=10) in contrast to their wild type littermates (9.5±0.957; n=4). The t-Test revealed a p-value of 0.001.

This indicated the ovulation failure of *Ncdn* homozygous females resulting in the subfertility. The main reasons causing impaired ovulation are non functional ovaries or disturbed estrous cycle. The functionality of ovaries was examined by analysing of

the ovarian response to external gonadotropins resulting in the induced ovulation. For this purpose animals were injected with Pregnant Mare's Serum gonadotropin (PMSG), which mimics follicle stimulating hormone (FSH) and with human Chorionic Gonadotropin (hCG), which action is similar to luteinising hormone (LH). PMSG stimulates follicular growth and hCG trigger ovulation and luteinization. Nine to ten moth old females were injected with 0,15 ml of PMSG and after 48 h with 0,15 ml of hCG. On the next day, ovulated oocytes were flushed from sacrificed animals and counted. Interestingly, the number of the ovulated oocytes, flushed from the homozygous females (n=9) was equal to the number of oocytes flushed from the heterozygous (n=3) and wild type littermates (n=5), indicating a positive response to the external hormonal stimulation (Fig. 13). Data were analysed by one-way ANOVA. Post-hoc analysis was conducted using Student-T test. Data presented in the figure are mean ±S.E.

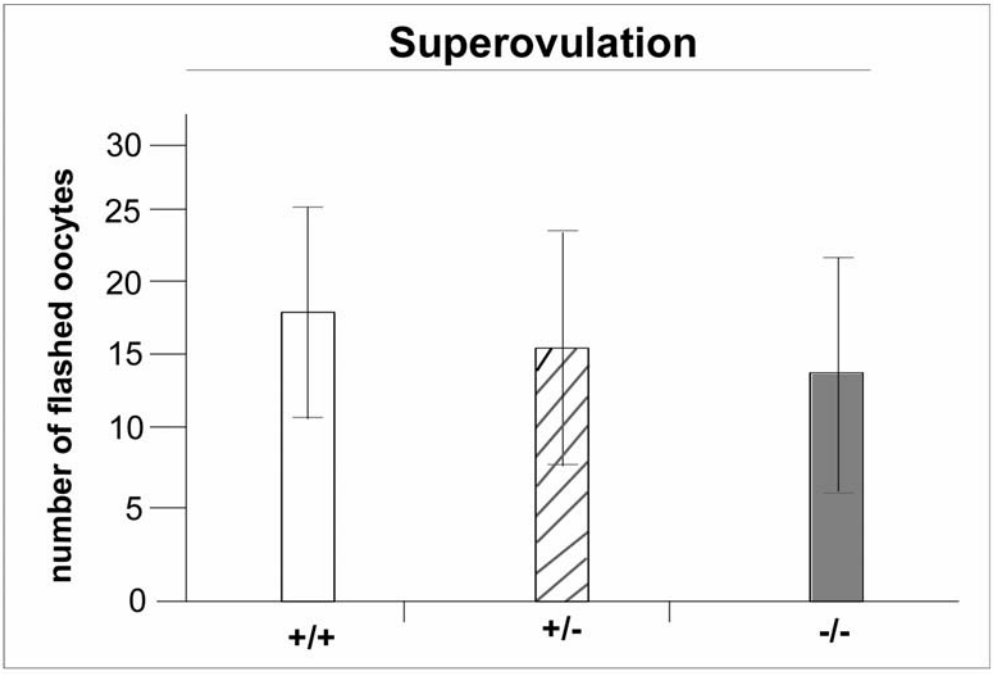

Fig. 13 Ovulation in the homozygous females can be induced by hormonal treatment

The number of ovulated oocytes is indicated on the Y-.axis. On the X-axis mice with different genotype which were injected IP with PMSG and hCG (0,15 ml each per mice). The number of the ovulated oocytes flushed from homozygous females (15.667±4.981; n= 9) was similar to the number of the ovulated oocytes flushed from heterozygous (17.333±7.535; n=3) and wild type (18.400±6.185; n=5) females.

The estrous cyclicity was analysed by evaluation of changes in the vaginal cytology. The vaginal smears were taken by flushing of the vaginal cells with a PBS. The smears were fixed shortly in the methanol, air dried and stained with HE (Fig.14). In the proestrus largely small round, nucleated cells are present singly or in sheets and no leucocytes are present (Fig.14 A). In estrus hundreds of large cornified cells (squames) with degenerated nucleus can be observed (Fig.14 B). Towards the end of the estrous stage the smear becomes “cheesy” and masses of adherent cornified cells are present. In metestrous (Fig.14C) many leucocytes and few cornified cells can be observed. In the diestrous vaginal smear is strongly mucous with entangled many leucocytes and a few nucleated cells (Fig.14 D).

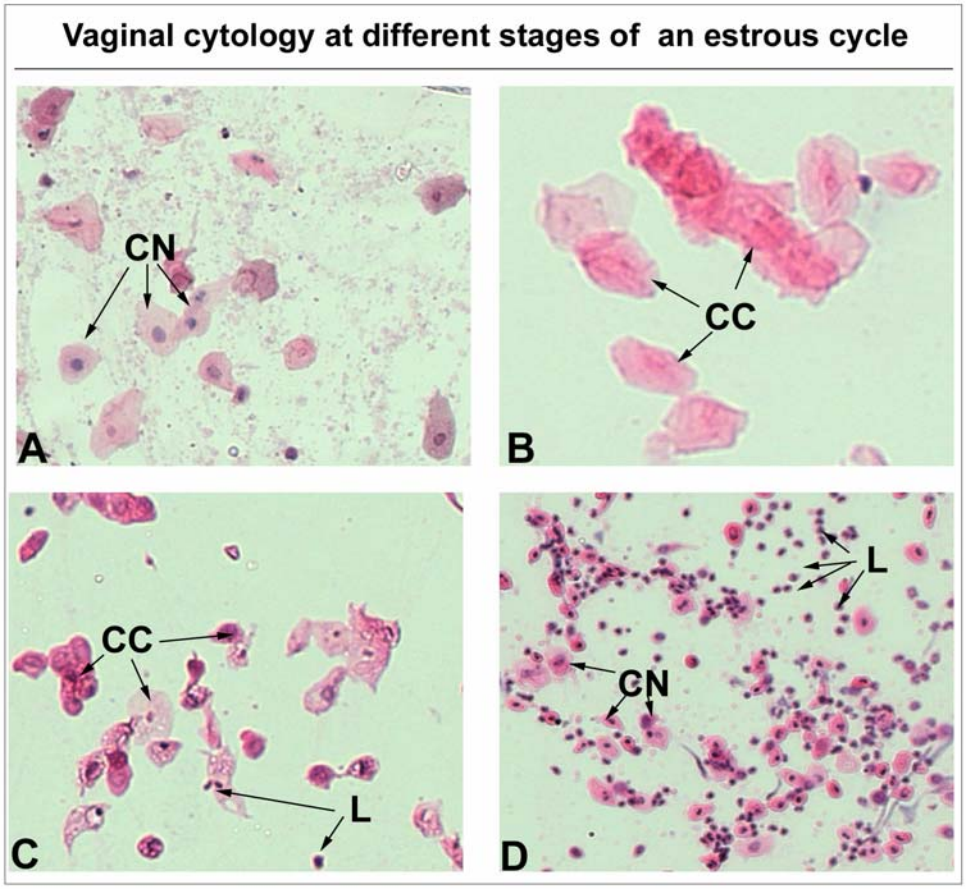

Fig. 14 Hematoxilin-eosin staining of vaginal smears

In proestrous (A) largely small round, nucleated cells are present singly or in sheets. There are no leucocytes. In estrus (B) – hundreds of large cornified cells (squames) with degenerated nucleus are present. In metestrous (C) – many leucocytes and few cornified cells are present. In the diestrous (D) vaginal smear is strongly mucous with entangled many leucocytes and a few nucleated cells.

Abbreviations: *CC* cornified cells; *CN* nucleated cells; *L* leucocytes

Vaginal smears were taken during 13 days from nine to ten month old females which were singly housed (n=10), to avoid synchronisation of the estrous cycle in group-housed females. Analysis of vaginal smears revealed irregular estrous cycle in *Ncdn* homozygous females with prolonged diestrous, which lasts in some animals until seven days (Fig.15). In contrast estrous cycle in the wild type littermates repeated every 4th or 5th day. This finding indicated possibly perturbed hormonal balance in *Ncdn* homozygous females.

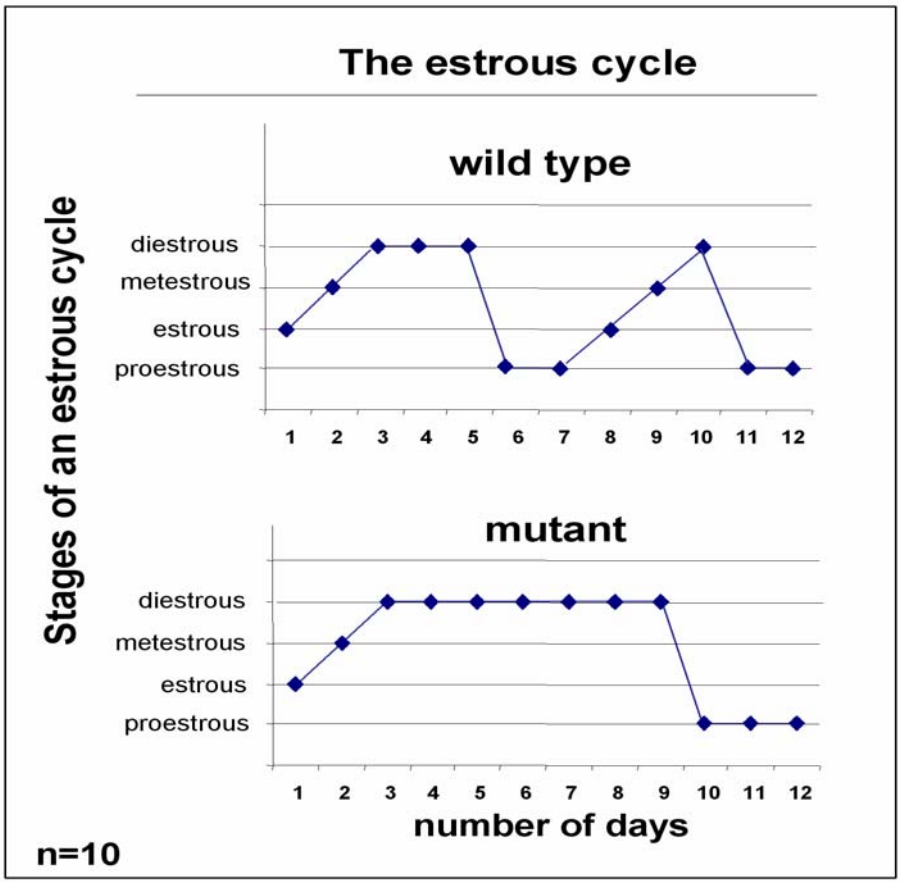

Fig.15 Homozygous females cycle irregularly

The homozygous female mice (n=10) were tested for duration and regularity of the estrous cycle. Vaginal smears were taken daily at the same time within 13 days. On the X-axis's number of the days and on the Y- axis's stages of an estrous are depicted. All ten tested homozygous female mice displayed an irregular estrous cycle. In five of them the diestrous lasted five to seven days in contrast with two to three day diestrous length in wild types.

The ovarian function including follicular maturation, ovulation and corpus luteum formation is regulated by hormones FSH, LH and prolactin (PRL). FSH, LH and PRL

are secreted from the gonadotroph and lactotroph cells of the anterior pituitary and get released into the circulating blood. The blood content of FSH LH and PRL was measured using radioimmunoassay (RIA) by Dr. T. Hämäläinen, Turku, Finland. The trunk blood samples were taken from nine to ten months old homozygous females (17 animals) and their wild type littermates (14 animals) at diestrous. Interestingly, the FSH and PRL levels in the blood of homozygous females were altered, while the level of LH was not changed. FSH was increased and the PRL was decreased in the trunk blood of homozygous females compared with their wild type littermates (Fig.16). Data were analysed by one-way or two-way ANOVA. Post-hoc analysis was conducted using Student-T test. Data presented in the figures are mean ±S.E.

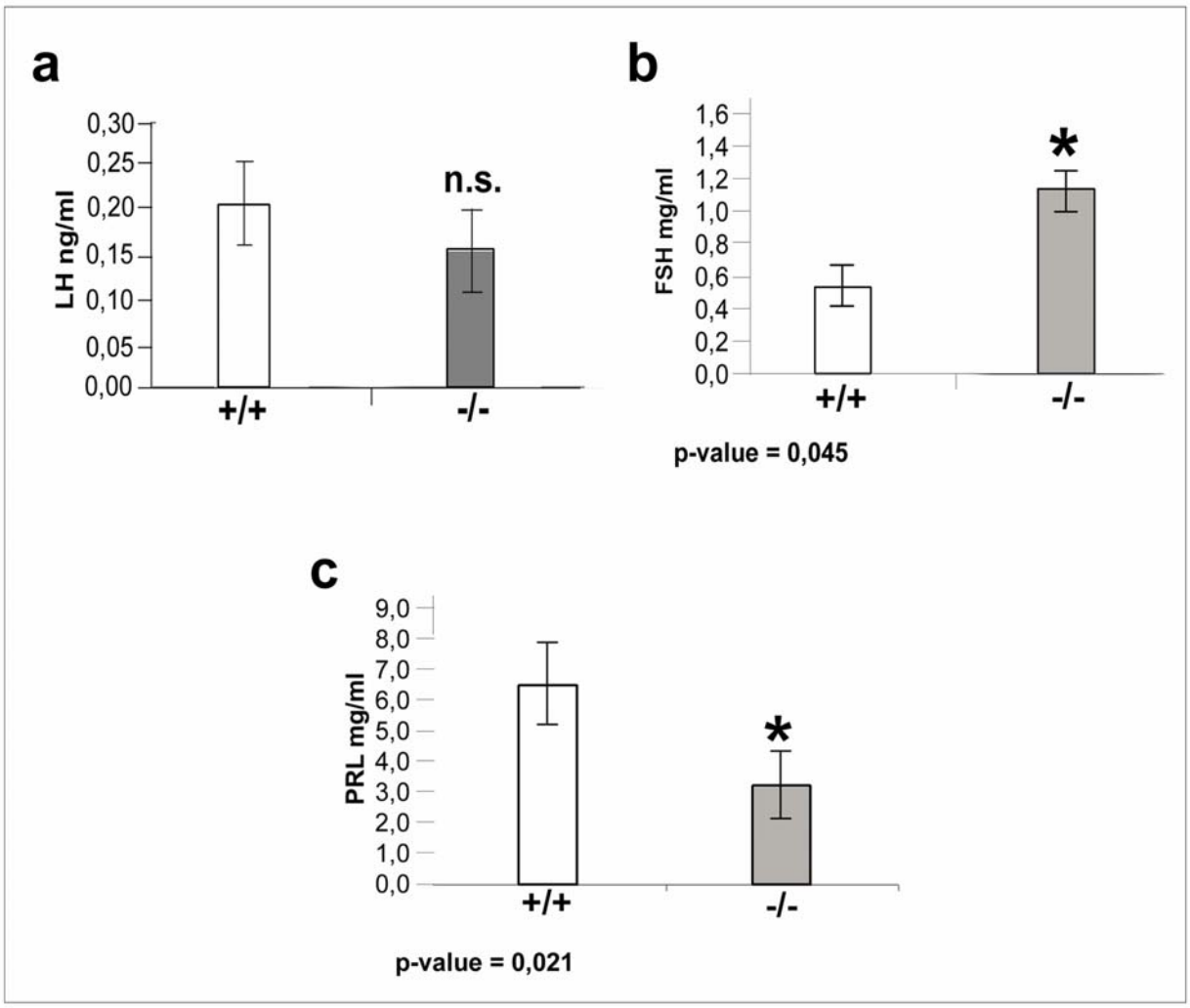

Fig. 16 FSH and PRL content in the trunk blood of homozygous females was altered at diestrous

The FSH and LH hormones were measured in the trunk blood taken from homozygous females and wild type littermates at diestrous by T.Hämäläinen, Turku, Finland. On the Y axis the hormone concentration in the blood (mg/ml) is indicated. The LH level in the trunk blood was unchanged in the homozygous females (0.153± 0.048; n=16) compared with their wild type littermates (0.205± 0.074; n=13) at the diestrous (a); the p-value = 0.56. The FSH level in the trunk blood of homozygous females (1.096± 0.255; n=16) was increased compared with their wild type littermates (0.518± 0.084; n=13) at diestrous of the estrous cycle. The t-Test revealed p-value = 0.045. The PRL content in the homozygous females (3.436 ± 0.7666; n=16), measured in the trunk blood taken at the diestrous was decreased compared with their wild type littermates (6.9 ± 1.294; n= 13). The t-Test revealed p-value = 0.021 (a).

The major factor regulating FSH and LH secretion is GnRH released from the GnRH releasing neurons of the brain. The GnRH expressing neuron bodies are located in the medial septum and diagonal band of Broca and send projections to the median eminence, there GnRH is released into the portal blood. The integrity of GnRH releasing neurons was analysed by immunostaining of 40 µm thick coronal sections of the brain with specific GnRH antibody (kindly provided by T. Braun, Halle, Germany). No obvious differences in distribution and number of GnRH expressing neurons were observed between *Ncdn* homozygous females and their wild type littermates (n=3) (Fig.17).

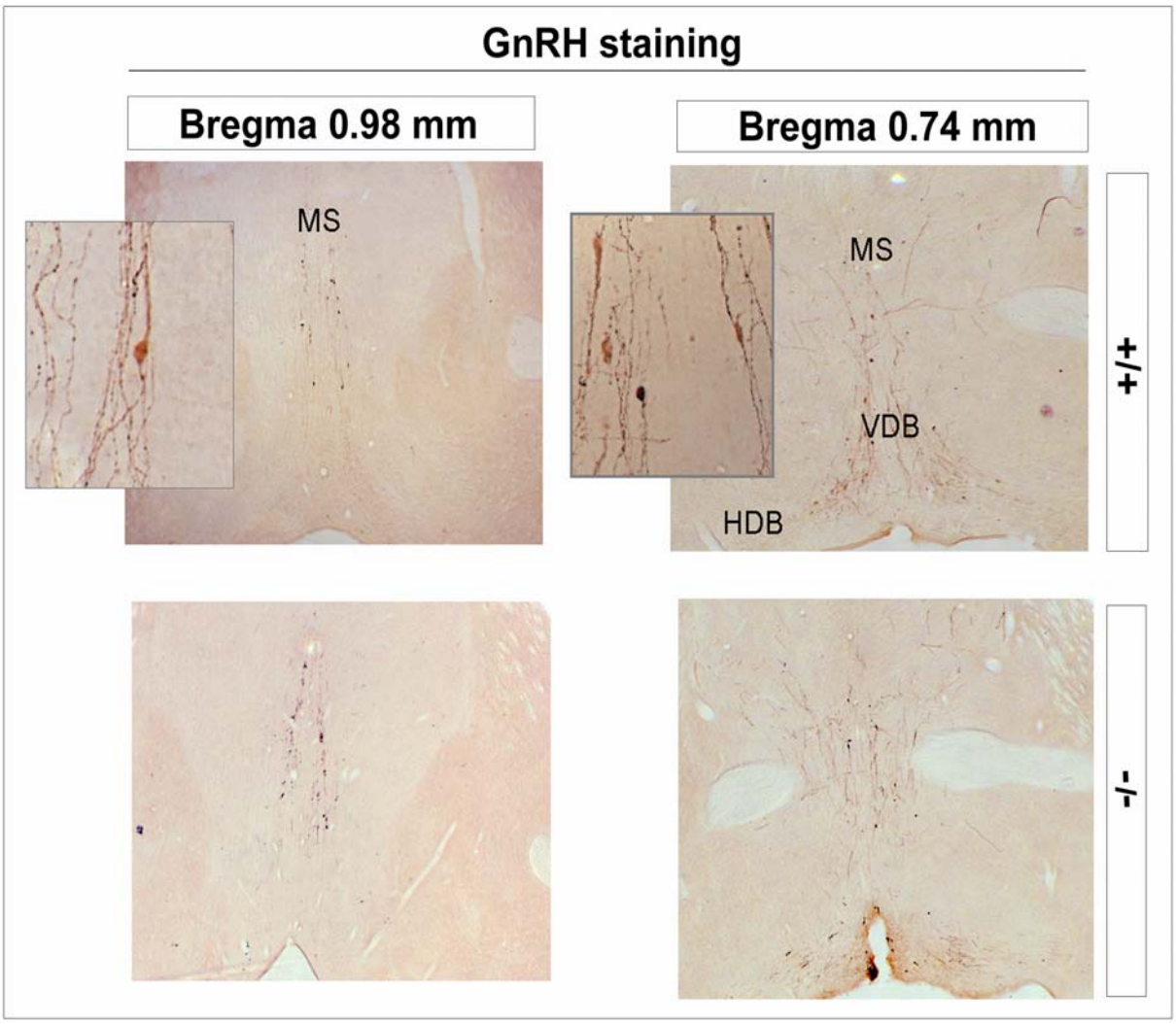

Fig.17 The number and distribution of the GnRH neurons was unchanged in the homozygous females (n=3)

The GnRH releasing neurons were detected by immunostaining with a GnRH polyclonal antibody on 40 µ thick sections of adult brains. No obvious differences in number and location of GnRH neurons between wild type (upper panel) and homozygous (lower panel) female mice were detected.
Abbreviations: *MS* medial septum, *VDB* vertical limb diagonal band, *HDB* horizontal limb diagonal band, *AcrH*- arcuate hypothalamic nucleus, *ME* median eminence

Since, the population GnRH expression neurons was not changed in the *Ncdn* mutants, an increased FSH could be resulting from the absent negative regulation of steroid hormone estrogen, produced by ovaries. As it was reported previously, high FSH was determined in females with starting ovarian failure due to low level of estrogen (Check et al., 2004). In order to analyse if this is a case in *Ncdn* homozygous females, measurement of estrogen was started at the time of writing of this thesis.

In order to identify reasons leading to the low level of PRL in the *Ncdn* homozygous females, the expression of the PRL gene was analysed by ISH with specific riboprobe for *Prl* gene (kindly provided by E. Borelli, Strasburg, France) and by immunostaining with PRL antibody on 8 µm thick paraffin sections of the pituitary. Interestingly, in the pituitaries of nine to ten months old homozygous females PRL level was dramatically increased on mRNA (Fig. 18a) and protein levels (Fig.18b) as compared to their wild type littermates.

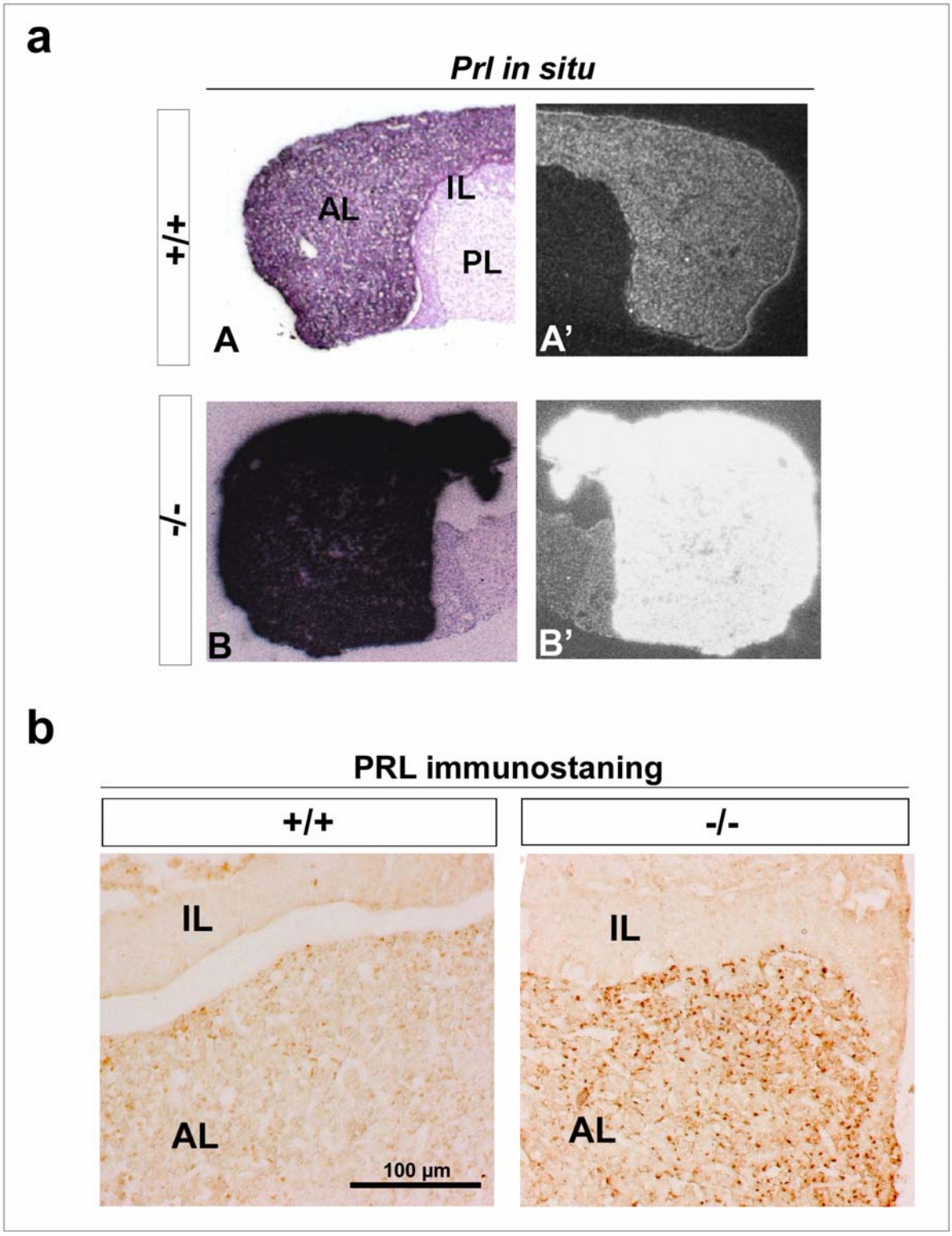

Fig. 18 Expression of PRL in the pituitary (*Prl* ISH n=4; PRL immunostaining n=3)

PRL expression was studied by ISH (a) and immunostaining (b) on 8µm thick paraffin sections of pituitaries. The homozygous females displayed dramatically elevated expression levels of PRL (B, B') on the mRNA level compared with wild type littermates (A, A'). The black coloured anterior lobe (AL) of homozygous mutant pituitary in the Nissl stain (B) was caused by high concentration of PRL mRNA

in this region. On the protein level PRL was still strongly increased in the pituitaries of homozygous females compared with their wild type littermates.

Abbreviations: *AL* anterior lobe*; IL* intermediate lobe*; PL* posterior lobe

Additionally to the increased PRL, the anterior lobes (AL) of nine to ten month old homozygous females were enlarged compared to their wild type littermates (Fig. 19). The posterior (PL) and intermediate lobes (IL) were not changed in size (data not shown). The pituitary size was estimated on paraffin section of the pituitaries (n=6) under light microscope supported by the software"Stereo Investigator" 5.05.4. Data were analysed by one-way ANOVA. Post-hoc analysis was conducted using Student-T test. Data presented in the figure is mean ±S.E.

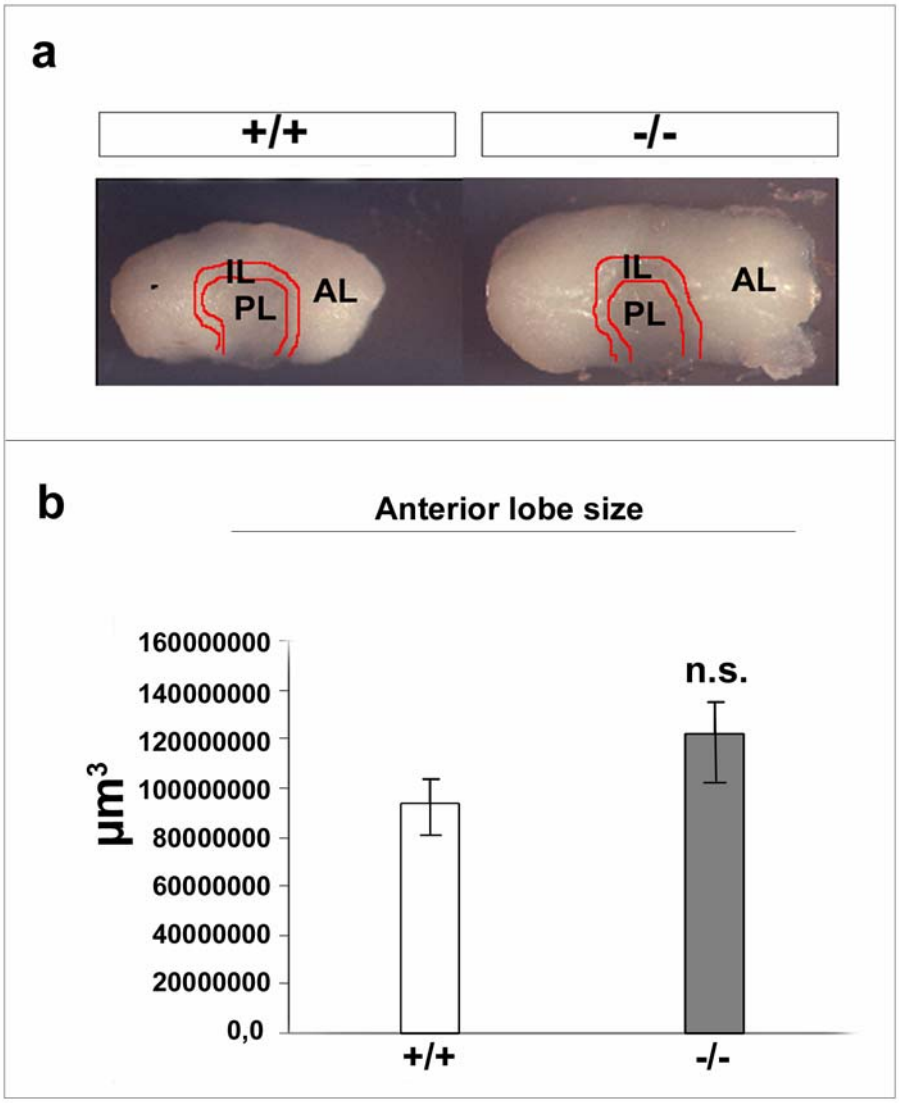

Fig.19 The enlarged anterior lobe of pituitaries in homozygous females

On the gross morphological pictures (a) *Ncdn* homozygous females (n=6) displayed enlarged anterior lobe compared with their wild type littermates. The anterior lobe size was measured after Cavalieri method on 8µm thick paraffin sections. The anterior lobe size of Ncdn homozygous females displayed non significant increase compared with the pituitaries of wild type littermates. The p-value measured by T-test = 0.11.
Abbreviations: *AL* anterior lobe; *IL* intermediate lobe; *PL* posterior lobe

Previously it was demonstrated that uncontrolled proliferation of the lactotroph cells is one of the main reasons leading to the enlargement of AL (Ben-Jonathan et al., 2000). The rate of proliferating cells in the pituitary was analysed by detection of 5-bromo-2´-deoxy-uridine (BrDU), which incorporates into the DNA during duplication in place of thymidine. Therefore, the BrDU is a useful marker for proliferating cells. Homozygous and wild type females were injected with BrDU in concentration 1000 µg per 100 g weight. Three hours later mice were sacrificed and perfused. Paraffin sections (8 µm thick) of pituitaries were stained with a specific monoclonal BrDU antibody. The BrDU positive cells were counted and followed up by one-way ANOVA. Post-hoc analysis was conducted using Student-T test. Data presented in the figure is mean ±S.E. Indeed, the number of the proliferating cells in ALs of *Ncdn* homozygous female animals was increased compared to their wild type littermates (Fig. 20).

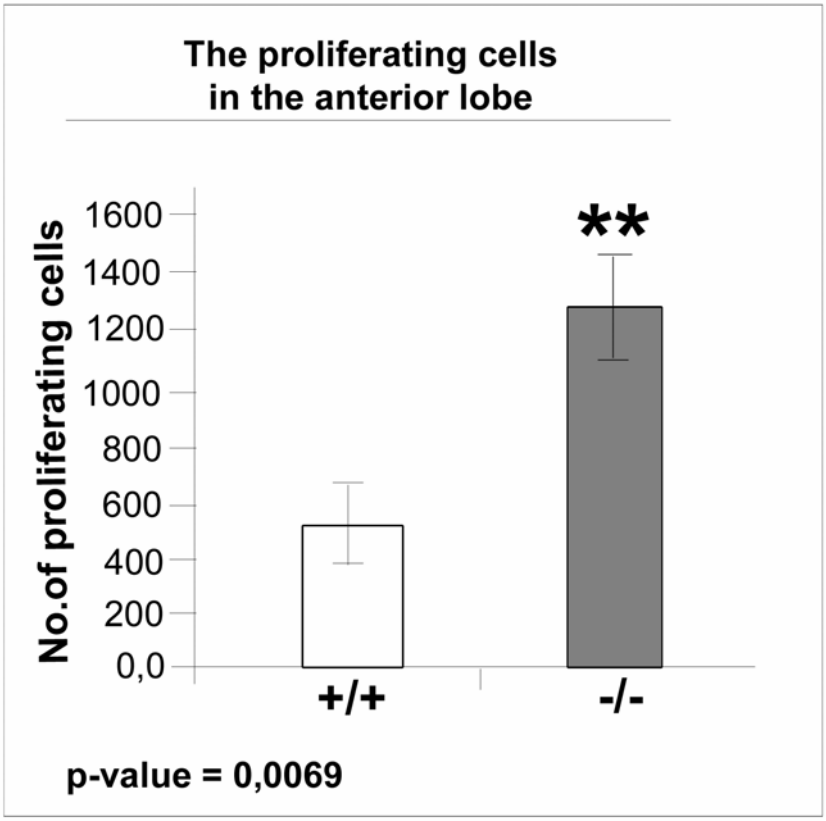

Fig.20 Number of proliferating cells was increased in pituitaries of homozygous mutant mice
The proliferating cells were detected by staining with the BrDU antibody. Homozygous females displayed an increased number of proliferating cells (1.230 ± 0.175; n=6) in the AL of pituitary compared to their wild type littermates (0.474 ± 0.129; n=6). The T-test revealed p value =0.0069

The proliferation of lactotroph cell as well as PRL synthesis and release are under negative control of neurotransmitter dopamine (DA), which is released from the A_{12} group of dopaminergic neurons, namely tuberoinfundibular dopaminergic (TIDA) neurons. Perikarya of TIDA neurons, which are located in the mediobasal hypothalamic arcuate nucleus and adjacent periventricular nucleus, project axons to the external layer of the median eminence. DA which is released from terminals of TIDA neurons in the median eminence does not enter a synapse but diffuses through fenestrated capillaries and is transported in the hypophysial portal blood to the anterior pituitary. In the pituitary DA activates dopamine receptor 2 (D2R), which is anchored in the cell membrane of lactotroph and melanotroph cells. The increased lactotroph proliferation and expression of PRL could be resulting from the impaired regulation of DA in the pituitary of *Ncdn* females. The number and distribution of TIDA neurons and the expression of D2R were analysed in the mutant mice

compared to their wild type littermates (n=5). For the analyses of TIDA neurons immunostaning for the tyrosine hydroxylase (TH) was done on the coronal cryosections sections of adult brains (30 µm thick). TH is the first enzyme in catecholamine biosynthesis and catalyses the conversion of L-tyrosine to L-DOPA, the precursor of DA. TH is therefore, a useful marker of dopaminergic neurons. No obvious differences in number and location of TIDA neurons were observed in the mutant (Fig. 21).

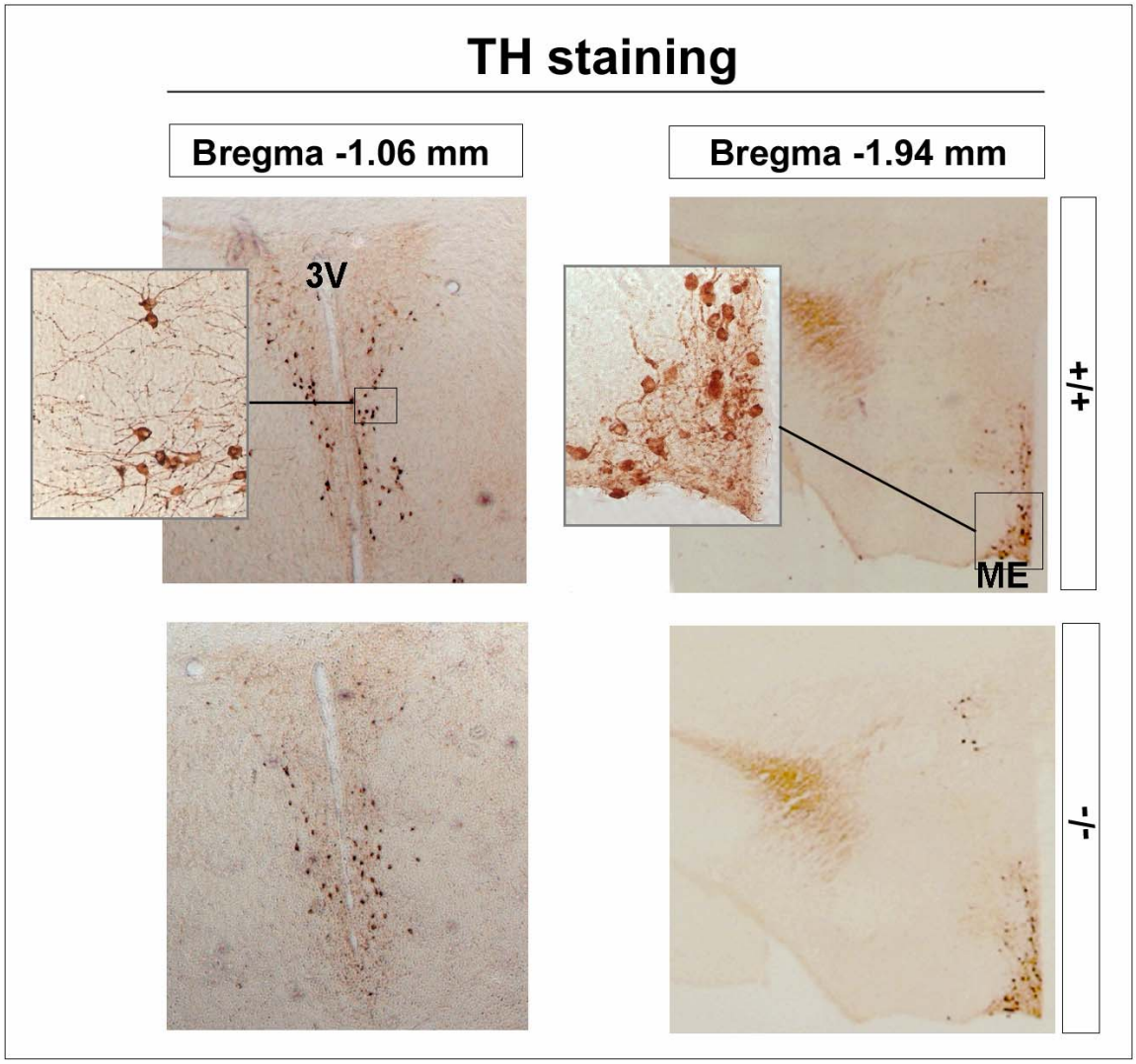

Fig.21 Number and distribution of TIDA neurons was not changed in the homozygous females
Immunostaining with a TH antibody was done on 30 µm thick cryo-sectons of adult brains. No obvious changes in number and location of TIDA neurons between wild type (upper panel) and homozygous mutants (lower panel) were detected (n=5).
Abbreviations: *3V* 3rd ventricle; *ME* medial eminence

The TIDA neurons seemed to be functional and were presented in unchanged number.

D2R was suggested as a main mediator of DA signalling in the pituitary (Saiardi et al., 1998). It belongs to a big family of seven transmembrane (7TM) G-coupled proteins (GPCRs) and is highly expressed in the CNS and in the pituitary. D2R exists in two isoforms: D2L (long) and D2S (short). Both isoforms are generated by alternative splicing from the same gene and differ by the insertion of a 29-amino acid within the putative third intracellular loop of D2R. The pharmacological and biochemical profiles of D2L and D2S are similar *in vitro*. Although, the antagonistic functions of two D2R isoforms *in vivo* were suggested due to coupling with different G-proteins (Usiello et al., 2000; Kim et al., 2004).

The expression of *D2R* isoforms was analysed by ISH with *D2L* and *D2S* specific riboprobes (kindly provided by P. Burbach, Utrecht, Netherlands) on paraffin section (8µm thick) of pituitaries. No obvious changes in the expression pattern of both *D2R* isoforms were observed in the pituitaries of *Ncdn* homozygous females compared to their wild type littermates (n=3) (Fig. 22).

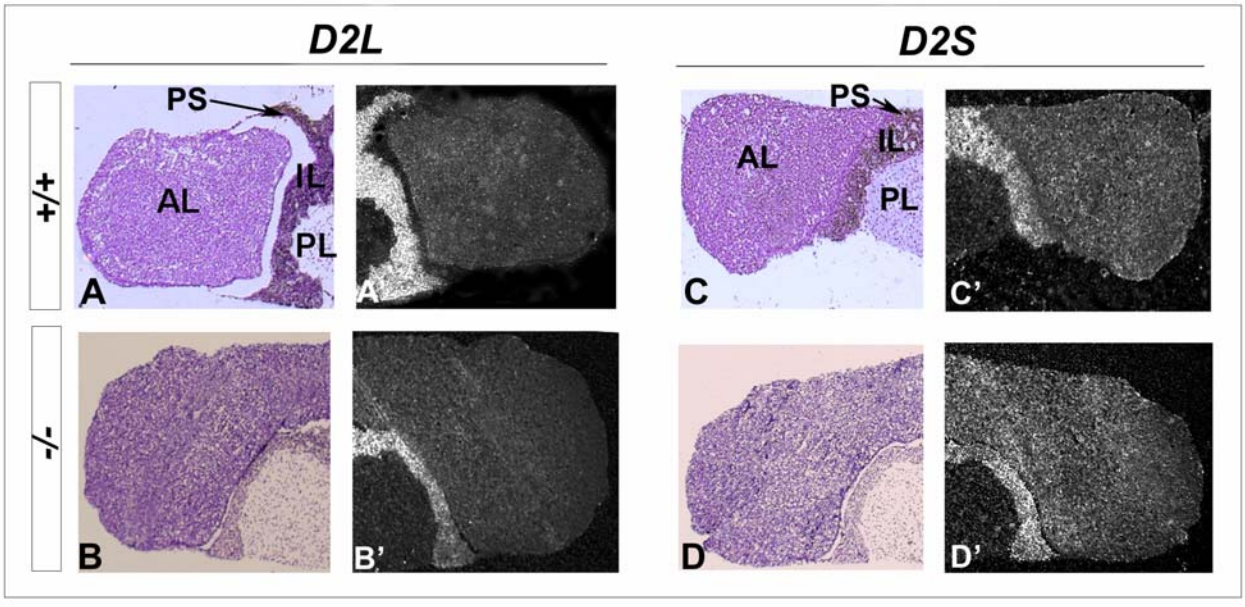

Fig. 22 Expression of the long and short isoforms of *D2R* was not changed in the pituitary of homozygous females

Expression analysis of short and long isoforms of *D2R* was performed with specific *D2L* and *D2S* riboprobes on 8µm thick paraffin sections (n=3).In the pituitary both isoforms are expressed in anterior and strongly in intermediate lobes. There were no obvious differences detected in the expression pattern of *D2L* and *D2S* in the pituitary of homozygous females compared to their wild type littermates.

Abbreviations: *Al* anterior lobe; *IL* intermediate lobe; *PL* posterior lobe; *PS* pituitary stalk

Interestingly, the expression pattern of D2R and *Ncdn* are similar in the pituitary (Fig. 23) and some brain regions, such as the striatum, hippocampus, hypothalamus, cortex, and olfactory tubercle (data not shown). The co-expression of D2R and *Ncdn* suggested a possible acting of these proteins in same pathways.

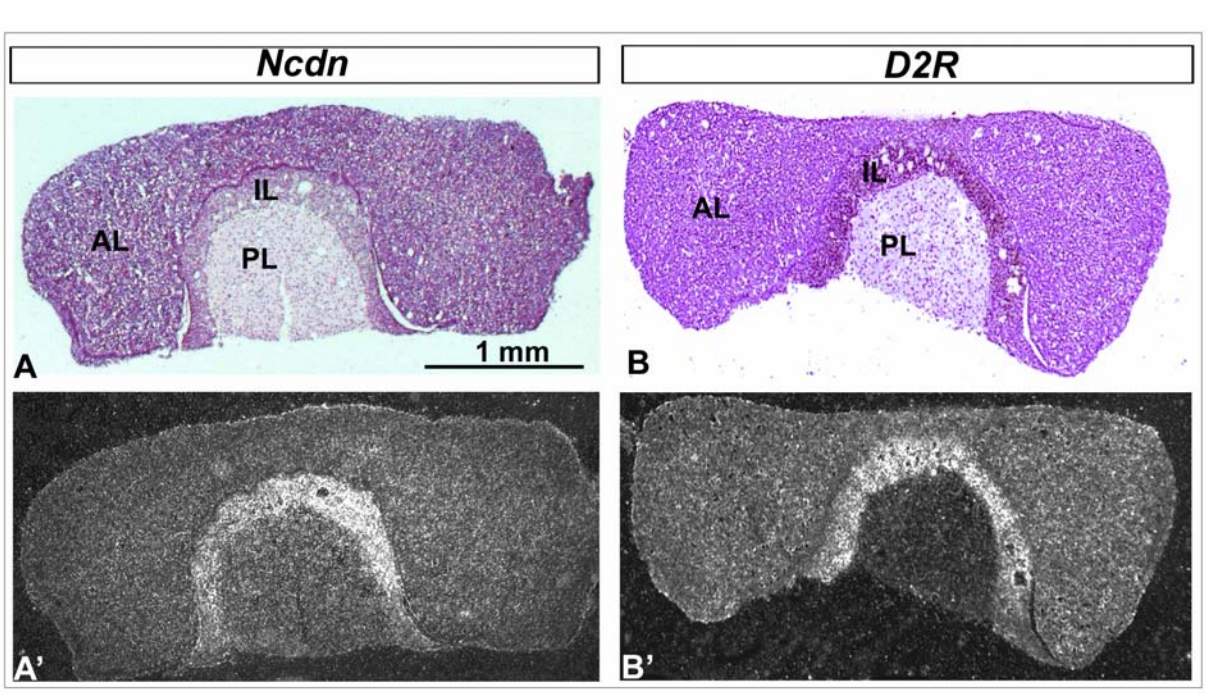

Fig.23 Co-expression of *Ncdn* and *D2R* in the pituitary

The expression of *Ncdn* and *D2R* was detected by *in situ* hybridisation with specific riboprobes on 8 µm thick paraffin sections of pituitaries. *Ncdn* (A, A') and D2R (B, B') are expressed in the anterior lobe and strongly in the intermediate lobe of the pituitary. Slight expression of *Ncdn* and *D2R* was detected in the posterior lobe.

Abbreviations: *AL* anterior lobe; *IL* posterior lobe; *PL* posterior lobe

Moreover, in the cytoplasmic tail of D2R a *Ncdn*-binding domain was determined by screening for proteins with sequences carrying a *Ncdn*-binding domain. Originally, the *Ncdn*-binding domain was identified by Dr. Bächner (personal communications) in the cytoplasmic tail of Melanin Concentrating Hormone Receptor 1 (MCHR1), which also belongs to the 7TM GCPRs. The *Ncdn*-binding domain (295 - 328aa sequence of MCHR1) was twice blasted using the position-specific iterated (PSI) BLAST trough protein data bases. D2R, somatostatin receptors 2 and 5 (SSTR2 and SSTR5) contained sequences with a highest homology to *Ncdn*-binding domain (Fig. 24). The

preliminary data of co-immunoprecipitation analyses supported a possible binding of *Ncdn* with D2R (Dr. Bächner, personal communication). However, the further investigations concerning this are still in process.

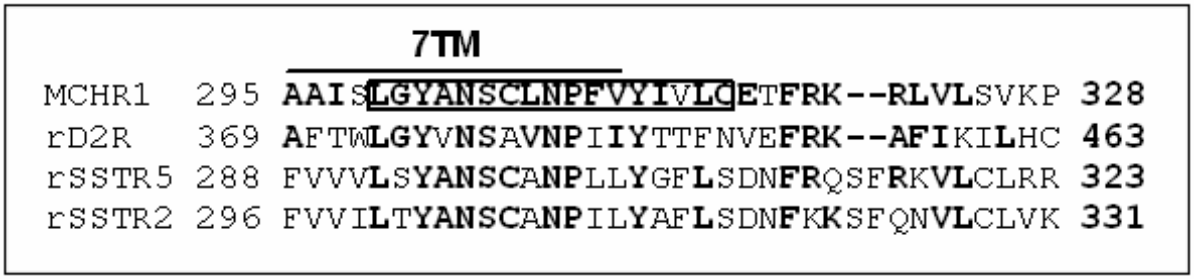

Fig. 24 Alignment of the *Ncdn* binding domain to most relevant GPCRs

The alignment of the *Ncdn* binding domain of MCHR1 (295 – 328 aa) revealed highest homology in D2R, SSTR5 and SSTR2. Identical amino acids are indicated in bold letters; the *Ncdn* binding domain in MCHR1 is boxed; 7TM is indicated with a bar.

Abbreviations: r rat.

The functionality of DA signalling via D2 *in vivo* can be analysed by determination of the Erk1/2 MAP Kinases activity in the pituitary or by challenge with D2R antagonists/ agonists. Previously it was reported that activation of D2R leads to the rapid phophorilation of Erk1/2 which is correlated with growth arrest of the cell proliferation (Usiello et al., 2000). Additionally, a decrease in the phosphorylation level of Erk1/2 in the pituitaries of D2R knock out mice due to impaired DA signalling was published by Iaccarino et al., 2002. The activity of Erk1/2 kinases was analysed in western blot with antibodies for phosphorylated forms of Erk1/2. The total protein was extracted from the anterior lobe of the pituitaries (n=3). The level of phophorylated Erk1/2 was decreased in the protein extracts from the *Ncdn* homozygous females, nine to ten month old (Fig.25). Staining with an HPRT antibody was used as a loading control.

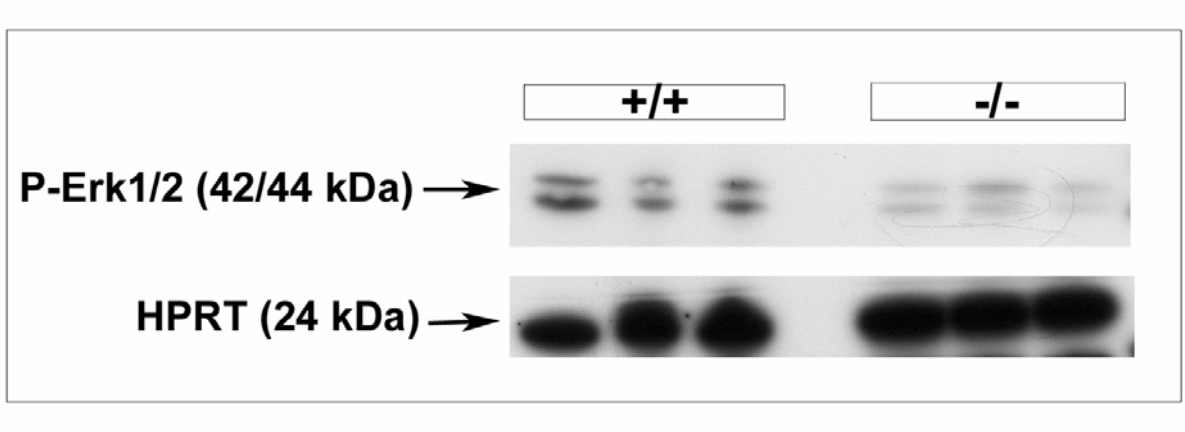

Fig.25 The phosphorylation level of Erk1/2 was decreased in ten months old homozygous females

The western blot was done on the protein isolated from the anterior lobes of the pituitary. The western blot was stained with phospho-Erk1/2 antibody. As a loading control staining with the HPRT antibody was used. The quantity of detected protein was determined using the "Bio-imager Intelligent Quantifier" software. The intencity of phosphorylated Erk1/2 was to 53 % decreased in 9-10 moths old homozygous female mice (n=3) compared with their wild type littermates.

Summarizing, *Ncdn* homozygous females are subfertile due to ovulation failure and display an irregular estrous cycle with prolonged diestrous and a hormonal imbalance. Analyses of factors, which are mainly involved in the regulation of the female fertility and are secreted from the brain and pituitary revealed following:

- *brain*: no altered number and distribution of TIDA and GnRH releasing neurons;
- *pituitary*: increased expression of PRL, decreased level of phophorilated Erk1/2; no altered expression of D2R
- *blood*: increased FSH, decreased PRL, no altered LH.

Additionally, the AL of the pituitary of *Ncdn* homozygous female was enlarged and contained the increased number of proliferating lactotrophs. The *Ncdn*–binding domain was identified in the cytoplasmic tail of D2R and in the pituitary co-expression of D2R and *Ncdn* was demonstrated.

All presented data suggest a role of *Ncdn* signalling in pathways regulating female fertility (Fig.26). In the pituitary, *Ncdn* was suggested to be involved in the regulation proliferation of lactotroph cells and PRL synthesis and release possibly via mediation of D2R signalling. However a specific role of *Ncdn* in the PRL release can not be

excluded since the PRL level in the blood of *Ncdn* homozygous females was decreased. On the other hand, *Ncdn* homozygous females displayed increased FSH in the blood at the age of nine to ten months. In contrast, in the blood of the younger female animals (five month old) FSH level was not altered, indicating starting ovarian failure in older mutant animals.

Finally, *Ncdn* expression was detected in the cells of the developing follicle. This suggest a possible involvement of *Ncdn* in feedback loops regulating pituitary and brain functions.

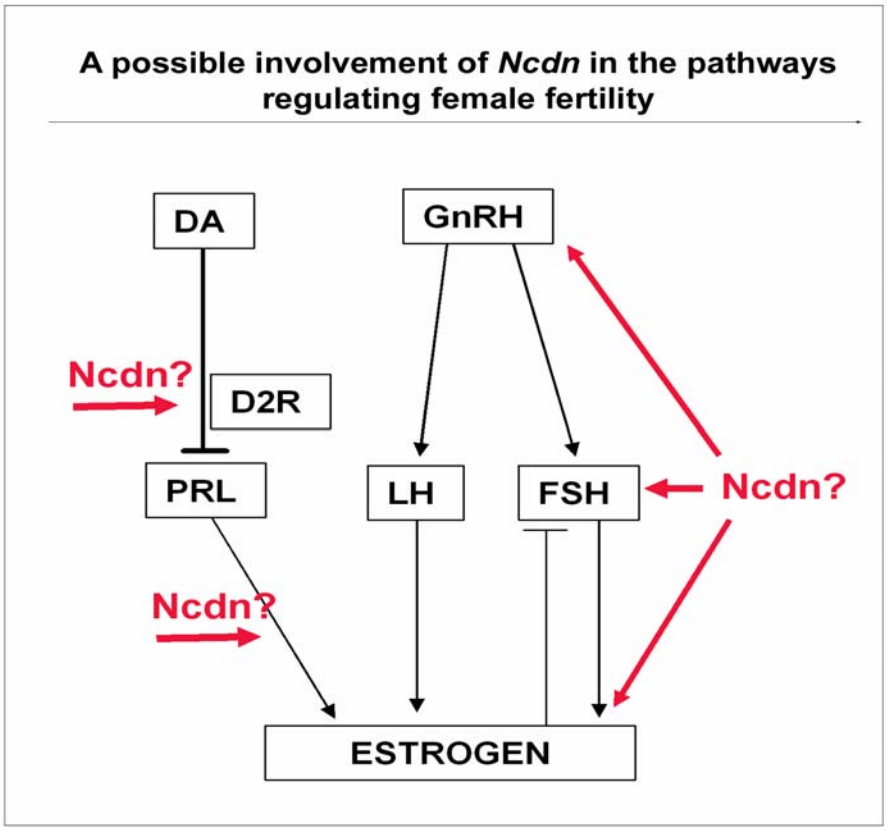

Fig. 26 A possible involvement of *Ncdn* in the regulation of female fertility

Ncdn is expressed in organs of reproductive axis: hypothalamus, pituitary and ovary and therefore can be involved in the regulation of female reproduction at all those levels. A possible involvement of *Ncdn* in DA signalling via binding to D2R was suggested based on the phenotypic analyses of *Ncdn* gene-trap mouse mutants. However, a specific function of *Ncdn* regulating PRL release beside of DA signalling was not excluded. Moreover, *Ncdn* can be involved in the regulation of female reproduction on the ovarian level by modulating feedback pathways regulating hypothalamic and pituitary factors.

Abbreviations: *AL* anterior lobe, *DA* dopamine*, FSH* follicle stimulating hormone, *GnRH* gonadotropin releasing hormone, *Hyp* hypothalamus, *IL* intermediate lobe, *LH* luteinising hormone, *PL* posterior lobe.

3 DISCUSSION

3.1 A possible role of *Ncdn* in the female fertility

In this study a possible involvement of *Ncdn* in the regulation of female fertility is suggested by the results of the phenotypic analyses of *Ncdn* gene-trap mouse mutant. *Ncdn* homozygous females are subfertile due to ovulation failure, possibly caused by hormonal imbalance. Mutants are characterised by decreased PRL, increased FSH and unchanged LH in the trunk blood. Morphologically, the ovaries of *Ncdn* homozygous females appeared normal and responded positively to external gonadotropins. The estrous cycle of mutant females was irregular with diestrous lasting till seven days in nine to ten month old animals. *Ncdn* is expressed at all levels of reproductive axis: brain, pituitary and ovary (Fig. 29) and therefore could be involved in the various pathways regulating female fertility.

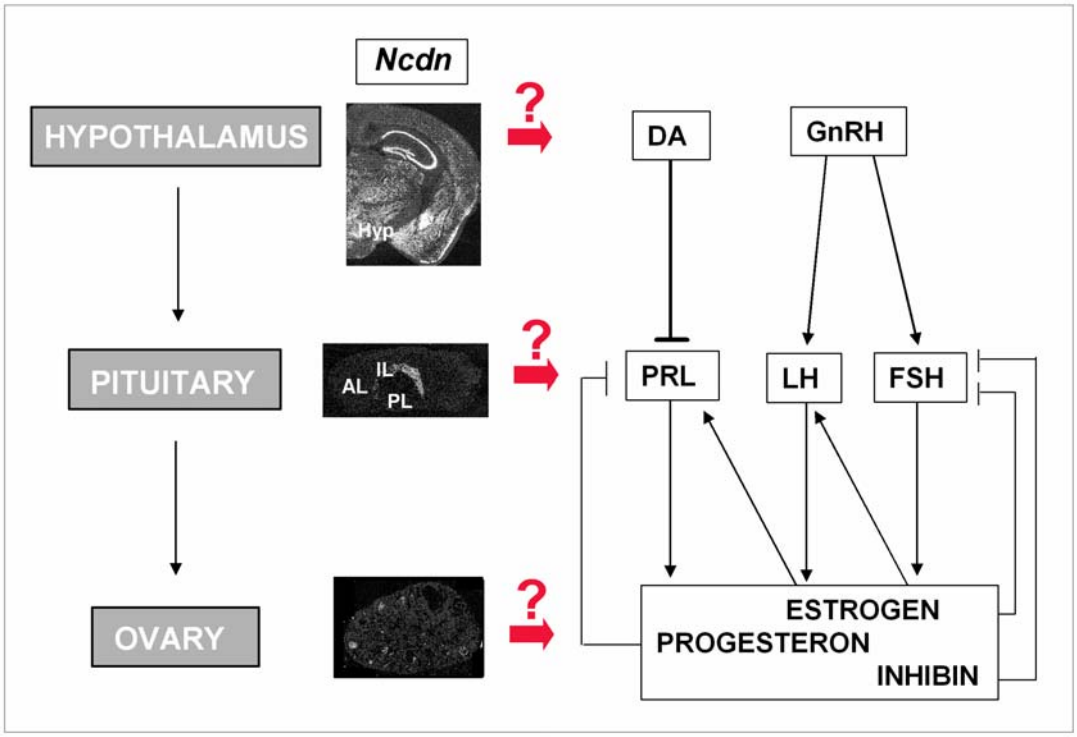

Fig.29 A possible involvement of *Ncdn* in the regulation of female fertility

Ncdn is expressed at all levels of HPG and therefore can be involved in the pathways regulating female fertility in the brain, pituitary and ovary. In the brain *Ncdn* is expressed in the arcuate nucleus, which includes TIDA and GnRH releasing neurons. In pituitary *Ncdn* is strongly expressed in the anterior and intermediate lobes, containing PRL, FSH LH and POMC secreting cells (lactotroph, gonadotroph and

melanotroph cells). In ovary it seems to be expressed in the granulosa cells. After being released into the portal blood, DA and GnRH activate their receptors in the pituitary and control secretion of FSH, LH and PRL, which stimulate steroidogenesis in the ovary. Additionally, FSH induces production of inhibin. In a feedback loop FSH is negatively regulated by inhibin. Whereby, estrogen stimulates the expression of LH and PRL in lactotroph cells and inhibits the secretion of FSH. Progesterone, produced from the CL in the negative feedback loop controls PRL release. Question marks denote the links that remain hypothetical.
Abbreviations: *FSH* follicle stimulating hormone, *DA* dopamine; *GnRH* gonadotropin releasing hormone; *LH* luteinising hormone.

Main hormones regulating female fertility, namely FSH, LH and PRL are secreted from anterior lobe of the pituitary. Their production and release are controlled by GnRH (Smith and Jennes, 2001) and DA (Freeman et al., 2000), secreted from the arcuate nucleus of the hypothalamus. Thereby, cyclic alterations in FSH, LH and PRL release regulate secretory patterns of the steroid hormones estrogen and progesterone, produced in the ovary. In a feedback loop estrogen negatively regulates FSH and stimulates LH release, while progesterone inhibits PRL release. FSH stimulates expression of inhibin, a glycoprotein which is secreted from granulosa cells of the ovary (Risbridger et al., 2001). Inhibin regulates in a negative feedback loop FSH release (Richards, 1980).

Thus, one of the reasons for altered FSH and PRL in the blood could be an impaired regulation from the hypothalamus. No change in the number and distribution of GnRH and DA releasing (TIDA) neurons was detected in the brains of *Ncdn* homozygous females. Therefore, knockout mutants with reproductive disorders in the pituitary and ovaries were compared to *Ncdn* phenotype (see Table 4, the common phenotypic characteristics are underlined).

Table 4 Knockout mutants with reproductive disorders

GENE	KNOCK OUT PHENOTYPE	REFERENCE
PITUITARY PHENOTYPE		
PRL	Female infertility; ovulation failure, pituitary hyperplasia; low estrogen in blood	Cruz-Soto et al., 2002
PRLR	Female infertility; due to impalantation defects increased PRL and decreased progesterone in blood; pituitary hyperplasia	Grosdemouge et al., 2003
D2R	Female subfertiliy, irregular estrous cycle, increased PRL on mRNA level and in the blood low estrogen in the blood	Saiardi et al., 1997
OVARIAN PHENOTYPE		
ERα	Female infertility associated with anovulation and development of ovarian cysts ;no plugs observed after maiting; large number of follicles at advanced stage of atresia; absence of mature CL; overexpression of gonadotropin mRNA; elevated LH in blood	Schomberg et al., 1999 Dupont et al., 2000
ERβ	Female subfertility, unchanged number of follicles; absence or scarceness of CL	Krege et al., 1998 Dupont et al., 2000
PR	Female infertile, due to ovulation failure, normal level of FSH, estrogen and progesterone; increased LH and slightly increased PRL	Lydon et al., 1996 Chappell et al., 1997
LHR (LurKO)	Female infertility due to anovulation, no preovulatory follicles and CL present in ovary, reduced size of reproductive organs	Zhang et al., 2001
Inhα	Female infertile; granulosa cell tumors, low estrogen, increased FSH in blood; point mutation in human INHα resulted in premature ovarian failure with increased FSH and decreased estrogen in blood	Shelling et al., 2000
P450 aromatase (*Cyp19*)	Female infertile due to block in follicular development and ovulation defects; increased FSH ,LH and testosterone in blood, decreased estrogen and progesterone, no CL present	Fisher et al, 1998

First two mutants with disrupted PRL signalling are infertile and display decreased level of steroid hormones in the blood. In PRL knockout mice infertility is caused by ovulation failure (Horseman et al., 1997), while PRLR knockout females are infertile due to

implantation defects caused by progesterone deficiency, thereby ovulation rates and estrous cycle are not affected (Grosdemouge et al., 2003). Particularly, PRL signalling was shown to be necessary for the expression of LHR, which is activated by LH, secreted from gonadotroph cells of anterior pituitary. In the ovary, activated LHR stimulates theca cell androgen production, triggers ovulation, and stimulates production of estrogen and progesterone of CL (Freeman et al., 2000). Therefore, phenotype of female mice with mutated LHR (LuRKO) is similar to the one of PRL and PRLR knock outs, namely female infertility due to anovulation, lack of preovulatory follicles and CL. The estrogen and progesterone levels are decreased in LuRKO females, while gonadotropin levels are increased consequently to absent negative feedback regulation. Comparison of PRL and PRLR mutants with *Ncdn* gene-trap mice suggested the decreased PRL in the blood of *Ncdn* homozygous females as a main reason leading to the subfertility. Interestingly, in contrast to low level of PRL released into the blood the PRL expression on mRNA and protein levels was dramatically increased in the pituitaries of *Ncdn* homozygous females. As it was previously mentioned, PRL secretion and release are mainly regulated by DA, released from TIDA neurons of the hypothalamus. After being released into the portal blood, DA is delivered to the pituitary and activates D2R, anchored in the lactotroph cell membrane (Ben-Jonathan et al., 2001). The number and distribution of the TIDA neurons, nor expression pattern of D2R (mRNA) were changed in *Ncdn* homozygous females. From the literature it is known, that D2R beside of regulating PRL production and release, mediates activation of MAP kinase pathway that is essential for the control of lactotroph proliferation in the pituitary (Iaccarino et al., 2002). Activated D2R elicits a rapid phosphorylation of ERK1/2 *in vitro* (Welsh et al., 1998; Yan et al., 1999; Oak et 2001; Vindis et al., 2001) and *in vivo* (Cai et al., 2001). *Ncdn* homozygous females displayed decreased level of phosphorylated Erk1/2 in anterior pituitary as compared to their wild type littermates. Moreover, pituitaries of *Ncdn* homozygous females were enlarged and contained an increased number of proliferating lactotrophs, possibly as a consequence of decreased Erk1/2 activity. The altered PRL expression and release; decreased Erk1/2 activity, increased rate of lactotroph proliferation and enlarged anterior lobe of the pituitary suggested a possible impairments in DA signalling downstream of D2R in *Ncdn* gene-trap mutants.

During screening for proteins with sequences homologous to the *Ncdn*-binding domain of MCHR1, originally detected by Dr. Bächner (personal communication), the C-terminal

part of D2R revealed a highest homology, suggesting a possible binding of it with *Ncdn*. Furthermore, expression patterns of D2R and *Ncdn* overlapped in the pituitary (anterior and intermediate lobes) and in some brain regions (striatum, hippocampus, hypothalamus, cortex, and olfactory tubercle), indicating a possible involvement of both molecules in the same pathway. Moreover, the pituitary phenotype of *Ncdn* gene-trap female mutants, namely an enlarged anterior lobe with increased number of proliferating lactotrophs and decreased level of phosphorylated Erk1/2 strongly resembled the pituitary phenotype of D2R-null homozygous females (Saiardi et al., 1997; Iaccarino et al., 2002). As *Ncdn* homozygous females, the D2R knockout females are subfertile and display an irregular estrous cycle with prolonged diestrous (Baik et al., 1995; Yamaguchi et al., 1996). However, decreased level of PRL in the blood of *Ncdn* gene-trap females is controversial to the increased PRL level in the blood of D2R knockout mice (Saiardi et al., 1997). This discrepancy could be explained by selective binding of *Ncdn* to one of D2R isoforms. As it was previously shown, D2R exist in two isoforms (D2L and D2S) that couples to distinct guanine nucleotide binding (G) proteins and activate different transduction pathways (Guiramand et al., 1995) depicted in the figure 30. Coupling of D2L via $G\alpha_0$ to potassium channels results in a decreased calcium influx and immediate suppression of PRL release. Whereas, D2S via coupling to $G\alpha_i$ suppresses PRL gene expression by inhibition of the cAMP-generating enzyme adenylyl cyclase and suppression of activated PKA (Ben-Johnatan et al., 2000). On the other hand, stimulation of D2S leads to the activation of Erk1/2 in the pituitary (Welsh et al., 1998; Yan et al., 1999). Beside of coupling with G-proteins, D2S was shown to activate phospholipase D (PLD) (Senogles, 2000), which is involved in the regulation of exocytose in various secretory cell types (Jones et al., 1999), such as neutrophils (Morgan et al., 1997), platelets (Haslam et al., 1993), and mast cells (Cohen et al., 2001). PLD1, one of two mammalian PLD, is a key factor for the exocytotic machinery in neuroendocrine cells (Vitale et al., 2001) and controls accumulation of phosphatidic acid (PA) at the late stage of Ca^{2+} -dependent exocytose (Humeau et al 2001). Thereby PA being a cone shaped lipid promotes negative curvature (Monck and Fernandes, 1994) and fusion of the membrane (Chernomordic et al., 1995).

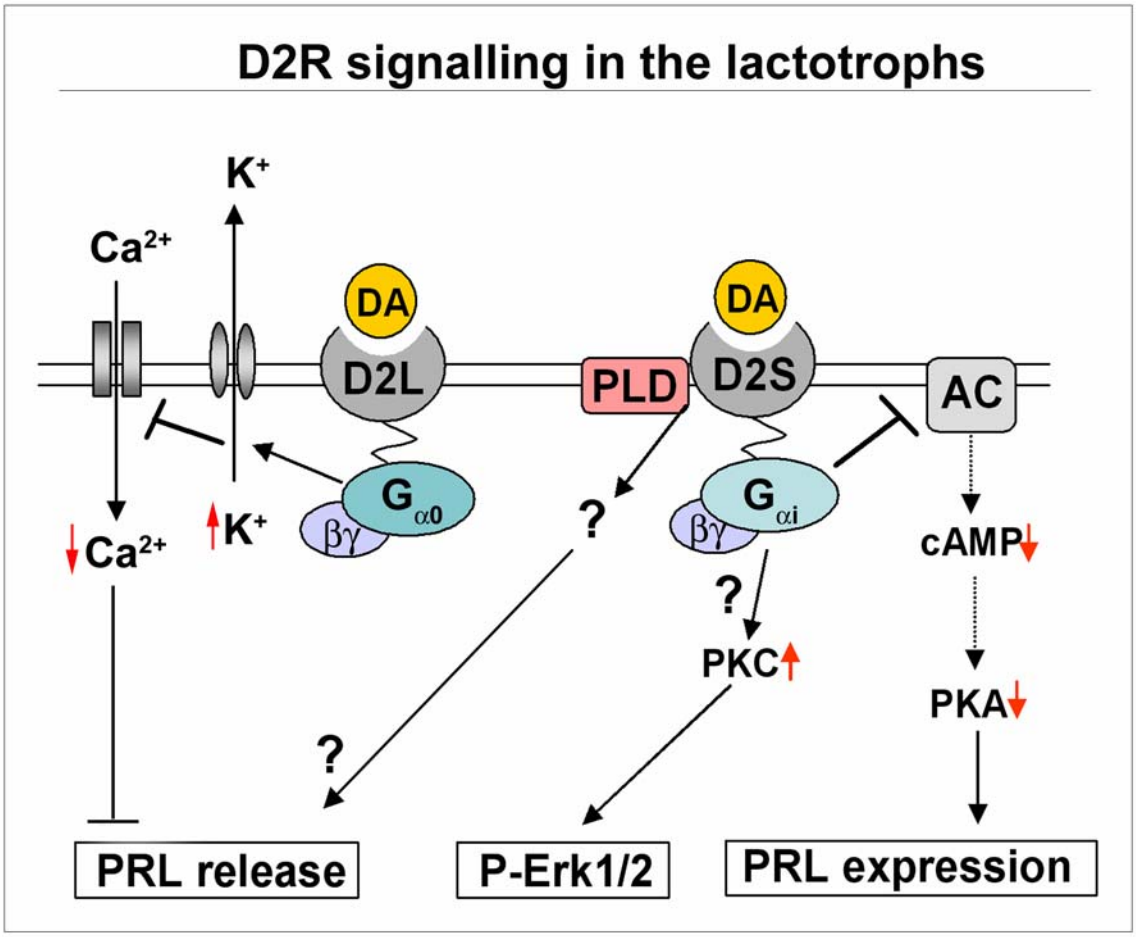

Fig.30 Signalling via D2L and D2S in lactotroph cells

Activated D2L couples either directly or indirectly via Gαo to potassium channels, leading to a decrease in calcium influx and immediate suppression of PRL release. Whereas, suppression of PRL expression is done by coupling of D2S to $G\alpha_i$ resulting in the inhibition of adenylyl cyclase (AC), decreased cAMP production. D2S also activates protein kinase C (PKC) through unknown mechanisms, resulting in the rapid phophorylation of Erk1/2 kinases. Beside of coupling with G-proteins, D2S was shown to bind directly to phospholipase D (PLD). Activated PLD was shown to regulate exocytose from the neuroendocrine cells and positively regulates PRL release.

In D2R knockout mutants, with absent both isoforms, PRL expression is increased, while phosphorylation of Erk1/2 is decreased in the anterior pituitary (correlated with loss of D2S); in the blood the PRL content is increased according to absent D2L. In D2L mutants, which still contain functional D2S, phosphorylation of Erk1/2 is increased in the anterior pituitary due to possibly higher density of D2S (Usiello et al., 2000). Thereby, PRL blood content of D2L mutants is not changed, suggesting a substitution by D2S of D2L functions in DA-mediated PRL secretion (Xu et al., 2002).

The increased expression of PRL and decreased phosphorylation of Erk1/2 in the pituitaries of *Ncdn* homozygous females suggest a possible impairment in DA signalling via D2S (Fig.31). Thereby, the D2L signalling is possibly not affected resulting in the increased suppression of PRL release. Furthermore, impaired D2S signalling could result in the altered stimulation of PRL release due to decreased activity of PLD. Interestingly, *Ncdn* was shown to bind with the middle third part of the protein to PA, a product of PLD1, (Ktistakis et al., 2003), suggesting a possible involvement in the D2S-PLD stimulated PRL release.

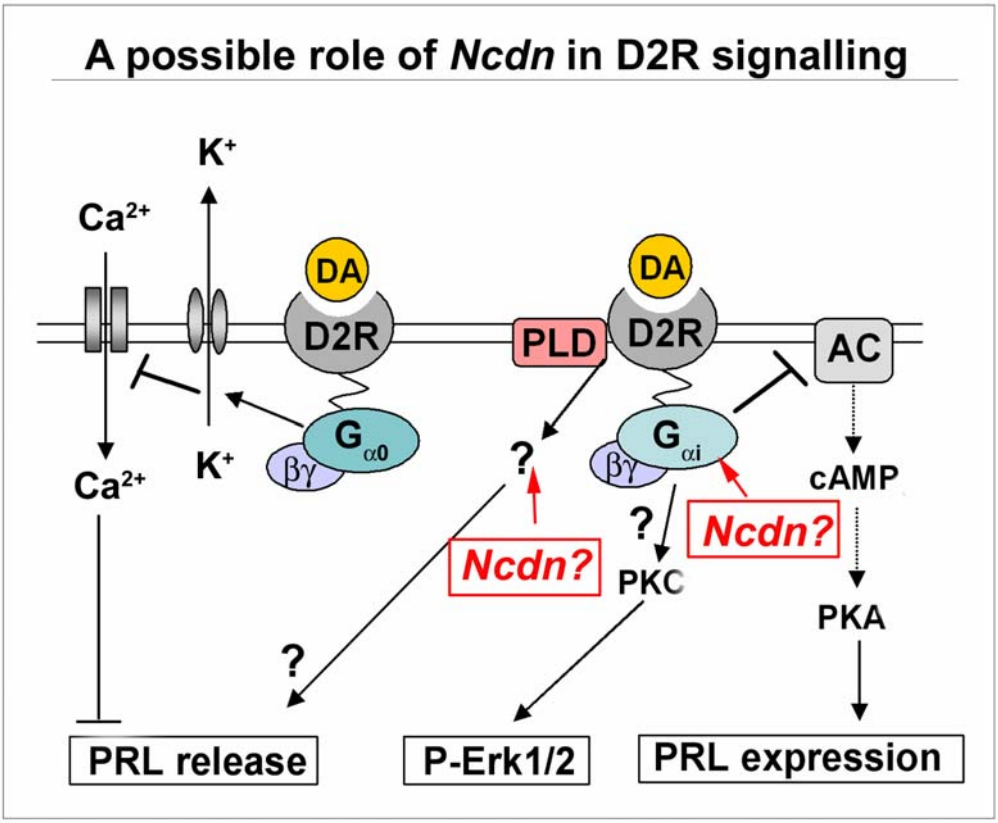

Fig.31 A possible role of *Ncdn* in D2S signalling in lactotroph cells

A possible involvement of *Ncdn* in DA signalling via binding with a C-terminal part of the protein with D2S, containing *Ncdn*-binding domain was suggested. *Ncdn* could be involved in the D2S- $G\alpha_i$ binding and act as a new scaffold factor. On the other hand, a possible involvement of *Ncdn* in PRL release, which is positively regulated by D2S.

Another aspect which has to be discussed here is the feedback regulation of PRL gene by factors released from the ovary (Fig.29).

The steroid hormones estrogen and progesterone regulate PRL gene expression via activating of their receptors ERs and PR. Estrogen regulates PRL secretion via

activation of ERα and ERβ at two levels. In the pituitary estrogen induces expression of PRL gene binding directly to the promoter region; in the hypothalamus estrogen modifies activity of the TIDA neurons (Freeman et al., 2000). Knock outs for both receptors display impaired fertility and elevated levels of gonadotropins in the blood (Schomberg et al., 1999; Krege et al., 1998; Dupont et al., 2000) similarly to *Ncdn* gene-trap females. Progesterone is secreted by CL and in a feedback loop negatively regulates PRL release via activation of PR in the pituitary. Absence of progesterone signalling results in the female infertility due to ovulation defects with associated uterine inflammation and disruption of the mammary gland morphogenesis (Lydon et al. 1995). The steroid hormone and FSH levels are not changed in PR knockouts, while LH and PRL are slightly increased in the blood (Lydon et al. 1996, Chapell et al 1997), which is controversial with increased FSH and decreased PRL in the blood of *Ncdn* gene-trap mutants.

Two knockout mouse mutants for P450 aromatase (*Cyp19*), which catalyzes final step in the biosynthesis of estrogen, and α-subunit of inhibin (Inhα), a tumour suppressor molecule, display reproductive disorders and increased FSH in the blood (Table 4). As *Ncdn*, both genes are expressed in the granulosa cells of the ovary. However, Inhα and P450 aromatase knock outs display disorders in the ovarian morphology, namely granulosa cell tumours in Inhα knock outs and absence of CL in P450 aromatase mutant mice, which were not detected in *Ncdn* mutants.

However, since *Ncdn* was shown to be expressed in ovarian follicles analysis of the ovarian factors is necessary to fully understand reasons leading to the subfertility of *Ncdn* gene-trap females.

3.2 Possible functions of *Ncdn* based on expression pattern and binding partners

The wide expression of *Ncdn* during embryogenesis in the central and peripheral neural system (Istvanffy et al., 2004) and early embryonic death (between 3.5 and 6.5 dpc) of *Ncdn*-null mutants (Moshizuki et al., 2003) indicated an essential function of it in early embryogenesis. In the adult brain, *Ncdn* is still widely expressed with strongest signals in the olfactory (olfactory pit, olfactory tubercle, piriform cortex) and limbic (amygdala, hippocampus, hypothalamus, nucleus accumbence) systems (Istvanffy et al., 2004). Strong *Ncdn* expression was also observed in the neuroendocrine system, particularly in

the arcuate nucleus of the hypothalamus (Istvanffy et al., 2004) and in the anterior and intermediate lobes of the pituitary. These expression patterns suggested a possible role of *Ncdn* in the formation of emotions (fear, aggression, and pleasure), memory and regulation of the endocrine system in the adulthood.

Tree binding partners of *Ncdn* were identified so far: semaphorin 4C (Ohoka et al., 2000), PA (Ktistakis et al., 2003), which was previously discussed and melanin-concentrating hormone receptor 1 (D. Bächner, personal communications).

Semaphorin 4C (S4C) was identified as a binding molecule of *Ncdn* in the screen for proteins expressed in the adult mouse brain. The intermediate part of *Ncdn* and juxtamembrane region of S4C was shown to be necessary for this binding identified *in vitro* (Ohoka et al., 2002). S4C is a transmembrane member of a large family of structurally distinct glycoproteins characterized by the presence of a conserved sema domain. Semaphorins provide crucial attractive and repulsive cues involved in the axon guidance (Tamagnone et al., 2000). Interestingly, the expression of human semaphorin IV was shown to be altered in patients with Alzheimer's disease (Hirsch et al., 1999). Recently another member of the semaphorin family - *SEMA5A* during two-tiered, whole-genome association study of Parkinson disease (PD) was found to be related to PD, which shares clinical, pathological, and etiological features with Alzheimer's disease (Maragnore et al., 2005). Strong expression of S4C in the developing neural tissue, such as the olfactory epithelium, epithelium of the vomeronasal organ, enamel epithelium of teeth, epithelium of the inner ear, and sensory ganglia, including trigeminal and dorsal root ganglia, while in adult it is markedly decreased suggesting an involvement of S4C in forming of the neural network during embryonic development (Inagaki et al.,1995). However, the S4C binding part of *Ncdn* (protein N-terminus) is not deleted by the inserted gene-trap vector and therefore could be still functional in the *Ncdn* gene-trap mutants. Moreover, the brain morphology appeared to be intact in the *Ncdn* homozygous mutants, indicating normal development of the neural tissue.

Other binding partner of *Ncdn*, melanin concentrating hormone receptor (MCHR1) is an orphan GPCR (An et al., 2001). *Ncdn* was reported to bind with C-terminla part of the protein to the last intracellular loop of MCHR1 (Bächner et al., 2004). MCHR1 is activated by melanin-concentrating hormone (MCH) a neuropeptide released from the lateral hypothalamus and modulate food intake and energy balance (Saper et al., 2002): Mice lacking MCH and MCHR1 are hyperactive, hyperphagic and have decreased lean

mass, lower body weight and altered metabolism (Marsh et al., 2002). Although in the *Ncdn* mutants the MCHR1 binding domain was truncated, the *Ncdn* mutants did not reproduce the behaviour phenotype of MCHR1 knock outs. This can be explained by still functional MCHR1 in *Ncdn* gene-trap mutants. Interestingly, in the brain of MCHR1 knockout mouse density of D2R was increased in the mesolimbic dopamine system (olfactory tubercle, ventral tegmental area, and nucleus accumbence (NAc)) as recently demonstrated by Smith et al., 2005. This data suggest a possible negative regulation by MCHR1 the D2R expression. As it was previously shown, both isoforms of D2R, in an adequate ratio, are required for the full expression of D2 normal functions. This tempted to speculate that similarly to MCHR1 KO *Ncdn* mutants could display altered density of D2R (in the brain and pituitary as well) leading to the impaired hormonal release.
Summarizing all discussed points, *Ncdn* plays and important role during embryonic development and could be involved in the establishment of the neural system via interacting with S4C. In the adulthood, *Ncdn* is important for the female reproduction. The subfertility of *Ncdn* homozygous females possibly is provoked by altered PRL secretion and release, due to impaired regulation from DA. The decreased activity of Erk1/2 kinases, which lead to the increased proliferation of lactotroph cells in the pituitary was related to the impaired D2R signalling as well. Furthermore, *Ncdn* could be involved in the PRL release from lactotrophs via transmitting of D2R signalling resulting in the activation of PLD and PA accumulation at the cell membrane. On the other hand, the D2R signalling in *Ncdn* gene-trap mutants could be impaired due to disrupted MCHR1 which was shown to modulat density of D2R expression.

In conclusion following experiments are suggested to fully understand *Ncdn* functions.

Firstly the expression of ovarian factors regulated by PRL was suggested to be studied in details. As it was previously reported PRL signalling activates LHR which is strongly expressed in the CL, preovulatory granulosa cells and lesser extent, theca and interstitial cells of the follicle (Fig.31). LHR is an important stimulator of luteal steroidogenesis and acutely upregulates progesterone production through the stimulation of steroidogenic enzymes (Risk et al., 2001). Thereby LH stimulates increases in intracellular cAMP, leading to subsequent stimulation of StAR mRNA (Steroidogenic Acute Regulatory protein) synthesis and StAR protein phosphorylation

and stimulation of progesterone synthesis *in vitro* (Arakane et al., 1997). StAR is known to permit the import of cholesterol to mitochondria. Expression of PRLR, LHR and StAR and steroid hormone level are decreased in the knock out mouse mutants with absent PRL signalling (Horseman et al. 1997; Grosdemouge et al., 2003). Expressional analyses of PRLR, LHR and StAR and measurements of steroid hormones (estrogen, progesterone and testosterone) in *Ncdn* gene-trap mutants were started during writing of this thesis.

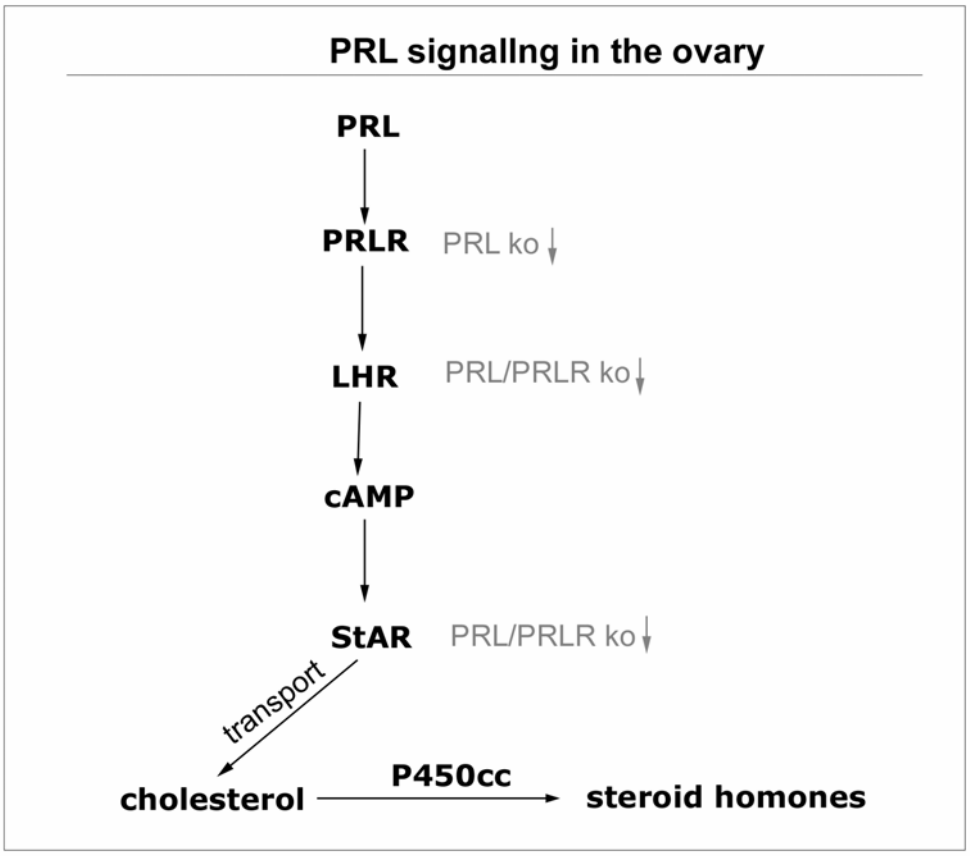

Fig.31 PRL signalling in the ovary

PRL via PRLR activates LHR, an important stimulator of luteal steroidogenesis. Activated LHR stimulates increases in intracellular cAMP, leading to subsequent stimulation of StAR mRNA synthesis and phosphorylation. StAR is known to permit the import of cholesterol to mitochondria, leading to the steroid hormone synthesis. The expression of PRLR, LHR and StAR and steroid hormone level as well are decreased in the knock out mouse mutants with absent PRL signalling

For the analysis of the D2R functionality in *Ncdn* mutant mice pharmacological studies (challenge with D2R agonist bromocriptine and D2R antagonist haloperidol) was suggested.
As it previously shown, *Ncdn* trapped mutants had no altered number and distribution of TIDA neurons, determined by immunostaining for TH enzyme, which is a key enzyme in the DA synthesis. This additionally indicated no alteration in DA synthesis by TIDA neurons, while alterations in DA release can not be excluded. Therefore measurements of DA content in ME are still required.

Finally, a possible binding/interaction of *Ncdn* with D2R or other receptors, containing the *Ncdn*-binding domain, should be studied on the cellular level using biochemical assays (immunopreciopitation, protein-protein binding assay).

4 MATERIALS AND METHODS

4.1 Chemicals/ enzymes/ equipment

Company	Chemicals / enzymes/ equipment
Amersham, Freiburg	Nylon transfer membrane Hybond N+, MicroSpin™ S-300HR columns, Megaprime™ DNA labelling systems, Redivue™[α-^{32}P]dCTP, [γ-^{32}P]ATP, 5'-End labelling Kit , T4 Polynucletid Kinase, Rapid-hyb-buffer, X-ray cassettes with Intensifier, ECL-Western-Blotting Detection Reagents
Abcam, Cambridge, UK	α-β-actin
BDH Lab. Supplies, Poole, GB	DPX embedding medium
Becton Dickinson, Sparks, USA	LB-Medium, Bacto™ Agar
Becton Dickinson, Europe (Schubert & Weiss, München)	Falcon®-tubes, canulas, syringes
Biozym	Agarose, PCR-tubes in stripes
BioRad, München	Triton®-X100
Bio LabsCell Signalling,	Rabbit α-rat p44/42 MAP kinase antibody; rabbit α-rat Phospho-p44/42 MAP kinase antibody (Thr202/Tyr204)
Biodesign (Dunna Labotechnik GmbH),	Rabbit α-rat FSH (Follicle stimulating hormone); Rabbit α-rat LH (luteinizing

Asbach	hormone)
Chemicon, CA, USA	Mouse α-bovine estrogen receptor (aa494-595) monoclonal antibody; Mouse α-bovine estrogen receptor monoclonal antibody (120-170aa), Rabbit α–prolactin polyclonal antibody
Eppendorf, Hamburg	Safe-Lock-reaction tubes (1,5/2,0 ml)
Fresenius AG, Bad Homburg	Ampuwa®-water
GIBCO BRL, Eggenstein	ART® Sterilfiltertips, 1kb$^+$-Ladder, formamid, restriction enzymes incl. 10x Buffer, PBS, fetal calf serum, goat serum, cell culture media
Invitrogen, Karlsruhe	TOPO TA Cloning® Kit, pCR II®TOPO®Vector *pCDNA3*®-Vector, E. coli TOP 10F® competent cells, Magic Mark Protein Ladder, Superscrit™ First-Strand Synthesis System for RT-PCR
Jackson Immuno Res., USA (Vertrieb Dianova, Hamburg)	Peroxidase conjugated and biotinylated Rabbit α-Goat IgG, peroxidase conjugated and biotinylated Goat α–Mouse IgG
Kodak, New Haven, USA (Vertrieb Sigma, Deisenhofen)	Autoradiography-emulsion (Type NTB-2) Developer (D-19), fixer, X-ray film (Biomax, X-OMAT)

MBI Fermentas, St. Leon-Roth	Restriction enzymes incl. 10x Buffer T4 DNA-Ligase, *Taq*-Polymerase, pre-stained Protein Ladder
Menzel Gläser, Braunschweig	Superfrost®Plus slides
Merck, Darmstadt	Natriumacetat, Magnesiumchlorid, Natriumhydroxid, Maltose, Calciumchlorid, Natriumchlorid, Isopropanol, Ethanol, Methanol, Formamid, Hydrochloric acid, Glacial acetic acid, Boric acid, Chloroform, Mayers Hämalaun
MILLIPORE, Neu Isenburg	Ultrafree®-MC filters (NMWL 30,000)
NEB, Frankfurt Main	Restriction enzymes incl. 10x Buffer
Pall, Ann Arbor, USA	BioTrace™PVDF-Membrane
Pel-Freeze, Rogers, USA	PK-antibody Rabbit α-TH IgG
Promega, Mannheim	Wizard® Genomic DNA Purification Kit *pGEM®-T, pGEM®-T Easy* Vector Systems for PCR-cloning, RNasin
QIAGEN, Hilden	QIAquick® PCR-purification Kit, QIAprep® Spin Miniprep Kit, QIAquick® Gel Extraction Kit, Qiagen® Plasmid Maxi Kit, RNeasy™ Kit
Roche, Mannheim	DNA-molecular weight standards, dNTPs, NTPs, DTT, Proteinase K, restrictions-enzymes incl.10x buffer, RNaseA, T4 DNA-Ligase, Klenow, T3-, T7-, SP6-RNA Poly-merase, *Taq*-Polymerase, RNase-Inhibitor t-

	RNA, Mouse monoclonal α–E. coli β– galactosidase, BrDU labelling and detection Kit II
Roth, Karlsruhe	Roti® Phenol/Chloroform, Rotiszint®-scintillation solution
Santa Cruz, Heidelberg	Rabbit α-human polyclonal HPRT (Hypoxantine-guanine phosphorybosiltransferase) antibody
Sigma, Deisenhofen	PEG, Sucrose, Glucose, Maltose, Kalium ferrocyanid, Kalium ferricyanid, Glycerol, Mineral oil, Natrium phosphate, Natrium hydrogenphosphate, MOPS, EDTA, EGTA, Desoxycholat, Nonidet-P40, Trizma® Base, Magnesiumsulfat, Glycin, DMSO, DMF, Bromphenolblau, Kresylviolet, DTT, SDS, 2-Mercaptoethanol, Citric acid, Natrium citrat, Paraformaldehyd, Glutar-aldehyd, Ampicillin, Kanamycin, Heparin, Methyl Salicylat, Poly-L-Lysine, Tween20,
Vector Laboratories, Burlingame, USA	Biotinylated Goat α-Rabbit IgG Vecta ®Stain ABC-Kit,
Whatman, Maidstone, GB	3MM-Filterpapier

4.2 Working with ribonucleic acids

4.2.1 Restriction of the plasmid DNA with endonucleases

For the restriction of 1 µg of the plasmid DNA 1-10 U of appropriate restriction enzyme were used. The reaction was carried under supplier conditions.

4.2.2 DNA agarose gel electrophoresis

DNA fragments were electrophoretically separated according to their molecular size on agarose gels (0,5-2%). The agarose was melted for 2-3 min in 1x TBE and cooled down till ~ 55°C. Before cooked agarose was poured into a gel caster ~0,05µg/ml ethidium bromide solution was added. The 1XTBE buffer was used as running buffer. The DNA loading buffer (0,2 – 0,5 of sample volume) was added to the DNA samples. The DNA samples were loaded into the wells of the gel and electrophoresis was carried out at a steady voltage (100-150 V or 3-4 V/cm2). Under this condition, the negatively charged DNA molecules moved towards the cathode. The DNA fragments were observed and photographed under UV light at a λ of 254 nm or 312 nm due to the intercalation of the fluorescent dye ethidium bromide into the double strand of DNA. Limitations of this method are under 5 – 10 ng DNA.

10 x TBE:	1 mM Tris-Base 0,83 mM Boric acid 20 mM EDTA
6X Sample buffer	0.2 % Bromphenolblue 60 % glycerine in H_2O

4.2.3 Plasmid DNA purification from the agarose gel

DNA was eluted with QIAquick Gel Extraction Kit (Qiagen, Cat.-Nr.: 28704) after manufacturer protocol. The gel bloc, containing DNA with appropriate size was melted in diluting and binding buffer at 55^0 C. After agarose bloc melted completely it

was applied on the column and centrifuged at 17 900 x g for 1 min. During this procedure DNA bounded selectively to the silica membrane of column. After washes with 70% ethanol DNA fragments were eluted with corresponding volume of Ampuwa H_2O or with 10mM Tris-HCl (pH 8,5). The purified DNA was stored in aliquots at -20°C.

4.2.4 Amplification of the DNA fragments using Polymerase-Chain- Reaction (PCR)

The PCR Reaction:

2.5 µl	10X Taq-Buffer with $MgCl_2$ (Roche Diagnostics)
10 ng	DNA-template (~ 100-200 ng genomic DNA)
0.2mM	dNTP (10 mM stock solution)
0.4 µm	of each primer (10 mM stock solution)
0.25 µm (1.25 U)	polymerase (Taq 5U/µl, Roche Diagnostics
	H_2O added till 25 µl

The amplified DNA fragments were separated on the agarose gel (5.1.2.2). The primers used in this thesis as well as special PCR conditions are listed in the appendix.

4.2.5 The synthetic oligonucleotides (primers)

All primers used in this work were synthesized by AG BIODV, GSF and were adjusted to a stock concentration of 100 pmol/µl with Ampuwa water. Primer stock solutions were stored at -20°. Primer melting temperatures were calculated with Oligo-Editor Program (AG BIODV).

4.2.6 Automatic sequencing of DNA

The principal of the nucleic acid sequencing is based on the chain termination method developed by Sanger (Sanger et al., 1977). In this method the template DNA was amplified by PCR with specially marked fluorescent 2´,3´ dideoxynucleotide triphosphates (ddNTP). The fluorescence signals were detected and processed by Spectrophotometer ABI Prism 3100 analyser (Applied Biosystems). Computer software 40100 identified each nucleotide based on the distinctive colour (emission wavelength) of each different dye. For the sequencing PCR the ABI Prism BigDye Terminator v3.1 kit was used.

The PCR-sequencing Mix
1.8 µl Big Dye Terminator
0.2 µl primer (20 pmol/µl)

H_2O added till 10 µl

The PCR programme was repeated 25 times and consists of following steps:

30 sec 95°C
15 sec at primer specific temperature
4 min 60°C

PCR products were precipitated with 4 volumes of 80% EtOH. The pellet was washed with 125 µl of 70% EtOH, air dried and diluted in 25 µl of H_2O. Sequencing data were analysed and edited using computer programmes Sequece-Navigator, Sequence-Analysis und VectorNTI™ (Version 6).

4.2.7 Radioactive labelling of the DNA-probe

DNA probes for the detection of specific nucleic acid sequences on the Southern and Northern membranes were P^{32} labelled with Megaprime™DNA labelling system (Amersham Life Science, Cat.Nr. RPN 1604/5/6/7). Membranes were pre-hybridised in Charge buffer for at least one hour. In case of Northern blot - *Rapid-hyb* buffer (Amersham, Cat.-Nr.: RPN 1635) was used. For labelling of dsDNA probe with corresponding size 700 – 1200 bp) pre-hybridisation and hybridisation were carried out 65°C. About 1 Mio cpm of labelled probe was used for 1 ml of hybridisation buffer. The labelled probe was denatured at 95°C for 5 min and chilled on ice for 2 min and then added to the hybridising buffer. The hybridisation was performed over

night under permanent rotation in the glass tubes. After hybridisation, the membrane was washed in the washing buffer at 55 – 60 °C.

4.3 Working with genomic DNA

4.3.1 Isolation of the genomic DNA from the mouse tissue, embryos and ES-cells

For the isolation of genomic DNA from the mouse tail tip Wizard®Genomic DNA Purification Kit (Cat.-Nr.: A1125) DNA isolation kit (Promega) were used.
After adding of 500 µl of Lysis buffer (P) and proteinase K (1 mg/ml) samples were incubated over night at 55°C. Tissue lysates were centrifuged 7 min at 13 000 rpm to separate denaturated proteins. DNA was precipitated by adding of 500 µl room temperature isopropanol to the supernatant and followed by 30 min centrifugation at 13 000 rpm. DNA pellet was washed with 75 % ethanol, dried and diluted in 600 µl of Ampuwa water. DNA samples were stored at 4°C. For the isolation of DNA from the embryonic tissue and ES-cells special lyses buffers were used.

Lyses buffer 1:	50 mM Tris-HCl (pH 8,0)
(Tissue)	50 mM EDTA
	10 mM NaCl,
	0,5% SDS
Lyses buffer 2:	10 mM Tris-HCL (pH 8,3)
(Embryos)	50 mM KCl
	0,45% NP40
	0,45% Tween 20
	0,1 mg/ml Gelatine
Lysispuffer:	10 mM Tris-HCl (pH 8,0)
(ES-Cells)	10 mM EDTA
	10 mM NaCl
	0,5% N-Laurylsarcosyl

4.3.2 Southern blot of the genomic DNA and hybridisation with DNA-probes

The genomic DNA was digested with concentrated enzymes (40U/µl) at the appropriate temperature over night. After digestion DNA was applied on the 0.8% agarose gel, in TBE buffer.

The Southern blotting technique (Southern, 1975) is based on the capillary transfer of denatured DNA molecules from agarose gels onto a nylon membranes (Hybond N, Amersham, Braunschweig) through diffusion of salt solutions. These membranes are then hybridized with a labelled DNA probe.

After electrophoresis, gel containing DNA fragments was denaturated 20 min in alkaline solution and then neutralized for 20 min in 2 X SSC. After DNA denaturation gel was placed on 20x SSC soaked Whatman™3MM-Filterpapier (Cat.-Nr.: 3030 917) paper which ends were immersed in transfer solution and a recipient with 20x SSC. The membrane was placed directly on the gel and covered by a layer of 2x SSC soaked Whatman paper. The air bubbles that could disturbe transfer were eliminated using a roller. On the top dry absorbent paper was placed. An object~500 g was placed on top for better transfer. The transfer was carried out overnight at RT.

After transfer the membrane was soaked in 2x SSC and DNA was covalently bounded to the membrane by UV cross-linking (120 mJ; UV Stratalinker TM 1800, Stratagene, Heidelberg).

Denaturation solution:	0,5 M NaOH 1,5 M NaCl
Neutralisation solution:	0,5 M Tris-HCl (pH 7,2) 1,5 M NaCl
20 x SSC:	3 M NaCl 0,3 M Natrimcitrat pH 7.0

4.3.3 Hybridisation of the genomic DNA with DNA probe

The membrane with transferred genomic DNA was hybridised with radioactively labelled DNA probe (5.2.7) in appropriate volume of Rapid Hyb Buffer (Amersham) at 65°C fro at least 3 hours. After hybridisation, the membrane was washed in buffers with increasing stringency: 2XSSC/0.1%SDS by RT; 1XSSC/0.1%SDS at 42°C or 0.5XSSC/0.1%SDS at 65°C dependent of the background binding. The hybridised membranes were exposed to Kodak X-ray films X-Omat AR (Sigma, Cat.-Nr.: F5263) in the X-ray cassettes (Amersham, Cat.-Nr.: RPN11645). The X-ray cassettes were placed dependent on the signal intensity 4 hours till 5 days at –80°C. The exposition time of genomic southern blots was about 6 till 14 hours. Northern blots were exposed till 5 days. After exposition films were developed after manufacturer protocol.

4.4 Working with Ribonucleic Acids (RNA)

4.4.1 Isolation of the total RNA from mouse tissues and cells

RNA is extracted in a denaturing solution of Guanidine-Isothiocyanate (GITC). Adult mice tissues (brain, pituitary) were collected and used immediately for the RNA isolation. 100 mg of each tissue was mixed with 1 ml of the GITC buffer solution (Total-RNA solution, Biomol) and then homogenized for 10-20 sec with an electric homogeniser (Ultraturrax T25) (Chomczynsky and Sacchi, 1997). 0.2 ml of chloroform was added to each sample for the generation of the phase gradient. After that samples were mixed and incubated 5 min at room temperature (RT). After centrifugation at 3.200x g for 10 min at 4^{o}C, the upper phase, containing RNA, was separated and mixed with 1 ml of isopropanol. After 15 min incubation on ice RNA was precipitated by centrifugation at 13.000x g at 4°C. RNA pellet was washed with 1 ml of ice-cold 75% ethanol. Pellets were dried at RT and finally re-suspended in 200 µl of DEPC-H_2O. To avoid contamination with proteins, samples were incubated at 65°C for 0.5-2 min, chilled on ice and denatured proteins were pelleted by centrifugation for 30 sec.

The RNA concentration was determined with a spectrophotometer. Absorption at 260nm (OD_{260}) is equal to 40 µg/ml (Sambrook et al., 1989). RNA samples were stored in small aliquots at -80°C.

DEPC water:	0,1% Diethyl Pyrocarbonat

4.4.2 RNA gel electrophoresis

For the RNA separation denaturating agarose gels were used. The electrophoresis chambers were treated with RNase ZAP (Ambion, Wiesbaden) to eliminate RNase, and finally rinsed with dH_2O. The agarose for the gel was melted in the 1 X FA-Gel buffer. After cooling down till 55°C, 37% formaldehyde (final concentration 2M) was added to the melted agarose and poured immediately into a gel bed. The running buffer 1 x FA contains 0,5 M formaldehyde. The formaldehyde concentration in the running buffer was equilibrated by permanent agitation of the running buffer. The RNA loading buffer was added to RNA sample (10-30 mg) and RNA lengh standard (Roche Cat.Nr.: 1 062 611). After incubation in the termoblock at 85°C, RNA samples were chilled on ice and loaded on the gel. Electrophoresis was carried out at 2 – 2,5 V/cm. The agarose gel was photographed under UV light (254 nm) and the RNA was used for the amplification of cDNA.

10 x FA-Gel-buffer: (pH 7,0 adjusted with NaOH)	200 mM 3-[N-Morpholino] propan- sulfonic acid (MOPS) 50 mM Natriumacetat 10 mM EDTA
1 x FA running buffer:	100 ml 10 x FA-Gel-Puffer 20 ml Formaldehyd 37% 880 ml DEPC-water
5 x RNA loading buffer:	16 µl saturated Bromphenolblue solution 80 µl 0,5 M EDTA (pH 8,0) 720 µl Formaldehyd 37% 2 ml Glycerol 3084 µl Formamid 4 ml 10 x FA-Gel-buffer ad 10 ml H_2O

4.4.3 RT-PCR using cDNA amplified on the total RNA

For the RT-PCR 1 mg of total RNA isolated from the brain and embryonic tissue was reverse transcribed with SuperScript™ First-Strand Synthesis System for RT-PCR (Invitrogen, Cat.Nr.:11904-018) kit. The first strange cDNA synthesis was catalyzed by SuperScript II RNase H^- reverse transcriptase. (recombinant form of Moloney-Mouse-Leukemia virus $RNaseH^+$) with random hexamers. The reverse transcription of cDNA was carried out after manufacturer protocol.

RT-PCR-conditions:

Hot start denaturation:	95°C	5min
Taq-Polymerase added	95°C	1min
Denaturation:	95°C	30sec
Annealing:	62°C	30sec
Extension:	72°C	30sec
Number of cycles	36	
Final Extension:	72°C	10min

PCR mix:

cDNA	2 µl
H_2O	37 µl
10X PCR buffer (with $MgCl_2$)	5 µl
dNTP's (10mM)	1 µl
DMSO	1,5 µl
Ex6	1 µl
Ex7	1 µl
Lac2	1 µl
Taq Polymerase	0,5 µl
Total volume	50 µl

4.4 General methods for working with *E. coli*

4.4.1 Storage of the bacterial cultures

The bacterial cultures are stored in the glycerine stocks (50%glycerine/ 50% of bacterial culture) at - 80°C.

4.4.2 Preparation of the competent cells

The plasmids are transformed into bacterial cells for multiplication. The highest acceptance of bacterial cell is in the log phase of grow, because of very thin cell membrane.

For preparation of competent cells 20 µl of *Escherichia coli (E.-coli)* DH5α-bacteria (s. Appendix) were inoculated in 20 ml Luria Broth (LB)-media and harvested at 37°C under 190U/min shacking till $OD_{(600)}$= max 0,3. The cell suspension was centrifuged at 4°C by 1000 x g for 10 min. The cell pellet was re-suspended carefully in 2 ml of ice cold TSS-buffer (Chung et al. 1989), shock frozen in 50 µl aliquots in liquid nitrogen and stored at –80°C until use.

LB-Medium:	1% Bakto -Trypton
(pH 7,2 adjusted with HCl)	0,5% Hefeextrakt
	0,5% NaCl
TSS solution:	50 mM $MgSO_4$
	10% PEG 3000
	5% Dimethylsufoxid (DMSO)
	ad 100 ml LB-Medium

4.4.3 Chemical transformation of the competent cells

50 µl of competent cells were slowly thawed on ice and carefully mixed with 25 – 100 ng of DNA. Cells were incubated on ice for another 30 min. After heat-shock at 42^0 C for 90 sec 250 µl LB-media were added and harvested at 37^0 C for 60 min with shacking at 180U/min. After incubation, 100-150 µl of the reaction mixture was spread on the selection plate with proper antibiotic (vector coding antibiotic resistance) and incubated overnight at 37°C.

4.4.4 Isolation of the recombinant DNA from bacterial cells

For the isolation of recombinant plasmid DNA the Qiagen® Plasmid Maxi Kit (Cat.-Nr.: 12162) and Qiaprep®Spin Miniprep Kit (Cat.-Nr.: 27104) were used after

manufacturer protocols. Both methods are based on alkali lyses of bacterial cells (Binboim and Dolly, 1979), selective binding of plasmid DNA on the silica-membrane (miniprep) or anion exchange resin (maxiprep) with following DNA elution under specific salt concentrations. Plasmid inserts used for hybridisations were sequenced and plasmid DNA was frozen at -20^0 C in small aliquots.

4.5 Culturing of the mammalian cells

For the culturing of the mammalian cells DMEM (Dulbecco's modified eagle medium (DMEM), Gibco BRL) with 10% fetal calf serum (FCS) was used. Cells were incubated at 37°C in 5%CO_2 reach atmosphere. Trapped cells were spread on the feeder cells

ES-Cell culture medium:	15% FCS (GibcoBRL) 0,1 mM 2-Mercaptoethanol (2-ME) 2 mM L-Glutamin 1.500 U/ml m-LIF in 500 ml DMEM high glucose
Feeder cells medium:	10% FCS (GibcoBRL) 2 mM L-Glutamin 2 mM MEM non essential aminoacids in 500 ml DMEM
2 x Freeze medium:	50% FCS (GibcoBRL) 30% ES-cell culture medium 20% DMSO
Wash medium:	ES cell culture medium without m-LIF

4.6 Working with mice

4.6.1 Mouse husbandry

All mice used for the analysis were kept at GSF Animal Husbandry in specific pathogen-free conditions under the Terms of animal welfare. Mice were kept five per cage after weaning at the age of 21 days in a room with controlled light and darkness cycle (12 hrs light, 12 hrs dark). The room temperature was 22 ± 2 °C and air humidity 55 ± 5%. Animals have free access to standard mouse chow and tap water.

4.6.2 Identification of the mouse embryonic stages

The embryonic stages of the mouse were determined after criteria of Theiler staging atlas (Theiler, 1989).

4.6.3 Superovulation with external gonadotropins

Seven to eight week old female mice were superovulated by intraperitoneal injections of 5IU of pregnant mare's serum gonadotropin (PMSG, Sigma St Louis, MO, USA) followed 44-48 hrs later by 5 IU of human chorionic gonadotrophin (HCG; Sigma). After second injection, females were housed overnight with males and were checked for a vaginal plug on the following morning. Zygotes were flushed from the oviduct of superovulated females. The female mice (1.5-2.5 days pc) were killed by cervical dislocation. The skin and peritoneum were opened with the large transverse incision to expose the abdominal cavity. The oviducts with the upper part of the uterus were dissected and placed into a drop of 0,1 M NaCl solution. Under dissection microscope, the needle attached to a 1 ml syringe was inserted in the fimbrial end of the oviduct. The needle was then held with forceps and oviducts were flashed with 0.05 ml of PBS. Embryos were collected with a pipette and washed through several PBS drops. Embryos were incubated in one drop of hyaluronidase for 3-5 min at 37^{o}C to remove cumulus cells. After dissolution of cumulus cells zygotes were counted under light microscope.

4.6.4 Determination of stages of an estrous cycle

For determination of the estrous cycle stages vaginal smears were applied on the slides, fixed in methanol for 10 sec and air dried. After slides were HE stained (5.9.2) and analysed under light microscope.

4.6.5 Blood samples

The trunk blood samples were taken pericardial and left for clotting at 4^{o}C over night. After clotting, samples were centrifuged for 30 min at 13000 rpm. The blood serum was transferred into fresh tubes and stored at -20^{o}C.

4.7 Biochemical methods

4.7.1 Isolation of the total protein

The animal tissue (hippocampus, pituitary, embryos) for protein extraction was homogenised in ice cold Protein extraction buffer by ultrasound handling for 1-2 min. After adding of 4x Laemmli loading buffer protein extracts were denaturated for 2 min at 95°C. Total protein samples were stored in aliquots at -20°C.

Protein extraction buffer:	250 mM Sucrose
	100 mM NaCl
	2,5 mM MgCl2
	10 mM EGTA
	20 mM HEPES
	1% Triton-X 100
	ad 100 ml H_2O

4 x Laemmli-loading buffer:	2,5 ml 1M Tris-HCl pH 6,8
	0,8 g SDS
	0,4 ml 2-ME
	0,001% Bromphenolblue
	7,1 ml H_20

4.7.2 SDS-polyacrilamide-gel electrophoresis (SDS-PAGE)

The discontinuous SDS-polyacrilamide gel electrophoresis for separation of denaturated proteins was carried out after Laemmli (1970) and Gallagher (1999). In this electrophoresis system buffers with different contents and pH were used to generate the voltage gradient. For the electrophoresis 10%, 4-10% and 4-20% Tris-HCl gels (BioRAD, Cat.-Nr.:161-1103) in the Mini-Protean®3 Apparatus (BioRad, Cat.Nr.: 165-3301) were used. As a running buffer 1x Tris-glycine buffer was used. From isolated total proteins 5 µl was loaded on the gel. Electrophoresis was carried out at 20 – 40 mA. Pre-stained Protein Ladder (MBI, Cat.-Nr.:SM0671) and Magic Mark Ladder (Invitrogen, Cat.-Nr.: LC5600) were used as protein weight standards.

10 x SDS-running buffer:	125 mM Tris-Base
	96 mM Glycine
	0,5% SDS
	ad 1000 ml H_2O

4.7.3 Western blotting

The total protein mix separated on the SDS-Polyacrylamid-Gel (10 %, 4-10% and 4-20%) was transferred on the BioTrace™PVDF membrane (Pall, Cat.-N.: P/N66543). Western blotting (Towbin et al., 1979; Burnette, 1981; Sassa and Gallagher, 2000) was performed in Criterion Blotter (BioRad, Cat.-Nr.:170-4070) under 250 mA for 3 hours at 4°C.

For blocking of unspecific binding sites membrane was incubated in the 5 % non-fat milk in 1X PBT solution over night at 4°C under smooth shaking. After 5 x 10 min wash in PBT membrane was incubated with diluted in PBT primary antibody (s. Materials and methods Table 1) for 12 hours at 4°C. The rests of the non coupled antibody solution was washed with PBT under permanent shaking. After washes membrane was incubated in secondary antibody (horse-reddish perocsidase coupled) diluted in PBT for one hour at room temperature. After incubation in the substrate ECL (Amersham, Cat.-Nr.: RPN2109D1) enzymatic activity of the horse-reddish perocsidase causes energy release in form of chemo luminescence. The chemo luminescence can be detected on the X-ray film and specifically detect proteins immobilised on the membrane.

1 x Protein-Transfer Buffer:	100 ml 10 x SDS running buffer
´ (PBT)	200 ml Methanol
	10 ml SDS 10%
	690 ml H_2O

4.8 Morphological methods

4.8.1 Intracardial perfusion

The intracardial perfusion was used for fixation of adult brain, pituitaries and ovaries. For the perfusion mice were narcotised with halothane, fixed, skin and thorax were opened with the large transverse incision till heart was open. The heart tip was cut and catheter was pushed into aorta trough the left heard ventricle. The catheter was fixed to aorta and attached to the electric pump. Blood vessels were washed first with 0,1 M PBS and after filled with 4%PFA in 0,1 M PBS. The perfusion was stopped after 10 min. Brains and other organs were sectioned and fixed by immersion in 4% PFA in 0,1 M PBS for 2-3 hours. Fixed organs were treated after scheme presented in Table 5 and embedded in paraffin. For the X-gal stain perfusion was done with LacZ buffers.

1XPBS (pH 7,4)	137 mM NaCl
	2,7 mM KCl
	10 mM NaH_2PO_4
	2 mM Na_2HPO_4
20%PFA in 1XPBS (pH 7.4, adjusted with NAOH)	Paraformaldehyde (PFA) is melted in 1XPBS at 70°C and stored in aliquots at -20°C.

4.8.2 Sectioning of the tissue

5.7.2.1 Cutting of paraffin sections on the microtome

Animal tissue was sectioned from the perfused animals (5.7.1) and dehydrated after Animal tissues were treated after schema presented below prior embedding in the paraffin.

	E10-10,5	E10,5-11,5	E12,5-13,5	E14,5-P0	adult
4% PFA	30 min	60 min	2 h	12 h	perfusion
70% Ethanol	15 min	15 -30 min	30 min	60 min	4 h
96% Ethanol	5 min	10 min	30 min	30 min	1 h
100% Ethanol	5 min	10 min	30 min	30 min	1 h
Rotihistol	≈ 5 min	≈ 10 min	≈ 30 min	≈ 30 min	≈ 1 h
Paraffin/Rotihystol 1:1	None	None	None	None	1 h
Paraffin	12 h	12 h	12 h	12 h	12 h

The mouse pituitaries and ovaries were treated I the same way like embryos day 10-10,5 (E10-10,5).

Paraffin sections were used for *in-situ* hybridisation, different immunohistochemical and histochemical stains. After dehydration tissues and organs were embedded in a paraffin mixture (ParaplastTM) with DMSO for a better infiltration in the tissue. Tissues and organs were transferred into embedding mould, which was filled with liquid Paraplast^{TM} and laid at RT to solidify. The paraffin blocks were cut on the microtome to 6-10µ thick consecutive sections. Sections were separated in the 39^{o} C water bath and strained on Superfrost®Plus slides. After drying at 37^{o} C slides were stored at 4^{o} C until use.

4.8.2.2 Cutting of frozen tissue on the cryotome

For preparation of cryo-sections tissues were fixed with 4 % PFA in 0,1 M PBS (s. Materials and Methods Table 5) or shock frozen on dry ice directly after sectioning. For the cryoprotection, fixed tissue was placed in 25 % sucrose solution in 0,1 M PBS over night. For cutting tissues were placed on the plate, covered by Cryo-embedding media, quick frozen at –50°C and 40µ thick sections were cut on the cryostat. The consecutive sections were strained on Superfrost®Plus slides and dried. Slides with cryosections were stored at –20°C.

For immunohistochemical stains sections were collected in cryopotection solution („free-floating“) and strained on slides after staining.

Cryoprotection solution: 125 ml Glycerol

125 ml Ethylenglycol
250 ml 0.1 M PBS

4.8.2.2 Cutting with vibrotome

For the X-gal stain of mouse adult brains 50-500 µm vibratome sections were preparated. The tissue was fixed by perfusion with LacZ-fixation solution and washed after perfusion with LacZ-wash buffer (5.7.1). Fixed brains were glued on the plate and cut in water bath. Sections were stained directly after cutting.

4.9 Histochemical staining

All histochemical staining were performed at RT on paraffin and cryo-sections. The paraffin sections prior to the staining were re-hydrated in the solutions with decreasing concentration of EtOH (96%, 70%, 50%, 25%) and distillate water.

4.9.1 Nissl staining

The kresyl violet solution used in Nissl staining colours RNA in the Nissl bodies (raw endoplasmatic reticulum) ribosomes attached to portions of endoplasmatic reticulum. Using Nisll stain cell bodies and cell nucleus were visualized. Paraffin sections were rehydrated in the decreasing series of ethanol and coloured in kresylviolet solution for 1 -2 min. After washes in H_2O und 70% ethanol sections were differentiated in the 96% ethanol with 1% of glacial acetic acid. Sections were dehydrated in increasing alcohol series and mounted directly from rotihistol with Roti® Histokit (Roth).

Kresylviolet-solution	2,5 g Kresylviolet
	0,102 g Natriumacetat
	1,55 ml glacial acetic acid
	ad 500 ml H_20

4.9.2 Hematoxylin eosin (HE) staining

The HE staining is used for differentiation of cell cytoplasm and cell nucleus. The cell cytoplasm is coloured by eosin in pink and cell nucleus by haemalaun solution in violet. The slides were stained for 2 -5 min in haemalaun solution. After differentiation

in differentiating solution for 10-60 sec slides were washed in tape water until the sections turn blue (2-3 min). In the next step sections were immersed in Eosin Y stain solution for 1-3 min. The stained sectiones were dehydrated in increasing alcohol series and mounted direct from rotihistol with Roti® Histokit (Roth).

Haemalaun solution	$C_{16}H_{14}O_6$ $Al_2(SO_4)_3$ C(OH)COOH in H_2O
Differentiating solution	0,1% HCL in 0,1M PBS
Eosin Y stain solution	0,1% in H_2O

4.9.3 X-gal staining

The histochemical staining procedure for *E. coli* β-galactosidase activity in adult mouse tissue was used to detect Lac Z expression of inserted sequence. The β-galactosidase, coded by LacZ-reporter, convert X-Gal (indol derivate) in the blue colour substance indigo in presence of ferro- and ferricyanids. For the X-gal stain vibratome and cryotome sections were used. Before incubation in the stain solutions at 37 ^{0}C over night, sections were washed 3 x for 15 min in LacZ-wash buffer under permanent shacking. After staining, sections were fixed over night in 4% PFA/PBS. Vibratome sectons were clarified with methylsalicylat. The cryosections were strained on the slides from PBS, air dried, rehydrated and lidded with Roti® Histokit.

Fixing solution:	4% PFA in PBS (pH 7,4) 5 mM EGTA 2 mM MgCl2
Wash-Buffer:	2 mM MgCl2 0,01% Deoxycholat 0,02% Nonidet-P40 in PBS

X-Gal stain solution:	0,1% X-Gal
	5 mM Kaliumferrocyanid
	5 mM Kaliumferricyanid
	in Wash-Buffer

X-gal stained sections were clarified in 1:2 mixture of benzyl alcohol and benzyl benzoate for 20 min.

4.10 Immunohistochemical staining

All washing steps were performed at RT. Paraffin sections were 2 X 30 min dewaxed in rotihistol, re-hydrated in decreasing series of ethanol (96%, 70%, 50%, 25%) and rinsed in H_20 for 10 min. For antigen retrieval sections were cooked for 5 min with 0,01 M Na-citrate buffer (pH 6.0) in microwave under 600 Watt. After cooling down sections were washed 2 X 5 min in PBS. For the cryo sections such pre-treatment was not necessary. In the following steps paraffin and cryo sections were treated in a same way. Endogenous peroxidases were inactivated by treatment with 0,1% H_2O_2 for 5 min. After washes 2 X 5 min in 0,1 M PBS sections were incubated for 1 hour in 10% FCS and 0,01% Triton-X in PBS at RT for blocking of unspecific bindings. Primary and secondary antibodies were diluted in 10% FCS/PBS (Appendix, Table 6). Sections were incubated with first antibody at 4°C over night and with secondary antibody for 1 hour at RT. After incubation with secondary antibody sections were washed 3 X 5 min in 0,1 M PBS and incubated with ABC (Avidin-Biotin-Complex) solution for intensifying of staining. After washes 2 X 5 min 0,1 M PBS and 5 min with 0,05 M Tris-HCl (pH 7,5) sections were developed in DAB solution. Due to activity of biotinelated horse-reddish peroxidase, which is coupled to the secondary antibody, brawn precipitate was formed from diaminobezidin substrate (DAB solution) in presence of H_2O_2 Stained sections were dehydrated in increasing alcohol series and lid slides with Roti® Histokit.

ABC reagent	reagent A 1 : 300
(Avidin-Biotin-Complex)	reagent B 1 : 300
	10% FCS
	in PBS (pH 7,4)

Blocking buffer:	10% FCS (fetal calf serum) 0,01% Triton-X100 in PBS (pH 7,4)
DAB stock solution	1% 3,3' Diaminobenzidin in H_20
DAB stain solution	1 ml DAB 1% 19 ml Tris-HCl (pH 7,4) 15 µl H_2O_2
Incubation solution	10% FCS in PBS (pH 7,4)
Natrium citrate buffer (pH 6)	10 mM Natriumcitrate in H_2O
Tris-HCl:	5 mM Tris-Base in H_2O (pH 7,4 adjusted with HCl)

4.11 *In situ* hybridisation with radioactively labelled probes on paraffin sections

In order to study mRNA expression on the paraffin sections the *in situ* hybridisation with radioactive labelled RNA probes was used. The *in situ* hybridisation was performed after modified method from Dagerlind (1992) and Wilkinson (1992).

4.11.1 Radioactive labelling of antisense riboprobes

The antisense riboprobes were transcribed from the plasmid DNA clones which contain gene specific sequences flanked by promotors for RNA polymerases of bacteriophags T3, T7 und SP6. The 5-10 µg of plasmid was linearised and purified with QIAquick PCR Purification Kit (Qiagen, Cat.-Nr.: 28104). The [α-thio ^{35}S]-UTP (Amersham, Cat.-Nr.: SJ 40383) was used for radioactive labelling of riboprobes.

Standard schema for 30 µl of labelling mix:

Linearised DNA (1µg)	1,5 µl

10x Transkriptionspuffer	3 µl
NTP-mix (rATP,rCTP,rGTP; each 10mM)	3 µl
DTT (0,5 M)	1 µl
RNase-Inhibitor (40U/µl)	1 µl
[α-thio ^{35}S]-UTP (40 µCi/ µl)	3 µl
RNA-Polymerase (20U/µl)	1 µl
DEPC-H_2O	16,5 µl
---	---
Total volume	30,0 µl

The reaction mix was incubated for at least 3 hours at 37°C. After first hour 20 U of RNA polymerases were added. The matrix DNA was degraded by adding of RNase free DNase 1 (2U) for 15 min at 37°C. The synthesised RNA was purified with RNeasy™ Mini Kit (Qiagen, Cat.Nr.: 74104) after manufacturer protocol. The purified RNA pobe was eluted in 50 µl of DEPC-H_2O. The activity of labelled probe was measured in scintillator. Activity of the riboprobes was usually in the range of 1 - 2,5 · 10^6 cpm/ µl.

4.11.2 Pre-treatment of the paraffin sections

The paraffin sections were pre-treated after following schema:

Dewax	2 x 15 min	Rotihistol
Rehydrate	2 x 5 min	100 % Ethanol
Rehydrate	5 min	70 % Ethanol
Rehydrate	3 min	DEPC-H_20
Rehydrate	3 min	PBS/DEPC
Postfixation	20 min	4 % PFA/PBS, on ice
Wash	2 x 5 min	PBS/DEPC
Tissue permeability increase	7 min	20 µg/ml Proteinase K in ProteinaseK buffer
Wash	5 min	PBS/DEPC
Postfixation	20 min	4 % PFA/PBS, on ice
Wash	5 min	PBS/DEPC
Acetylation	10 min	200 ml 0,1 M TEA (pH8) (Triethanolamine-HCl)

		600 µl Acetic anhydrid
Wash	2 x 5 min	2xSSC
Dehydrate	1 min	60 % Ethanol/DEPC
Dehydrate	1 min	70 % Ethanol/DEPC
Dehydrate	1 min	95 % Ethanol/DEPC
Dehydrate	1 min	100 % Ethanol
Air dry	30 min	

1 x Proteinase K buffer: (pH 7,8 adjasted with HCl)	50 mM Tris-HCl (pH 7,6) 5 mM EDTA (pH 8,0)
2X SSC	300 mM NaCl 20 mM Natriumcitrate
Triethanolamin (TAE 0,1 M):	10,1 g in DEPC-H_2O

4.11.3 Hybridisation of the pre-treated paraffin sections

Sections were pre-hybridised with hybridisation buffer in wet chamber at 65°C for at least 60 min. Each slide was covered by glass lids. The hybridisation chamber was filled with 50% formamid in 4 x SSC. After pre-hybridisation slides were covered by 100 µl of hybridisation buffer with radioactive labelled and denaturated at 95°C riboprobe. The hybridisation solutions contained 7.000.000 cpm per each slide. The hybridisation was carried out at 65°C over night in wet chamber.

Chamber buffer	100 ml Formamid 105 ml DEPC-H_2O 20 ml 20 x DEPC-SSC
Deionised Formamid:	10 g ion exchanger Resin (BioRad AG501-X8) 100 ml Formamid

Hybridisation buffer:	50% Formamid
	20 mM Tris-HCl (pH 8,0)
	300 mM NaCl
	5 mM EDTA (pH 8,0)
	10% Dextransulfat
	0,02% Ficoll 400
	0,02% PVP 40
	0,02% BSA
	0,5 mg/ml tRNA
	0,2 mg/ml blocking -DNA
	200 mM DTT

Yeast-tRNA 10 mg/ml: The tRNA (Roche Diagnostics) in the pulver form was dissolved 50 ml Falcon tubes with water till concentration 2.5 mg/ml. After two time extraction with Phenol/Chlorophorm (centrifuged for 5min at 2800 g) the water-phase, containing tRNA was separated and pelleted with 1/10 volume of 3M Na-acetat and 2,5 volumes of of 100% EtOH. After 30 min of incubation on ice samples were centrifuged at 2800 g. The pellet was washed with 70% EtOH and air dried. The tRNA was dissolved in water till final concentration 10 mg/ml. The 1ml aliquots were stored at -80°C.

Carrier DNA (10 mg/ml): 0.5 g of salmon sperm DNA (Sigma) was dissolved in water (7.5 ml) at RT 15min till2 hours with agitation. After 1.25 ml of 2M HCl was added and precipitated DNA was kneaded for 1 min with a pipette tip and incubated at RT for 15 min. DNA clod was dissociated by adding of 1.75 ml of 2M NaOH and incubation fro 15 min at 37°C with agitation. To the dissolved DNA 5 ml of 1M Tris-HCl (pH 7.4) and water till 20 ml of final volume were added (pH 7.4 , adjusted with 2M HCl). DNA is incubated with 1/10 volume of Na-acetate and 2.5 volumes of 70% EtOH on ice and centrifuged at 11500 g. DNA pellet is washed with 70 %EtOH and air dried. After DNA is diluted till the final concentration of 10 mg/ml, denaturated at 95°C, shock cooled on ice and stored in aliquots at -20°C. For the quality control 0.5 till 3 mg of DNA are tested on the 1,5% agarose gel. The size of the fragments is between 50 and 300 bp.

4.11.4 Washing of the hybridised sections

The unspecific bounded riboprobe was digested with RNaseA and washed out with different buffers. The DTT added to wash buffers oxidate disulfides of riboprobe. The stringency of wash buffers increases with decreasing of SSC concentration:

4 x 5 min	RT	4xSSC
20 min	37 °C	NTE (20µg/ml RNaseA)
2 x 5 min	RT	2 x SSC/1 mM DTT
10 min	RT	1 x SSC/1 mM DTT
10 min	RT	0,5 x SSC/1mM DTT
2 x 30 min	64 °C	0,1 x SSC/1 mM DTT
2 x 10 min	RT	0,1 x SSC
1 min	RT	30 % Ethanol in 300 mM NH_4OAc
1 min	RT	50 % Ethanol in 300 mM NH_4OAc
1 min	RT	70 % Ethanol in 300 mM NH_4OAc
1 min	RT	95 % Ethanol
2 x 1 min	RT	100 % Ethanol
30 min	RT	

1 x NTE: 500 mM NaCl
10 mM Tris-HCl (pH 8,0)
5 mM EDTA (pH 8,0)

RNaseA: 10 mg/ml dissolved in water

4.11.5 Exposure to X-ray film and development of hybridised sections

The hybridised slides were exposed to X-ray film (Kodak; Biomax, Cat.-Nr.: 870 1302) for 48 h at RT in order to control hybridisation. After developing of the X-ray film slides were covered by a thin sheet of photoemulsion (Kodak; NTB-2, Cat.-Nr.: 165 4433) and exposed in the black box with silica gel perls for 4 – 6 weeks. After exposition slides were developed for 3 – 4 min in developer (Kodak; Developer D19, Cat.-Nr.: Sigma P5670), 5 – 7 min fixed (Kodak; Fixer, 197 1720), washed in water. The backside of slides was cleaned from photoemulsion sections were air dried.

Finally sections were Nisll stained (5.9.1) and after dehydration mounted with Rotihistokit.

4.11.6 Documentation of histological results

Hybridised sections were analysed under microscope Zeiss, Axioplan 2 (Objective 5x – 100x) and binocular microscope Zeiss, Stemi SV 6 (Planobjectiv S 1,0 x) in dark and light fields. Sections were photographed with digital-camera AxioCam MRC / HRC supplied by computer programme Axiovision 3.1; 4.0. The identification of anatomic structures was done using following histological atlases: Kaufmann, 1992; Drews, 1993; Schambra et al., 1992; Altmann and Bayer, 1995; Alvarez-Bolado and Swanson , 1996; Franklin and Paxinos, 1997; Jacobowitz and Abbot, 1998).

5 REFERENCES

Arbogast LA, Ben-Jonathan N. (1988) The preovulatory prolactin surge: an evaluation of the role of dopamine. *Endocrinology*. 123(6):2690-5

Adra, C. N., Boer, P. H. & McBurney, M. W. (1987) Cloning and expression of the mouse pgk-1 gene and the nucleotide sequence of its promoter *Gene* 60, 65-74.

An S., Cutler G, Zhao J.J., Huang S.-G., Tian H., Liang L., Rich M., Bakleh A., Du J., Dai K. (2001) Identification and characterization of a melanin-concentrated hormone receptor *Proc. Natl. Acad. Sci. USA*, 98 No 13. 7576-7581

Altman J., Bayer S.A. (1995): Atlas of prenatal rat brain development. *CRC Press, Inc.,* Boca Raton, Florida

Alvarez-Bolado G., Swanson L. W. (1996): Developmental brain maps: structure of embryonic rat brain. *Elsevier Science B. V.,* Amsterdam

Bartke A. (1979) Prolactin-deficient mice. *Animal Models for Research on Contraception and Fertility.* Harper and Row, Hagerstown, pp 360–365

Ben-Jonathan N. and Hnasko R. (2001) Dopamin as a prolactin (PRL) inhibitor *Endocrin Reviews* 22(6):724-763

Bjurulf E., Selstam G., Olofsson J.I. (1994) Increased LH receptor mRNA and extended corpus luteum function induced by prolactin and indomethacin treatment in vivo in hysterectomized pseudopregnant rats. *J Reprod Fertil*. 102(1):139-45.

Blobe G.C., Liu X., Fang S.J., How T., Lodish H.F., (2001) A novel mechanism for regulating transforming growth factor beta (TGF-beta) signalling. Functional modulation of type II TGF-beta receptor expression through interaction with the PDZ domain protein, GIPC, *J.Biol Chem* 276: 39608-39617

Blum M., McEwen B.S., Roberts J.L. (1989) Transcriptional analyses of tyrosine hydroxylase geen expression in the tiberoinfundibular dopaminergic neurons of the rat arcuate nucleus after estrogen treatment. *J. Biol. Chemistry* 262:817-821

Booth R.A., Cummings C., Tiberi M, Liu X.J. (2002) GIPC participates in G protein signalling downstream of insulin-like grow factor 1 receptor. *J. Biol Chem* 277: 6719-6725

Bowen J.M., Keyes P.L., Warren J.S., Townson D.H. (1996) Prolactin-induced regression of the rat corpus luteum: expression of monocyte chemoattractant protein-1 and invasion of macrophages. *Biol Reprod*, 54:1120-1127

Boulay J.L. and Paul W.E. (1992) The interleukin-4-related lymphokines and their binding to hematopoietin receptors. *J Biol Chem* 267:20525–20528

Britt K.L. and Findlay J.K. (2002) Estrogen actions in the ovary revisited. *J Endocrinology* 175, 269-276

Burnette W. N. (1981): Western Blotting: Electrophoretic transfer of proteins from sodium dodecyl sulfate polyacrylamide gels to unmodified nitocellulose and radiographic with antibody and radioiodinated protein. *A. Anal. Biochem*. 112, 195-203

Cai G., Zhen X., Uryu K., and Friedman E. (2000) Activation of extracellular signal-regulated protein kinases is associated with a sensitized locomotor response to D(2) dopamine receptor stimulation in unilateral 6-hydroxydopamine-lesioned rats. *J. Neuroscience* 20, 1849–1857.

Chappell P.E., Lydon J.P., Conneely O.M., O'Malley B.W., Levine J.E. (1997) Endocrine defects in mice carrying a null mutation for the progesterone receptor gene. *Endocrinology*, 138 (10): 4147-4152

Chappell P.E., White R.S., and Mellon P.L. (2003) Circadian Gene Expression Regulates Pulsatile Gonadotropin-Releasing Hormone (GnRH) Secretory Patterns in the Hypothalamic GnRH-Secreting GT1–7 Cell Line. *J Neuroscience*, 23(35):11202–11213

Chang C., Chen Y.T., Yeh S.D., Xu Q., Wang R.S., Guillou F.(2004) Infertility with defective spermatogenesis and hypotestosteronemia in male mice lacking the androgen receptor in Sertoli cells. *Proc. Natl. Acad. Sci. USA..*101 6876–6881.

Check M.L., Check J.H., Kaplan H. (2004) Pregnancy despite imminent ovarian failure and extremely high endogenous gonadotropins and therapeutic strategies: case report and review*. Clin Exp Obstet Gynecol.*31(4):299-301

Chernomordic L.V., Chanturia A, Green J. and Zimmerberg J. (1995) The hemifusion intermediate and its conversion to complete fusion: regulation of membrane composition. *Biophys, J*. 69, 922-929

Cho B.N., Suh Y.H., Yoon Y.D., Lee C.C., and Kim K. (1993) Progesterone inhibits the estrogen-induced prolactin gene expression in the rat pituitary. *Mol Cell Endocrinology* 93: 47-52

Cho B-N, McMullen M.L., Pei L.., Yates J.,. Mayo K.E. (2001) Reproductive deficiencies in transgenic mice expressing the rat inhibin α-subunit gene *Endocrinology* 142(11): 4994-5004

Choi E.Y., Jeong D., Won K., Park H., Baik J.H. (1999) G protein mediated mitogen-activated protein kinase activation by two dopamine D2 receptors. *Biochem Biophys Res Commun* 5, 256 (1): 33-40

Cohen, J. S. & Brown, H. A. (2001) Phospholipases stimulate secretion in RBL mast cells*. Biochemistry* 40, 6589–6597.

Cruz M.E., Villegas G., Dominguez-Gonzalez A., Chavira R., Dominguez R.(2001) Ovulation delay induced by blockade of the cholinergic system on dioestrus-1, is related to changes in dopaminergic activity of the preoptic anterior-hypothalamic area of the rat. *Brain Res Bull.* 1;54(4):339-44.

Cruz-Soto M.E., Schreiber M.D., Gregerson K.A., Boivin G.P., Horseman N.D. (2002) Pituitary tumorigenesis in prolactin gene disrupted mice. *Endocrinology* 143(11): 4429-4436

Dateki M., Horii T., Kasuya Y., Mochizuki R., Nagao Y., Ishida J., Sugiyama F., Tanimoto K., Yagami K., Imai H., Fukamizu A. (2005) Neurochondrin negatively regulates CaMKII phosphorylation, and nervous system-specific gene disruption results in epileptic seizure. *J Biol Chem*. 27;280 (21):20503-8.

Dagerlind A., Friberg K., Bean A. J, Hökfeld T: (1992) Sensitive mRNA detection using unfixed tissue: combined radioactive and non-radioactive in situ hybridization histochemistry. *Histochemistry 98*, 39-49

Dexter D.T., Carayon A., Vidailhet M., Ruberg M., Agid F., Agid Y., Lees A.J., Wells F.R., Jenner P., Marsden C.D. (1990) Decreased ferritin levels in brain in Parkinson's disease. *J Neurochem.* 55(1):16-20.

Dierich A., Sairam M.R., Monaco L., Fimia G.M., Gansmuller A., LeMeur M. and Sassone-Corsi P. (1998) Impairing follicle-stimulating hormone (FSH) signaling in vivo: targeted disruption of the FSH receptor leads to aberrant gametogenesis and hormonal imbalance. *Proc. Natl. Acad. Sci. USA.*.95 13612–13617.

Diczfaluzy E. and Fraser I.S. (1998) The discovery of reproductive steroid hormones and recognition of their physiological roles. *Estrogens and Progesterones in Clinical Practice*, pp 3-17.

De Vries L., Elenko E., Hubler L., Jones T., and Gist Farquhar M. (1996) GAIP is membrane-anchored by palmitoylation and interacts with the activated (GTP-bound) form of Gai subunits. *Proc. Natl. Acad. Sci. USA.*. 93, pp. 15203–15208, Cell Biology

De Vries L., Lou X., Zhao G., Zheng B., and Farquhar M.G. (1998) GIPC, a PDZ domain containing protein, interacts specifically with the C-terminus of RGS-GAIP *Proc. Natl. Acad. Sci. USA.*95, 12340-12345

Donadeu F.X., Ascoli M. (2005) The differential effects of the gonadotropin receptors on aromatase expression in primary cultures of immature rat granulosa cells are highly dependent on the density of receptors expressed and the activation of the inositol phosphate cascade. *Endocrinology* 146(9):3907-16

Dorshkind K., Horseman N.D. (2000) The role of prolactin, growth hormone, insulin-like growth factor-I, and thyroid hormones in lymphocyte development and function: insight from genetic models of hormone and hormone receptor deficiency. *Endocrin Rev* 21: 292-312

Dorshkind K., Horseman N.D. (2001) Anterior pituitary hormones, stress and immune system homeostasis. *BioEssays* 23: 288-294

Drummond A.E. and Findlay J.K. (1999) The role of estrogen in folliculogenesis *Mol Cell Endocrinology* 151 57-64

Drews U. (1993): Taschenatlas der Embryologie. *Georg Thieme Verlag,* Stuttgart

Dupont S., Krust A., Gansmuller A., Dierech A., Chambon P., and Mark M. (2000) Effects of single and compound knockouts of estrogen receptors α (ERα) and β (ERβ) on mouse reproductive phenotype. *Development* 127, 4277-4291

Eddy E.M., Washburn T.F., Bunch D.O., Goulding E.H., Gladen B.C., Lubahn D.B., and Korach K.S. (1996) Targeted disruption of the estrogen receptor gene in male mice causes alteration of spermatogenesis and infertility. *Endocrinology,* 137 4796–4805.

Elvin J.A. and Matzuk M. (1998) Mouse models of ovarian factors. *Rev Reproduction* 3, 183-195

Escalera G., Choi A.L., Weiner R.I. (1992) Generation and synchronization of gonadotropin-releasing hormone (GnRH) pulses: intrinsic properties of the GT1–1 GnRH neuronal cell line. *Proc. Natl. Acad. Sci. USA..*89:1852–1855.

Ferguson J.N., Young L., Hern E., Matzuk M., Insel Th.R, and Winslow J. (2000) Social amnesia in mice lacking the oxytocin gene *Nat Genetics* 25,284-288

Finkelstein J.S., Whitcomb R.W., O'Dea L.S., Longcope C., Schoenfeld D.A., Crowley Jr W.F. (1991) Sex steroid control of gonadotropin secretion in the human male. I. Effects of testosterone administration in normal and gonadotropin-releasing hormone deficient men. *J Clin Endocrinol Metab* 73:609–620

Finidori J., Kelly P.A. (1995) Cytokine receptor signalling through two novel families of transducer molecules: Janus kinases, and signal transducers and activators of transcription *J. Endicrinology* 147, 11-23

Fisher C.R., Graves K.H., Parlow A.F., Simpson E.R. (1998) Characterisation of mice deficient in aromatase (ArKO) because of targeted disruption of the *cyp19* gene *Proc. Natl. Acad. Sci. USA.* 95: 6965-6970

Forte G., Bocca B., Senofonte O., Petrucci F., Brusa L., Stanzione P., Zannino S., Violante N., Alimonti A., Sancesario G. (2004) Trace and major elements in whole blood, serum, cerebrospinal fluid and urine of patients with Parkinson's disease. *J Neural Transm.* 111(8):1031-40

Franklin, K. B. J., Paxinos, G: The mouse brain in stereotactic coordinates. *Academic Press, Inc.,* San Diego (1997)

Freeman M.E. (1994) The neuroendocrine control of the ovarian cycle of the rat. In: *The Physiology of Reproduction,* pp. 613–658.

Gafvels M., Bjurulf E., Selstam G. (1992) Prolactin stimulates the expression of luteinizing hormone/chorionic gonadotropin receptor messenger ribonucleic acid in the rat corpus luteum and rescues early pregnancy from bromocriptine-induced abortion. *Biol Reprod.* 47(4):534-40.

Gray G.D., Soderstein P., Tallentire D., Davidson J.M .(1978) Effects of lesions in various structures of the suprachiasmatic-preoptic region on LH regulation and sexual behavior in female rats. *Neuroendocrinology* 25:174–191.

Geijsen N., Horoschak M., Kim K., Gribnau J., Eggan K., and Daley G.Q. (2004) Derivation of embryonic germ cells and male gametes from embryonic stem cells. *Nature* 427 148–154.

de Gendt K., Swinnen J.V., Saunders P.T., Schoonjans L., Dewerchin M., Devos A. (2004) Sertoli cell-selective knockout of the androgen receptor causes spermatogenic arrest in meiosis. *Proc. Natl. Acad. Sci. USA.*101 1327–1332.

Gharib S.D., Wierman M.E., Shupnik M.A., and Chin W.W. (1990) Molecular biology of the pituitary gonadotropins. *Endoc Reviews* 11; 177-199
Grosdemouge I., Bachelot A., Lucas A., Baran N., Kelly P., Binart N. (2003) Effects of deletion of the prolactin receptor on ovarian gene expression. *Reproductive Biol Endocrinology*, 1: 12.

Greco T.L., Duello T.M., and Gorski J. (1993) Estrogen receptors, Estradiol, and Diethylstilbestrol in early development: the mouse as a model for the study of estrogen receptors and estrogen sensitivity in embryonic development of male and female reproductive tracts. *Endoc Reviews,* 14; 59-71

Gonzalez-Robayna I.J., Falender A.E., Ochsner S., Firestone G.L., and Richards J.S. (2000) Follicle-Stimulating hormone (FSH) stimulates phosphorylation and activation of protein kinase B (PKB/Akt) and serum and glucocorticoid-lnduced kinase (Sgk): evidence for A kinase-independent signaling by FSH in granulosa cells. *Mol Endocrinology* 14 1283–1300

Gorczynska E., Spaliviero J., and Handelsman D.J .(1994) The relationship between 30,50-cyclic adenosine monophosphate and calcium in mediating follicle-stimulating hormone signal transduction in Sertoli cells. *Endocrinology* 134 293–300.

Gore A.C., Oung T., Yung S., Flagg R.A., and Woller M.J. (2000) Neuroendocrine mechanisms for reproductive senescence in the female rat: gonadotropin-releasing hormone neurons. *Endocrinology* 13 315–323.

Guiramand J., Monmayeur J.P., Ceraline J., Bhatia M., and Borelli E. (1995) Alternative splicing of the dopamine D2 receptor directs specificity of coupling to G-proteins. *J. Biol Chem* 270, 7354-7358

Haslam R. J. and Coorssen J. R. (2001) Hayes *et al.* • Role of Inhibin B in FSH Regulation in Men *J Clin Endocrinol Metab,* 86(11):5541–5546 5545

Heckert L.L. and Griswold M.D. (2002) The expression of the follicle-stimulating hormone receptor in spermatogenesis. *Rec Prog Horm Research* 57 129–148.

Hentges S. and Low M. (2002) Ovarian dependence for pituitary tumorogenesis in D2 dopamine receptor-deficient mice. *Endocrinology* 143(12):4536-4543

Hess R.A., Bunick D., Lee K.H., Bahr J., Taylor J.A., Korach K.S., and Lubahn D.B. (1997) A role for oestrogens in the male reproductive system. *Nature* 390 509–512.

Hirsch E., Hu L.J., Prigent A., Constantin B., Agid Y., Drabkin H., Roche J. (1999) Distribution of semaphorin IV in adult human brain. *Brain Research* 27;823(1-2):67-79.

Hitz C., Vogt Weisenhorn D., Ruiz P., Wurst W., Floss T. (2005) Progressive loss of the spongiotrophoblast layer of Birc6/Bruce mutants results in embryonic lethality. *Genesis* 43(4):216.

Hisaw F.L. (1947) Development of graafian follicle and ovulation *Phys Reviews* 27 95-119

Horsemann N.D., and Yu-Lee L.Y (1994) Transcriptional regulation by the helix bundle peptide hormones: growth hormone, prolactin, and hematopoietic cytokines. *Endocr Rev* 15: 627–649,

Horseman N.D., Zhao W., Montecino-Rodriguez E., Tanaka M., Nakashima K., Engle S.J., Smith F., Markoff E., Dorshkind K. (1997) Defective mammopoiesis, but normal hemtopiesis, in mice with targeted disruption of the prolactin gene. *EMBO J* 16: 6926-6935

Hu L.A., Che W., Martin N.P., Whalen E.J., Premont R.T., and Lefkowitz R.J. (2003) GIPC interacts with the beta-1-adrenergic receptor and regulates beta-1-receptor-mediated ERK activation *J.Biol. Chem* 278, 26295-26301

Hu Y.C., Wang P.H., Yeh S., Wang R.S., Xie C., Xu Q., Zhou X., Chao H.T., Tsai M.Y., Chang C. (2004) Subfertility and defective folliculogenesis in female mice lacking androgen receptor. *Proc. Natl. Acad. Sci. USA.*3;101(31):11209-14.

Hubner K., Fuhrmann G., Christenson L.K., Kehler J., Reinbold R., De La Fuente R. (2003) Derivation of oocytes from mouse embryonic stem cells. *Science,* 300, 1251–1256.

Humeau Y., Vitae N., Chasserot-Golaz S., Dupon J-L, Du G., Frohman M.A., Bader M-F, and Polain B (2001) A role for phospholipase D1 in neurotransmitter release *Proc. Natl. Acad. Sci. USA.*98; No26 15300-15305

Iaccarino C., Samad T.A., Mathis C., Kercret H., Picetti R., Borrelli E. (2002) Control of lactotrop proliferation by dopamine: essential role of signaling through D2 receptors and ERKs. *Proc. Natl. Acad. Sci. USA.*29;99(22):14530-5

Ishikawa J. (1992) Luteinizing hormone requirement for ovulation in the rat *Biol Reproduction* 46, 1144-1150

Istvanffy R., Vogt Weisenhorn D.M., Floss T., Wurst W.. (2004) Expression of neurochondrin in the developing and adult mouse brain. *Dev Genes Evol*. 214(4):206-9

Jannini E.A., Ulisse S., Cecconi S., Cironi L., Colonna R., D'Armiento M., Santoni A., and Cifone M.G. (1994) Follicle-stimulating hormone induced phospholipase A2 activity and eicosanoid generation in rat Sertoli cells. *Biol of Reproduction* 51 140–145.

Jacobowitz D. M., Abbott L. C. (1998): Chemoarchitectonic atlas of the developing mouse brain. *CRC Press, Inc.,* Boca Raton, Florida

Jeanneteau F., Guillin O., Diaz J., Griffon N., and Sokoloff P. (2003) GIPC recruits GAIP (RGS19) to attenuate dopamin D2 receptor signalling. *Mol Biol Cell* 15, 4926-4937

Jones E.E., Naftolin F. (1990) Estrogen effect on the tuberoinfundibullar dopaminergic system in the female rat brain. *Brain Res* 510: 84-91

Jones D., Morgan C., and Cockcroft S. (1999) Phospholipase D and membrane traffic. *Biochim. Biophys. Acta* 1439, 229–244.

Kanuka H., Matsuyama S., Ohnishi M., Matsumoto Y., Nishihara M., and Takahashi M. (1997) Prolactin expresses differential effects on apoptotic cell death of luteal cells *in vivo* and *in vitro*. *Endocr J* 44: 11–22

Kakar S.S., Musgrove L.C., Devor D.C., Sellers J.C., Neill J.D. (1992) Cloning, sequencing, and expression of human gonadotropin releasing hormone (GnRH) receptor. *Biochem Biophys Res Commun*. 30;189(1):289-95.

Kaufman M. H. (1992): The atlas of mouse development. *Academic Press Ltd.,* London

Khan Z.U., Mrzljak L., Gutierrez A., de la Calle A. and Rakic, P.S. (1998) Prominence of the dopamine D2 short isoform in dopaminergic pathways *Proc. Natl. Acad. Sci. USA.*95, 7731-7736

Ktistakis N.T., Delon C., Manifava M., Wood E, Ganley I., and Sugars J.M. (2003) Phopholipase D1 and potential targets of its hydrolysis product, phosphatidic acid *Biochem Soci Transactions* 31, 1, 94-97

Kraus S., Naor Z., and Seger R. (2001) Intracellular signaling pathways mediated by the gonadotropin-releasing hormone (GnRH) receptor. *Arch Med Research* 32 499–509.

Krege J.H., Hodgin J.B., Course J.F., Enmark E., Warner M., Mahler J.F., Sari M., Korach K.S., Gustafsson J-A, Smithes O. (1998) Generation and reproductive phenotype of mice lacking estrogen receptor β. *Proc. Natl. Acad. Sci. USA.* 95: 15677-15682

Kumar T.R., Wang Y., Lu N., and Matzuk M.M. (1997) Follicle stimulating hormone is required for ovarian follicle maturation but not male fertility. *Nat Genetics* 15 201–204.

Lalevee N., Pluciennik F., and Joffre M. (1997) Voltage dependent calcium current with properties of T-type current in Sertoli cells from immature rat testis in primary cultures. *Biol Reproduction* 56, 680–687.

Lei Z.M., Mishra S., Zou W., Xu B., Foltz M., Li X., and Rao C.V. (2001) Targeted disruption of luteinizing hormone/human chorionic gonadotropin receptor gene. *Mol Endocrinology* 15 184–200.

Leong D.A., Frawley L.S., and Neill J.D. (1983)Neuroendocrine control of prolactin secretion. *Annu Rev Physiol* 45: 109–127,

Li H. Li S.H., Yu Z.X., Shelbourne P., Li X.J. (2001) Huntingtin aggregate-associated axonal degeneration is an early pathological event in Huntington's disease mice. *J. Neurosci.* 21:8473–81

Limm M.M., Bielsky I.F., Young L. (2005) Neuropeptides and social brain: potential rodent models of autism *Int J Dev Neurosci* 23 (2-3): 235-243

Liscovitch M., Czarny M., Fiucci G., and Tang X. (2000) Phospholipase D: molecular and cell biology of a novel gene family. *Biochem. J.* 345, 401–415.

Lou X., Yano H., Lee F., Chao MV and Farquhar M.G. (2001) GIPC and CAIP form a complex with TrkA: a putative link between G protein and receptor tyrosine kinase pathway *Mol Biol Cell* 12: 615-627

Lou X., McQuistan T., Orlando R.A, and Farquhar M.G. (2002) GAIP, GIPC and Galfa are concentrated in endocytic compartments of proximal tubule cells: putative role in regulating megalin's function *J.Am. Soc. Nephrol.* 13 918-927
Lloyd J.M., Hoffman G.E., and Wise P.M. (1994) Decline in immediate early gene expression in gonadotropin-releasing hormone neurons during proestrus in regularly cycling, middle-aged rats. *Endocrinology* 134 1800–1805.

Lubahn D.B., Moyer J.S., Golding T.S., Couse J.F., Korach K.S., and Smithies O (1993) Alteration of reproductive function but not prenatal sexual development after insertional disruption of the mouse estrogen receptor gene. *Proc. Natl. Acad. Sci. USA.* 90 11162–11166.

Luo L., and O'Leary D. (2005) Axon Retraction and Degeneration in Development and Disease *Annu. Rev. Neurosci*.. 28:127–56
Lydon J.P. (1995) Reproductive phenotpes of the progesterone receptor null mutant mouse. *J. Steroid Biochem. Mol. Biol.* 56, 67-77

Ma X., Dong Y., Matzuk M.M.m, and Kumar T.R. (2004) Targeted disruption of luteinizing hormone beta-subunit leads to hypogonadism, defects in gonadal steroidogenesis, and infertility. *Proc. Natl. Acad. Sci. USA*.101 17294–17299.

Maraganore D.M., de Andrade M., Lesnick T.G., Strain K.J., Farrer M.J., Rocca W.A., Pant P.V., Frazer K.A., Cox D.R., Ballinger D.G. (2005) High-resolution whole-genome association study of Parkinson disease *Am J Hum Genet.* 77(5):685-93.

Marsh D.J., Weingarth D.T., Novi D.E., Chen H.Y., Trumbauer M.E., Chen A.S., Guan X.M., Jiang M.M., Feng Y., Camacho R.E., Shen Z., Frazier E.G., Yu H., Metzger J.M., Kuca S.J., Shearman L.P., Gopal-Truter S., MacNeil D.J., Strack A.M., MacIntyre D.E., Van der Ploeg L.H., Qian S. (2002) Melanin-concentrating hormone

1 receptor-deficient mice are lean, hyperactive, and hyperphagic and have altered metabolism. *Proc. Natl. Acad. Sci. USA.* 5;99(5):3240-5.

Matsumoto A.M., Bremner W.J. (1984) Modulation of pulsatile gonadotropin secretion by testosterone in man. *J Clin Endocrinol Metab* 58:609–614

Matzuk M.M., Finegold M.J., Su J.G., Hsuen A.J., Bradley A. (1992) α-Inhibin is a tumour-supressor gene with gonadal specificity in mice *Nature* 360: 313-471

Matzuk M.M. and Lamb D.J. (2002) Genetic dissection of mammalian fertility pathways. *Nat Cell Biology* 4 Suppl S41–S49.

Mason A.J., Hayflick J.S., Zoeller R.T., Young W.S., Phillips H.S., Nikolics K., and Seeburg P.H. (1986) A deletion truncating the gonadotropin- releasing hormone gene is responsible for hypogonadism in the hpg mouse. *Science* 234 1366–1371.

McArdle C.A., Franklin J., Green L., and Hislop J.N. (2002) Signalling, cycling and desensitisation of gonadotrophin-releasing hormone receptors. *J Endocrinology* 173 1–11.

McCehsney R., Sealfon S.C., Tsutsumi M., Dong K.W., Roberts J.L., Bancroft C. (1991) Either isoform of the dopamine D2 receptor can mediate dopaminergic repression of the rat prolactin promoter. *Mol Cell Endocrin* 79: R1-R7

Menon K.M.J., Utpal M., Munshi C., Clouser A., and Nair K. (2004) Regulation of Luteinizing Hormone/Human Chorionic Gonadotropin Receptor Expression: A perspective. *Biol Reproduction* 70, 861–866

Meroni S.B., Riera M.F., Pellizzari E.H., and Cigorraga S.B. (2002) Regulation of rat Sertoli cell function by FSH: possible role of phosphatidylinositol 3-kinase/protein kinase B pathway. *J Endocrinology* 174 195–204

Miles L.E., Hanyaloglu A.C., Dromey J.R., Pfleger K.D., and Eidne K.A. (2004) Gonadotropin-releasing hormone receptor-mediated growth suppression of immortalized LbetaT2 gonadotrope and stable HEK293 cell lines. *Endocrinology* 145 194–204.

Mochizuki R., Dateki M., Yanai K., Ishizuka Y., Amizuka N., Kawashima H., Koga Y., Ozawa H., Fukamizu A. (2003) Targeted disruption of the neurochondrin/norbin gene results in embryonic lethality. *Biochem Biophys Res Commun.* 31;310(4):1219-26.

Monck J.R., and Fernandes J.M. (1994) The exocytotic fusion pore and neurotnasmitter release *Neuron* 12 707-716

Montmayeur J. P., Bausero P., Amlaiky N., Maroteaux L., Hen R. and Borrelli, E. (1991) *FEBS Lett.* 278, 239–243.

Morgan C. P., Sengelov H., Whatmore J., Borregaard N., and Cockcroft S. (1997) ARF-regulated phospholipase D activity localizes to secretory vesicles and mobilizes

to the plasma membrane following fMetLeuPhe stimulation of human neutrophils. *Biochem. J.* 325, 581–585.

Morgan D., Grant K., Gage D.H., Mach R.H., Kaplan J.R., Prioleau O., Nader S.H., Buchheimer N., Ehrenkaufer R, and Nader M.A. (2002) Social dominance in monkeys: dopamine D2 receptors and cocaine self-administration *Nat Neuroscience* 5 no 2 169-174

Mulac-Jericevic B., Mullinax R.A., DeMayo F.J., Lydon J.P., and Conneely O.M. (2000) Subgroup of reproductive functions of progesterone mediated by progesterone receptor-B isoform. *Science* 289 1751–1754.

Mulac-Jericevic B:, Lydon J:P:, DeMayo F:J:; and Conneely O.M. (2003) Defective mammary gland morphogenesis in mice lacking the progesterone receptor B isoform. *Proc. Natl. Acad. Sci. USA.*100 9744–9749.

Nelson D.R., Kamataki T., Waxman D.J., Guengerich F.P., Estabrook R.W., Feyereisen R., GonzalesF.J., Coon M.J., Gunsalus I.C., Goth O. (1993) The P450 superfamily: update on new sequences, gene mapping, accession numbers, early trivial names of enzymes, and nomenclature. *DNA Cell Biol* 12, 1-51

Neill J.D. (2002) GnRH and GnRH receptor genes in the human genome. *Endocrinology* 143 737–743.

Norwitz E.R., Jeong K.-H., Chin W.W. (1999) Molecular mechanisms of gonadotropin-releasing hormone receptor gene regulation. *J Soc Gynecol Invest* 6, No 4 169-178

Oak J. N., Lavine N., and Van Tol H. H. (2001) Dopamine D4 and D2L Receptor Stimulation of the Mitogen-Activated Protein Kinase Pathway Is Dependent on *trans*-Activation of the Platelet-Derived Growth Factor receptor. *Mol. Pharmacol.* 60, 92–103.

Orikasa C., Kondo Y., Hayashi S., McEwen B.S., and Sakuma Y. (2002) Sexually dismorphic expression of estrogen receptor b in the anteroventral periventricular nucleus of the rat preoptic area: implication in luteinising hormone surge. *Proc. Natl. Acad. Sci. USA.5* vol.99 , No 5, 3306-3311

Pelletier G., Li S., Phaneuf D., Martel C., Labrie F. (2003) Morphological studies of prolactin-secreting cells in estrogen receptor α and estrogen receptor β knock out mice. *Neuroendocrinology*, 77:324-333

Petroni M.L., Albani G., Bicchiega V., Baudo S., Vinci C., Montesano A., Izzo G., Bertocco P., Mazzotta S., Zorzetto E., Balzola F., Mauro A. (2003) Body composition in advanced-stage Parkinson's disease. *Acta Diabetol*. 40 Suppl 1:S187-90.

Rao M., Midgley A., and Richards J. (1978) Hormonal regulation of ovarian cellular proliferation *Cell* 14 71–78

Richards J.S. (1980) Maturation of ovarian follicles: actions and interactions of pituitary and ovarian hormones on follicular cell differentiation. *Phys Reviews* 60 51-89

Richards J. (1994) Hormonal control of gene expression in the ovary. *Endoc Reviews* 15 725–751

Richards J.S. (2001) Perspective: the ovarian follicle – a perspective in 2001. *Endocrinology* 142 2184-2193

Risbridger G.P., Schmitt J.F., Robertson D.M. (2001) Activins and inhibins in endocrine and other tumors*. Endocr Rev*. 22(6):836-58. Review

Risk M., Gibori G: (2001) Mechanisms of luteal cell regulation by prolactin. *Boston, Kluwer Academic Publishers* 1, 265-295

Roy A., Matzuk M.M., (2006) Deconstructing mammalian reproduction: using knockouts to define fertility pathways. *Reproduction* 131(2):207-19.

Ruf F., Fink M.Y., and Sealfon S.C. (2003) Structure of the GnRH receptor-stimulated signaling network: insights from genomics. *Frontiers in Neuroendocrinology* 24 181–199.

Saiardi A., Bozzi Y., Baik J.H., Borelli E. (1997) Antiproliferative role of dopamine: loss of D2 receptors causes hormonal dysfunction and pituitary hyperplasia. *Neuron* (19): 115-126

Sambrook J., Fritsch E. F., Maniatis T. (1989): Molecular Cloning: A Laboratory Manual. *Cold Spring Harbor Laboratory Press,* 2nd Edition

Santen R.J. (1975) Is aromatization of testosterone to estradiol required for inhibition of luteinizing hormone secretion in men. *J Clin Invest* 56:1555–1563

Saper C.B., Chou T.C., Elmquist J.K. (2002) The need to feed: homeostatic and hedonic control of eating. *Neuron* 36:199 –211.

Sasse J., Gallagner S. R., (2000*)*: *Current Protocols in Molecular Biology 10.6.1-13,* John Wiley and Sons Inc

Schomberg D.W., Course J.F., Mukherjee A., Lubahn D.B., Sar M., Mayo K.E., Korach K.S. (1999) Targeted disruption of the estrogen receptor-α -gene in female mice: characterisation of ovarian responses and phenotype in adult. *Endocrinology* 140: 2733-2744

Schambra U.B., Lauder J.M:, Silver J. (1992): Atlas of the prenatal mouse brain. *Academic Press, Inc.,* San Diego

Senogles S.E. (2000) The D2s dopamine receptor stimulates phospholipase D activity: a novel signaling pathway for dopamine. *Mol Pharmacoogy* 58(2):455-62.

Senogles S.E. (2003) D2s dopamine receptor mediates phospholipase D and antiproliferation. *Mol Cel Endocrinology* 209 (2003) 61–69

Sherins R.J., Loriaux D.L. (1973) Studies on the role of sex steroids in the feedback control of FSH concentrations in men. *J Clin Endocrinol Metab* 36:886–893
Shelling A.N., Burton K.A., Chnad A.L., van Ee C.C., France J.T., Farguhar C.M., Milsom S.R., Love D.R., Gersak K., Aittomaki K., Winship I.M. (2000) Inhibin: a candidate gene for premature ovarian failure. *Hum reproduction* 15: 2644-2649

Simoni M., Gromoli J., and Niesclag E. (1997) The follicle-stimulating hormone receptor: biochemistry, molecular biology, physiology, and pathophysiology. *Endoc Reviews* 18 739–773.

Simpson E.R. (2003) Sources of estrogen and their importance. *J Steroid Biochem* and Mol Biol 86, 225-230

Smith D., Tzavara E., Shaw J., Luecke S., Wade M., Davis R., Salhoff C., Nomikos G.G., and Gehlert D.R. (2005) Mesolimbic Dopamine Super-Sensitivity in Melanin-Concentrating Hormone-1 Receptor-Deficient Mice*. J Neuroscience*, 26, 25(4):914 – 922

Smith M.J. and Jens L. (2001) Neural signals that regulate GnRH neurons directly during the oestrous cycle. *Reproduction* 122, 1-10

Southern E. M. (1975): Detection of specific sequences among DNA fragments separated by gel electrophoresis. *J. Mol. Biol. 98*, 503-517.

Soyal S.M., Amleh A. and Dean J. (2000) FIG alfa, a germ cell-specific transcription factor required for ovarian follicle formation. *Development* 127 4645-4654

Spain B.H., Koo D., Ramakrishnan M., Dzudzor B., Colicelli J. (1995) Truncated forms of a novel yeast protein suppress the lethality of a G protein alpha subunit deficiency by interacting with the beta subunit. *J Biol Chem.* 27;270(43):25435-44.

Staub C. (2001) A century of research on mammalian male germ cell meiotic differentiation in vitro. *J Andrology* 22 911–926.

Tamagnone L., and Comoglio P. M. (2000) Signalling by semaphorin receptors: Cell guidance and beyond. *Tend in Cell Biol* 10, 377-383

Tobet S.A., Bless E.P., and Schwarting G.A. (2001) Developmental aspect of the gonadotropin-releasing hormone system. *Mol Cel Endocrinology* 185 173–184.
Toyooka Y., Tsunekawa N., Akasu R., and Noce T. (2003) Embryonic stem cells can form germ cells in vitro. *Proc. Natl. Acad. Sci. USA.*100 11457–11462.

Towbin H., Staehelin T., Gordon J., (1979): Electrophoretic transfer form polyacrylamide gels to nitrocellulose sheets: procedure and some applications. *Proc. Natl. Acad. Sci. USA. 76*, 4350-4354

Tronche F., Kellendonk C., Kretz O., Gass P., Anlag K., Orban P. C., Bock R., Klein R., and Schutz G. (1999) Disruption of the glucocorticoid receptor gene in the nervous system results in the reduce anxiety *Nat. Genet.* 23, 99–103

Tsai J., Grutzendler J., Duff K., Gan W.B. (2004) Fibrillar amyloid deposition leads to local synaptic abnormalities and breakage of neuronal branches. *Nat. Neurosci.* 7:1181–83

Vainio S., Heikkila M., Kispert A., Chin N., and McMahon A.P. (1999) Female development in mammals is regulated by Wnt-4 signalling. *Nature* 397 405-427

Veldhuis J.D., Rogol A.D., Samojlik E., Ertel N.H. (1984) Role of endogenous opiates in the expression of negative feedback actions of androgen and estrogen on pulsatile properties of luteinizing hormone secretion in man. *J Clin Invest* 74:47–55

Vindis C., Seguelas M. H., Lanier S., Parini A., and Cambon C. (2001) Dopamine induces ERK activation in renal epithelial cells through H_2O_2 produced by monoamine oxidase. *Kidney Int*. 59, 76–86.

Vitae N., Caumont A-S, Chasserot-Golaz S., Du G., Wu S, Sciorra VA, Morris J, Frohman M.A. and Bader M-F (2001) Phospholipase D1: a key factor for the exocytotic machinery in neuroendocrine cells. *EMBO* 20 No 10 2424-2434

Wang L.H., Kalb L.G. and Strittmatter S.M. (1999) A PDZ protein regulates the distribution of the transmembrane semaphorin, M-SemF. *J. Biol. Chem*. 274, 14137-14146

Wang Y, Xu R. Sasoka T, Tonegawa S, Kung MP, and Sankoorikal EB (2000) Dopamine D2 long receptor-deficient mice display alterations in striatum-dependent functions. *J. Neuroscience* 20, 8205-8314

Walker W.H., Fucci L., and Habener J.F. (1995) Expression of the gene encoding transcription factor adenosine 30, 50-monophosphate (cAMP) Response element-binding protein: regulation by follicle-stimulating hormone-induced cAMP signaling in primary rat Sertoli cells*. Endocrinology* 136 3534–3545.

Welsh G. I., Hall D. A., Warnes A., StrangeP. G., and Proud C. G. (1998) Activation of microtubule-acssociated protein kinase (Erk) and p70S6 kinase by D2 dopamin receptors. *J. Neurochem.* 70, 2139–2146.

Wells J.A., DeVos A.M. (1996) Hematopoietic receptor complexes *Annu Rew Biochem* 65, 609-634

Weiner R.I., Martinez de la Escalera G. (1993) Pulsatile release of gonadotrophin releasing hormone (GnRH) is an intrinsic property of GT1 GnRH neuronal cell lines. *Hum Reprod* 2:13–17.

Wetsel W.C., Valenca M.M., Merchenthaler I., Liposits Z., Lopez F.J., Weiner R.I., Mellon P.L., Negro-Vilar A. (1992) Intrinsic pulsatile secretory activity of immortalized LHRH secreting neurons. *Proc. Natl. Acad. Sci. USA.* 89:4149 – 4153

Wierman M.E. (1996) Gonadotropin-releasing hormone. *In Repr Endocrinology, Surgery, and Technology,*1, 666–681

Wiles M.V., Vauti F., Otte J., Fuchtbauer E.M., Ruiz P., Fuchtbauer A., Arnold H.H., Lehrach H., Metz T., von Melchner H., Wurst W. (2000) Establishment of a gene-trap sequence tag library to generate mutant mice from embryonic stem cells. *Nature Genet.*, 24, 13–14

Wilkinson J. W. (1992) Whole mount in situ hybridization of vertebrate embryos. In: Wilkinson DG (ed) In situ hybridization: a practical approach. IRL Press, Oxford, 75-83

Winslow J.T., Insel T.R. (2002) The social deficits of the oxytocin knockout mouse *Neuropeptides* 36, (2-3): 221-229

Winters S.J., Janick J.J., Loriaux D.L., Sherins R.J. (1979) Studies on the role of sex steroids in the feedback control of gonadotropin concentrations in men. Use of the estrogen antagonist, clomiphene citrate. *J Clin Endocrinol Metab* 48: 222–227

Usiello A., Baik J.H., Rouge-Pont F., Picetti R., Dierich A., LeMeur M., Piazza P.V., Borrelli E. (2000) Distinct functions of the two isoforms of dopamine D2 receptors. *Nature* 9; 408(6809):199-203

Xu R., Parlow A.F., Wang Y. (2002) The effects of dopamine and D2 receptor antagonist on pituitary hormone secretion are intact in mice lacking dopamin D2L receptor. *Brain research*, 939 (95): 95-99

Yan J., Feng A., Fienberg A., and Greengard P. (1999). D2 dopamine receptors induce MAPK and CREB phosphorylation in neurons. *Proc. Natl. Acad. Sci. USA..* 96: 11607-11612

Yamaguchi H., Aiba A., Nakamura K., Nakao K., Sakagami H., Goto K., Kondo H., Katsuki M. (1996) Dopamin D2 receptor plays a critical in cell proliferation and propiomelanocrtin expression in the pituitary. *Genes Cells* 1:253-268

Yao H.H., Matzuk M.M., Jorgez C.J., Menke D.B., Page D.C., Swain A., and Capel B. (2004) Follistatin operates downstream of Wnt4 in mammalian ovary organogenesis *Dev Dynamics* 230 210-215

Zhang F., Poutanen M., Wilbertz J., and Huhtaniemi I. (2001) Normal Prenatal but Arrested Postnatal Sexual Development of Luteinizing Hormone Receptor Knockout (LuRKO) Mice *Mol Endocrinology* 15(1): 172–183

6 APPENDIX

6.1 Synthetic oligonucleotides (primers)

Name	Sequence 5'→ 3'	Tm[°C]
E6	CAAGGGAGACTGCTTCTAGCTGCCAACGTG	68.8
E7	CTCCTAATGGCCCGGCTCCTTAGC	63.8
F	TCCCTGATAGGAGGGAGGTC	51.6
LacZ	CTCAAGAGACCTGGGACCAA	51.4
L2	CAAGGCGATTAAGTTGGGTAACG	57.7
R	CAAGGCGATTAAGTTGGGTAA	56.7

6.2 Antibodies

Primary antibody	Secondary antibody	ABC
BrDU Mouse α –BrDU 1:10 Roche, Cat.-Nr. 1299964	Biotynilated α –Mouse 1:500	1 : 300 Vector Lab., Cat.-Nr.. PK-6100
β–actin polyclonal antibody 1:1000 Abcam, Cat.-Nr 9809	HR-Peroxidase conjungatetd Goat α-mouse IgG, 1 :2000 Chemicon, Cat.-Nr.: AQ127P	1 : 300 Vector Lab., Cat.-Nr.. PK-6100
β-gal monoclonal antibody 1:1000 Roche, Cat.-Nr.7564	HR-Peroxidase conjungatetd Goat α-mouse IgG, 1 :2000 Chemicon, Cat.-Nr.: AQ127P	1 : 300 Vector Lab., Cat.-Nr.. PK-6100
Calbindin α-Calbindin 1 : 2000 Chemicon, Cat.-Nr.:AB960	Biotinylated Goat α-Rabbit IgG 1 : 300 Vector Lab., Cat.-Nr.: BA 1000	1 : 300 Vector Lab., Cat.-Nr.. PK-6100
HPRT (FL-218) polyclonal antibody 1:1000 Santa Cruz Biotechnology, Cat.-Nr.	Biotinylated Goat α-Rabbit IgG 1 : 300 Vector Lab., Cat.-Nr.: BA 1000	1 : 300 Vector Lab., Cat.-Nr.. PK-6100

Ncdn (N-terminal) serum 1:300 K. Maruyama, Japan, personal communications	HR-Peroxidase conjungatetd Goat α-Rabbit IgG, 1 :2000 Chemicon, Cat.-Nr.: 8965	1 : 300 Vector Lab., Cat.-Nr.. PK-6100
Ncdn (C-terminal) serum 1:300 K. Maruyama, Japan, personal communications	HR-Peroxidase conjungatetd Goat α-Rabbit IgG, 1 :2000 Chemicon, Cat.-Nr.: 8965	1 : 300 Vector Lab., Cat.-Nr.. PK-6100
Parvalbumin Rabbit α-parvalbumin 1:5000 Swant, Cat-Nr.	Biotinylated Goat α-Rabbit IgG 1 : 300 Vector Lab., Cat.-Nr.: BA 1000	1 : 300 Vector Lab., Cat.-Nr.. PK-6100
p44/42 Map Kinase (THr202/Tyr24) polyclonal antibody 1:1000 Cell signaling, Cat.-Nr 9102	Biotinylated Goat α-Rabbit IgG 1 : 300 Vector Lab., Cat.-Nr.: BA 1000	1 : 300 Vector Lab., Cat.-Nr.. PK-6100
phospho-p44/42 (THr202/Tyr24) polyclonal antibody 1:1000 Cell signaling, Cat.-Nr 9101	Biotinylated Goat α-Rabbit IgG 1 : 300 Vector Lab., Cat.-Nr.: BA 1000	1 : 300 Vector Lab., Cat.-Nr.. PK-6100
Prolactin 1 : 2000 Chemicon, Cat.-Nr.:AB960	Biotinylated Goat α-Rabbit IgG 1 : 300 Vector Lab., Cat.-Nr.: BA 1000	1 : 300 Vector Lab., Cat.-Nr.. PK-6100
TH IgG 1 : 5000 PelFeeze, Cat.-Nr.:P4010	Biotinylated Goat α-Rabbit IgG 1 : 300 Vector Lab., Cat.-Nr.: BA 1000	1 : 300 Vector Lab., Cat.-Nr.. PK-6100

6.3 DNA probes used for the hybridisation of southern blots

DNA probe	Insert size	DNA-Vektor / Enzyme	Reference
neo	800 bp	*pKJ -1/Pst1*	Adra et al, Gene, 60; pp. 65-74.
En-1 3' extern	700 bp	*ESEN* / *Eco*RI; *Hind*III	J. Guimera, personal communications

6.4 DNA probes used for the generation of the antisence riboprobe

Gene	Insert size [bp]	Vector, enzyme and RNA polymerase	Reference
Ncdn	550	pBlueScript II KS, *EcoRI* / T7	K. Maruyama, Japan personal communications
D2RL	922	pCR-Script Amp	P.Burbach, pesonal communications
D2RS	833	pCR-Script Amp	P.Burbach, pesonal communications
α-GSU	580	pGEM T*, HindIII* /T7	E.Borelli, France, personal communications
GH	800	pBlueScript II-SK *, Sal*/T7	E.Borelli, France, personal communications
POMC	600	pGEM T, *NcoI* / T3	E.Borelli, France, personal communications
TSH	2100	pBlueScript II-SK, *BamHI* / T7	E.Borelli, France, personal communications
TRH	250	pBlueScript II-SK, *PstI* / T7	E.Borelli, France, personal communications

6.5 Bacterial strains, ES-cells and mouse lines

Bacterial stains: E. coli DH5α, for cloning K-12 strain, F- Φ80lacZΔM15 Δ(LacZYA-argF) U169 deoR recA1 endA1 hsdR17 (rk -, mk+) phoA supE44; λ- thi-1 gyrA96 relA1

ES cells: TBV-2 ES cells

Mouse lines: C57BL/6 (inbreed strain with black coat colour, obtained from the GSF)
Ncdn-trapped (2nd backcross generation to C57BL/6 mice).

6.6 Abbreviations

3-AT	3-Amino-1,2,4-triazol
Ac	Acetate
Amp	Ampicilline
Bp	Base pare
°C	Grad Celsius
cDNA	coding DNA
CNS	Central neural system
cpm	counts per minute
dATP	Desoxyadenintriphosphate
dCTP	Desoxycytosintriphosphat
DAB	Diaminobenzidin
DEPC	Diethylpyrocarbonat
dGTP	Desoxyguanintriphosphat
DNA	Desoxyribonucleic acide
DNAse	Desoxyribonuclease
dNTP	Desoxynukleosidtriphosphat
DTT	Dithiothreitol
dTTP	Desoxythymintriphosphat
E	Embryonic day
EDTA	Ethylen diamintetraacetate
E.coli	Escherichia coli
et al.	et alteres
EtBr	Ethidiumbromide
EtOH	Ethanol
Fig.	Figure
g	Gramm
g	Acceleration due to gravity
His	Histidin
ISH	*in-situ* Hybridisation
Kb	Kilobase pare
KDa	Kilodalton
l	Liter
Leu	Leucin
LB	Luria-Bertami
µ	micro
m	milli
M	Molarity
min	Minute
mRNA	messenger-RNA
n	Number of probes
NAc	Nucleus accumbence
Nr.	Number
PA	Phosphatidic acid
PBS	Phosphate buffered saline

PCR	Polymerase Chain Reaktion
PEG	Polyethylenglycol
PFA	Paraformaldehyd
pd	postnatal day
PD	Parkinson's disease
RNA	Ribonucleic acid
RNAse	Ribonuclease
rpm	rounds per minute
RT	Room temperature
RT-PCR	Reverse Transcriptase-PCR
SDS	Sodiumdodecylsulfat
sec.	Second
Tris	Trishydromethylaminoethan
Trp	Tryptophan
U	Unit
wt	Wilde type
X-Gal	5-Brom-4-Chlor-3-indolyl-β-D-Galactopyranosid

The scientific terms are written in cursive letters. The abbreviations of genes correspond to the nomenclature of the International Committee of Standardised Genetic Nomenclature for mice are written in cursive letters. The proteins are abbreviated similar as genes, but not in cursive. The chemical elements and restriction enzymes are abbreviated corresponding to the standard symbols.

6.7 Curriculum vitae

Ruzanna Istvanffy (Shachbasian)

2002 – present: Ph.D. student at the Institute of Developmental Genetics, GSF Research Center
Thesis title: The molecular and functional analysis of neurochondrin mouse mutant

1995-1998 Graduate student at the Institute of Molecular Genetics, Moscow, Russia

Diploma (equal to Masters Degree) from Yerevan State University, Yerevan, Armenia
Thesis title: Cloning of levanase gene SacC in Ti-plasmid of Agrobacterium tumefacies

SEMINARS, CONGRESSES AND EXCURSIONS

13.11.2005	SfN 35th Annual meeting, Program Nr: 242.7 (Society for Neuroscience)	Oral presentation
29.0904	3rd Weimar Conference on Genetics (Society of German Genetics)	Poster
15.12.04	Developmental biology seminars, Munich (Society of German Genetics)	Oral presentation

PUBLICATIONS

Istvanffy R., Vogt Weisenhorn D.M., Floss T., Hölter, S., Kallnik M., W. Wurst (2005) A possible involvement of neurochondrin in dopamine signalling via the D2R in the pituitary Abstract SfN 35th Annual meeting, Nov. 13, Program Nr. 242.7

Istvanffy R., Vogt Weisenhorn D.M., Floss T., Wurst W. (2004) Expression of neurochondrin in the developing and adult mouse brain Dev Genes Evol, Apr; 214(4):206-9

Neumivakin L.V., Solovjev V.P., Sokhansanj A., Tilba V.A., Moseiko N.A., Shachbasian R.V., Piruzian E.S.(1995). Increase in osmotolerance of Rhizobium fredii soybean isolate BD32 by the proB proA operon of Escherichia coli, Biochem Biophys Res Commun. 26; 217(3):796-801

6.8 Acknowledgments

I would like to express my deepest gratitude to Prof. Wolfgang Wurst for his excellent guidance, caring, patience, and providing me with an excellent atmosphere for doing research.

I would like to thank Dr. Thomas Floss who gave me an opportunity to analyse the *Ncdn* gene-trap mouse line and patiently corrected my writing.

I would also like to thank Dr. Daniela Vogt Weisenhorn for helping me to develop my background in morphology, histochemistry and immunohistochemistry and for fruitful discussions.

I thank Dr. Claudia Seisenberger for proof reading of my thesis and suggestions to my work.

Many thanks to my friends Alexandra Black, Eleonora Minina and Thorsten Naserke for the grate support and helpful suggestions during my graduate studies.

I would like to thank all the members of IDG for the friendly relationship and nice working atmosphere.

Special thanks to Prof. Yuri Popov for the helpful comments and suggestions to my work.

Finally, I would like to thank my parents, my sister, my daughter and my husband, who supported and encouraged me.

6.9 Selbständigkeitserklärung

Hiermit erkläre ich, dass ich diese Arbeit selbst verfasst und keine anderen als die angegebenen Quellen und Hilfsmittel benutz habe. Ich versichere, dass die Arbeit in dieser oder einer anderer Form beim keiner andere Prüfungsbehörde vorgelegt wurde.

München, den 27.03.2006

Ruzanna Istvanffy